BEHAVIOUR OF ARCH DAMS UNDER STATIC AND DYNAMIC LOADS

A Dissertation
submitted in partial fulfilment
of the requirements for the degree
of
MASTER OF ENGINEERING
in
EARTHQUAKE ENGINEERING
With Specialization in Structural Dynamics

By
R. K. GUPTA

DEPARTMENT OF EARTHQUAKE ENGINEERING
UNIVERSITY OF ROORKEE
ROORKEE (INDIA)
September, 1972

C O N T E N T S

C E R T I F I C A T E

CERTIFIED that the thesis entitled " BEHAVIOUR OF ARCH DAMS UNDER STATIC AND DYNAMIC LOADS" which is being submitted by Sri Radhey Krishna Gupta in partial fulfilment for the award of the degree of Master of Engineering in " STRUCTURAL DYNAMICS " Earthquake Engineering of the University of Roorkee, Roorkee is a record of student's own work carried out by him under our supervision and guidance. The matter embodied in this thesis has not been submitted for the award of any other degree or diploma.

This is further to certify that he has worked for a period of 7 months from March 1972 to September 1972 for preparing this thesis for Master of Engineering Degree at this University.

S. S. Saini.

Dr. S. S. Saini.
Reader in Civil Engg.
W. R. D. T. C.
At University of Roorkee
ROORKEE.

Dr. A. R. Chandrasekaran
Professor of Structural Dynamics
S.R.T.E.E., University of Roorkee
ROORKEE, U. P., INDIA

ACKNOWLEDGEMENT

The author wishes to express his deep sense of gratitude towards Dr.A.R.Chandrasekaran, Professor of Structural Dynamics, Department of Earthquake Engineering, University of Roorkee for his invaluable guidance and encouragement, without which this thesis would have not been satisfactorily completed.

The author is extremely grateful to Dr.S.S.Saini, Reader in Water Resources Development and Training Centre, University of Roorkee, for his valuable advice when he was in the Department of Earthquake Engineering, University of Roorkee.

Thanks are due to staff members of Computer Centre, S.E.R.C., Roorkee and Delhi, School of Economics, Delhi University for providing facilities in the use of IBM 1620 and IBM 360/44 computer.

S Y N O P S I S

The behaviour of cylindrical arch dams, has been studied under static and dynamic type of loads. Different geometrical parameters have been varied. In addition, an actual profile of a dam in a non-symmetrical valley has also been analysed. In all cases deflections and stresses have been worked out. Finite element technique has been used in the analysis. In the static analysis hydrostatic and dead load have been considered. Earthquake forces have been represented equivalent static lateral loads having three different distribution along the height namely, (i) Rectangular, (ii) Inverted triangular, and (iii) Inverted parabolic. The fundamental frequencies and corresponding mode shapes have been calculated for the two cases.

CHAPTER 1

INTRODUCTION

Considerable change has occurred in the design of arch dams in recent years. The trend now is toward higher and thinner arch dams, more complex shapes, and adoption to more difficult site circumstances.

Most recently designed dams are doubly curved, that is, curved in both the vertical and horizontal planes. By carefully proportioning arch thickness along with proper shaping, efficient structural properties, and economy may be achieved. A number of comprehensive methods for the analysis of arch dams are available. These include structural models, trial-load method, shell theory, finite element method, dynamic relaxation, energy method, etc. A brief review of all these methods have been given in Chapter 2 and their comparison and suitability to adopt for a particular site has been discussed. It is found that finite element method is a generalized method of structural analysis and can take into account any form of geometrical shape, thickness variation and boundary conditions and hence adopted in the present analysis.

In the present analysis, the dam profile has been assumed to be the assemblage of flat rectangular elements. Chapter 2 gives the details of the procedure adopted.

Because of the time and expense required to analyse arch dams in the past usually only a single

combination of loads was considered namely, self weight normal full reservoir water, and minimum concrete temperature. The use of computers has made possible the investigation of various other combinations of loads which may occur at any particular site. For example, many reservoirs operate at a low level during late summer or fall. At this time maximum concrete temp. may occur. This combination of load often produces high tensile stresses on the intrados of the arch along the abutments. The possibility of resonance occurring in a dam as a result of earthquakes has generally been ignored until recently. Methods have been devised to estimate the natural frequency of a dam, and if resonance is a possibility, to compute its effect on the structure.

All of these loading conditions and the capability to analyze their effects on an arch dam have a direct relationship to the safe, and efficient design of such structures.

One of the more recent trend in arch dam design is to adopt these structures to wider, the non-symmetrical sites. The ideal configuration for an arch dam site is a narrow V-shape. As sites become wider a greater proportion of the applied load is carried vertically to the foundation in the central part of the dam. To overcome this tendency and to keep stresses within allowable limits, the arches must be thickened or shaped to improve their

load carrying ability. Increased vertical curvature also assists in keeping the dam relatively thin and controlling a tendency for tensile stresses along the abutment extrados.

Non-symmetrical sites present a particularly difficult problem for designers. There is a strong tendency in such sites for the load to go to the steepest abutment. The dam must therefore be proportioned so that the load will be uniformly distributed throughout the structure.

Six cases of cylindrical arch dams with different parameters have been considered to evaluate deflections and stresses. Deflections and stresses have been calculated for hydrostatic and dead loads. Earthquake forces has been replaced by equivalent static load. Three types of load variations along the height of the dam has been considered keeping the free cantilever base moment the same and type of load distribution which will give worst results has been discussed. Lastly, the static and dynamic stresses have been combined for different cases and the total stress distribution curves have been drawn for some typical cases. Finite element method has also been used to determine the fundamental frequency and corresponding mode shape for some typical cases.

Because of the inherent safety and outstanding

aesthetic qualities of arch dams, prospects for the future design and construction of these structures are unlimited. Continued and increased emphasis on foundation investigations is essential. Arch dams may be built in wider and more difficult sites.

After studying the behaviour of cylindrical arch dams in symmetrical as well as non-symmetrical valley with different geometrical parameters we conclude that for economical and safe design V-shaped valley should De preferred but it will be economical to construct an arch dams in other shapesof valleys also as compared to gravity dams. Central angle of dam should lie between 95° to 110° and an increase in thickness vertically as well as horizontally gives an economical design. The weight of an arch dam is small in comparison to gravity dam. Therefore the inertia forces are also small and consequently the stresses due to earthquake load is very small as compared to the stresses due to static loads particularly in moderate earthquake zones.

CHAPTER 2

REVIEW OF THE METHODS OF ARCH DAM ANALYSIS

The use of the arch dam form for dam design has increased considerably in recent times, about 500 of this type having been constructed in the last 25 years,[8] The first interim report on research into the Design of Arch Dams was published in September 1963. A wide variety of methods are available for the analysis of dams of simple geometrical form. New methods were continually being tried out. These would need to be applied to the curved and doubly curved dams before being recommended for general use.

There are several techniques available for analysis as given in second interim report[18]. The methods, both analytical and model techniques, will undoubtedly have a much broader application in fields other than arch dam design.

In any discussion of a proposed method for the analysis of a structure it is always very important to investigate the basic assumptions made. These assumptions may be of a more or less mathematical nature but nevertheless they will also have a physical interpretation. It is by the examination of the basic assumptions that the similarities and divergencies of different methods of analysis can be found.

Some of the following methods have been described briefly and comparison of proposed methods has been given considering various factors and suitability of methods.

1. The three dimensional solution,
2. Trial load method,
3. Complete adjustment method,
4. Method of Energy,
5. Shell Theory,
6. Finite Difference Approach,
7. Finite Element Method.

Three dimensional solution of arch dams

The relaxation process[3] for the stress analysis of arch dam was used in 1956. This process enables mathematical equations to be solved numerically to any desired degree of accuracy. The exact elastic equations for the dam were formulated in terms of displacements instead of the more usual stress functions, and were solved by relaxation. Calculations were made of the stresses due to gravity loads and water pressure acting separately and also of those due to variations in temperature.

A cylindrical-polar system of co-ordinates, r,z, and θ, was adopted and the displacements of any point denoted by u(radial), v(vertical) and w(tangential), each taken positive in the corresponding positive direction of the coordinates r,z, and θ respectively.

At any point the six components of stress can be expressed in terms of the three displacements by the relation (1) given in Appendix A. Thus, once the displacements have been determined, values of the stress components may be deduced directly from them.

The displacements themselves are found by solving the three governing differential equations (2) which result from substitution of the expression (1) for the stresses into the equations of equilibrium for the point. These equations have to be solved, subject to stated boundary conditions to determine the values of u,v, and w throughout dam and the adjoining rock-foundation.

2. TRIAL LOAD METHOD[9]

The trial load method considers the agreement between radial (horizontal) and tangential displacements and rotations of the vertical axis of the arches and cantilevers but ignores the vertical displacements and the rotations of horizontal axis. Conditions of equilibrium are taken into account only for radial, tangential, and vertical twist loads and for certain internal forces since not all of these forces are considered. This method considers, on the arches, radial, tangential, and twist triangular unit loads not related to the position of cantilevers. Thus, the conditions set at each intersection of elements are only approximate. The final value of such loads was determined by trial until equal deformations were obtained.

3. COMPLETE ADJUSTMENT METHOD[13]

The complete adjustment method is based on the principles used in the theory of shells, i.e., the conditions of equilibrium of an element (voussoir)limited by two verticals and two horizontal planes and the conditions of compatibility of deformations (displacements and rotations) undergone by that element. In those planes the voussoir is acted upon by 10 internal forces in its faces and mass by external loads. The equations of equilibrium being six, four conditions of compatibility will be necessary to find the internal loads. Since shearing and twist forces are not independent, the internal forces can be reduced to eight and the equations of equilibrium to five, only three equations of compatibility being necessary.

In the arches or cantilevers considered, the forces in the horizontal and vertical forces are assimilated to external loads. The integration of the equations of equilibrium and compatibility is made by simply considering certain unit loads on the voussoirs of intersection which produce certain deformations of the arches or cantilevers. The total internal loads are determined by a system of equations involving all those voussoirs of intersection. This method makes the method completely exact, allowing a correct determination of all the principal stresses in the dam. When the curvature of the dam is different at each level, the cantilevers are

twisted elements generated by two horizontal (radial) segments perpendicular to the level lines upstream and at a unit distance at the upstream face. For double curvature shells, arches and cantilevers could be taken as the same type of twisted elements normal to the upstream face. The arches could be a half element from each abutment to the crown. For the analysis of displacement and deformations, effect of twist and shear, equations of equilibrium and conditions of compatibility, and analysis of arches and cantilevers, reference[13] may be consulted.

4. METHOD OF ENERGY[17]

This method is based on by minimizing the functional representing the internal energy of strain diminished by the work done by the external forces. Adopt cylindrical coordinates. The strains in a plane situated at a distance z from the middle surface are then given by the relations

$$\epsilon^{xz} = \frac{\partial u}{\partial x} - z\,\frac{\partial^2 w}{\partial x^2}$$

$$\epsilon^{yz} = \frac{R}{R+Z}\left[\frac{dv}{dy} + \frac{w}{R} + z\,\frac{\partial}{\partial y}\left(\frac{v}{R} - \frac{dw}{dy}\right)\right]$$

$$r^{z} = \frac{\partial v}{\partial x} + z\left(\frac{1}{R}\,\frac{\partial v}{\partial x} - \frac{\partial^2 w}{\partial x\,\partial y}\right) + \frac{R}{R+Z}\left(\frac{\partial v}{\partial y} - z\,\frac{\partial^2 w}{\partial x\,\partial y}\right)$$

where R = radius of middle surface.

For a plane condition of stress, the strain energy per unit volume E_v at a distance Z from the middle surface is given by:

$$E_v = \frac{E}{2(1-\mu^2)}\left[(\epsilon^{xz}+\epsilon^{yz})^2+2(1-\mu)(\tfrac{1}{4}\gamma^{z^2}-\epsilon^{xz}\epsilon^{yz})\right]$$

where E is the modulus of elasticity and μ the poisson's ratio for the dam.

The energy per unit surface area of the middle surface E_s is then given by

$$\int_{-h}^{+h} E_v(R+\frac{h}{R})dh$$

where h is the half thickness of the shell and $R+\frac{h}{R}$ represents the variation of the length of the fibres with Z. Substituting the expressions for the strains and making the approximation that $(1+\frac{Z}{R})^{-1} = 1 - \frac{Z}{R}$, we get

$$E_s = \frac{Eh}{1-\mu^2}\left[\left(\frac{\partial u}{\partial x}\right)^2+\left(\frac{\partial v}{\partial y}+\frac{w}{R}\right)^2+\frac{1}{2}(1-\mu)\left(\frac{\partial u}{\partial y}+\frac{\partial v}{\partial x}\right)+2\mu\,\frac{\partial u}{\partial x}\left(\frac{\partial v}{\partial y}+\frac{w}{R}\right)\right]$$

$$+\frac{Eh^3}{3(1-\mu^2)}\left[\left(\frac{\partial^2 w}{\partial x^2}\right)^2+\left(\frac{\partial^2 w}{\partial y^2}\right)^2+2(1-\mu)\left(\frac{\partial^2 w}{\partial x\,\partial y}\right)^2\right.$$

$$-\frac{2u}{R}\,\frac{\partial v}{\partial y}\,\frac{\partial^2 w}{\partial x^2}+2\mu\,\frac{\partial^2 w}{\partial x^2}\cdot\frac{\partial^2 w}{\partial y^2}-\frac{2}{R}\cdot\frac{\partial u}{\partial x}\cdot\frac{\partial^2 w}{\partial x^2}$$

$$+\frac{1-\mu}{R}\,\frac{\partial u}{\partial y}\,\frac{\partial^2 w}{\partial x\,\partial y}-\frac{3(1-\mu)}{R}\,\frac{\partial v}{\partial x}\cdot\frac{\partial^2 w}{\partial x\,\partial y}$$

$$\left.+\frac{3(1-\mu)}{2R^2}\left(\frac{\partial v}{\partial x}\right)^2-\frac{1}{R^2}\left(\frac{\partial v}{\partial y}\right)^2-\frac{2w}{R^3}\,\frac{\partial v}{\partial y}+\frac{2w}{R^2}\cdot\frac{\partial^2 w}{\partial y^2}\right]$$

Work done by the external forces

The external forces acting on the dam can be resolved along the three directions of the axes. Supposing

the three components at any point x,y to be X,Y,Z the work done can be written as Xu+Yv+Zw, since the contribution of X,Y,Z themselves to the displacement u,v,w is very small.

FUNCTIONAL AND ITS EQUIVALENT EXPRESSION AS A SUM

The functional to be minimized thus becomes $\int\int_S E_s \, dxdy - \int\int_S (Xu+Yv+Zw)dxdy$, the integration being done on the entire middle surface of the dam.

We find that the expression for E_s contains w and its second derivatives while the derivatives of u,v are of the first order only. This suggested the use of separate networks for u,v,w, the nodes for v being placed in the middle of the nodes for w in the x-direction. Now we define small surface areas with respect to the networks. Two types of such unit areas are needed-Type A, having a w node at its centre, the v node at the middle of the two sides y = constant and the u nodes on the middle of the sides x = constant - Type B, having the w nodes at the four corners, the v nodes at the middle of the sides x = constant and the u nodes at the middle of the sides y = constant (fig.1).

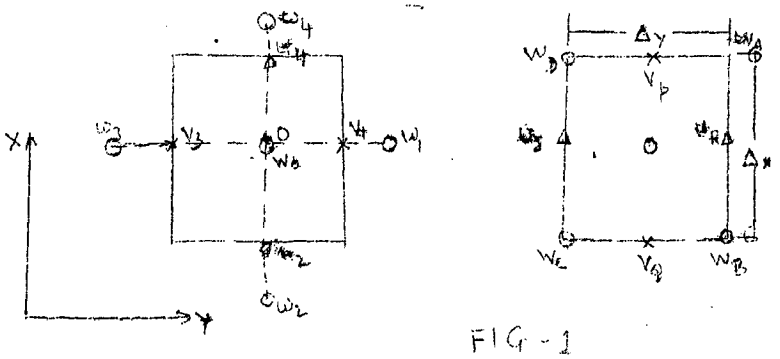

FIG - 1

unit area type A

$$\frac{\partial v}{\partial y} = \frac{v_1 - v_3}{\Delta_y}$$

$$\frac{\partial u}{\partial x} = \frac{u_4 - u_2}{\Delta_x}$$

$$\frac{\partial^2 w}{\partial x^2} = \frac{w_4 + w_2 - 2w_o}{\Delta_x^2}$$

$$\frac{\partial^2 w}{\partial y^2} = \frac{w_1 + w_3 - 2w_o}{\Delta_x^2}$$

unit area type B

$$\frac{\partial v}{\partial x} = \frac{v_p - v_Q}{4x}$$

$$\frac{\partial u}{\partial y} = \frac{u_R - u_S}{\Delta_y}$$

at O $$\frac{\partial^2 w}{\partial x \partial y} = \frac{W_A - W_B + W_C - W_D}{\Delta_x \Delta_y}$$

} At O

Type A is used for expressing the terms in E_s given by E_{SA}, where

$$E_{SA} = \frac{Eh}{1-\mu^2}\left[\left(\frac{\partial u}{\partial x}\right)^2 + \left(\frac{\partial v}{\partial y} + \frac{w}{R}\right)^2 + 2\mu \frac{\partial u}{\partial x}\left(\frac{\partial v}{\partial y} + \frac{w}{R}\right)\right] + \frac{Eh^3}{3(1-\mu^2)}\left[\left(\frac{\partial^2 w}{\partial x^2}\right)^2 + \left(\frac{\partial^2 w}{\partial y^2}\right) - \frac{2\mu}{R}\frac{\partial v}{\partial y}\cdot\frac{\partial^2 w}{\partial x^2} + 2\mu \frac{\partial^2 w}{\partial x^2}\cdot\frac{\partial^2 w}{\partial y^2} - \frac{2}{R}\frac{\partial u}{\partial x}\cdot\frac{\partial^2 w}{\partial x^2} - \frac{1}{R^2}\left(\frac{\partial v}{\partial y}\right)^2 - \frac{2w}{R^3}\left(\frac{\partial v}{\partial y}\right) + \frac{2w}{R^2}\cdot\frac{\partial^2 w}{\partial y^2}\right]$$

while the type B is used for expressing the remaining terms given by E_{SB}, where

$$E_{SB} = \frac{Eh}{1-\mu^2}\cdot\frac{1}{2}(1-\mu)\left(\frac{\partial u}{\partial y}+\frac{\partial v}{\partial x}\right)^2+\frac{Eh^3}{3(1-\mu^2)}\left[2(1-\mu)\left(\frac{\partial^2 w}{\partial x\partial y}\right)^2\right.$$

$$\left.+\frac{1-\mu}{R}\cdot\frac{\partial u}{\partial y}\cdot\frac{\partial^2 w}{\partial x\partial y}-\frac{3(1-\mu)}{R}\cdot\frac{\partial v}{\partial x}\cdot\frac{\partial^2 w}{\partial x\partial y}+\frac{3(1-\mu)}{2R^2}\left(\frac{\partial v}{\partial x}\right)^2\right]$$

It is supposed that the average energy in the unit surface area is given by the energy at its centre, where the derivatives are calculated in the finite difference form. The E_s so calculated, when multiplied by the area of the unit surface gives the contribution to the integral from the unit area. The sum total of the products of E_s with the areas, so obtained, gives the equivalent of the first part of the functional:

$$\iint_s E_s dxdy = \sum_{\substack{\text{all unit}\\ \text{areas of A}}} E_{SA}\Delta x\Delta y + \sum_{\substack{\text{all unit}\\ \text{areas of B}}} E_{SB}\,\Delta x\Delta y = S_1$$

The equivalent sum has the squares of the displacements u,v,w or the products of two displacements, the coefficients of the terms depending upon the values of E,μ, h, R, Δx and Δy.

Similarly, three different unit areas will be needed to express the work done by the external forces, these having respectively the nodes u,v,w at their centres and denoted by type D, type C, and type A, giving the equivalent relation:

$$\iint_s (Xu+Yv+Zw)dxdy = \sum_{\substack{\text{all unit}\\ \text{areas of D}}} Xu\Delta x\Delta y + \sum_{\substack{\text{all unit}\\ \text{areas of C}}} Yv\Delta x\Delta y$$

$$+ \sum_{\substack{\text{all unit}\\ \text{areas of A}}} Zw\,\Delta x\Delta y = S_2$$

Displacements and Stresses

The functional, modified by the elimination of some displacements by the use of boundary conditions, can now be differentiated with respect to each reamining displacement, thus obtaining the required number of linear simultaneous equations. The differentiation of S_1 gives the matrix while that of S_2 gives the second term. The matrix so obtained is symmetrical. Once the displacements are known the stresses can be calculated.

5. SHELL-THEORY[17]

Theory of shells for constant angle arch dams is given in Appendix B. There is no doubt that the most precise and comprehensive theory of thin arch dams can be created on the basis of the shell theory. But for thicker structures, shell theory may not present the reliable results. For such structures the moment theory of shells is to be used. However, in order to apply such a theory successfully to thicker structures of shell dams it is necessary for the equilibrium conditions of the differential element of the arch-dam-shell to include also the transverse forces with their components in directions both normal and tangential to the shell. Accordingto Lombardi, there is very good ground for applying the shell theory to arch dams which have a ratio of wall thickness to radius $d/r \leqslant 0.2$.

This method is deduced by starting from the complete system of differential equations of the moment theory

The sum, so obtained, has the displacements multiplied by coefficients depending upon the values of X, Y, Z and Δx and Δy.

We are thus able to replace the integralsby two sums, one S_1 having the second power of the displacements, and the other S_2 having the first power only. If the three displacements are taken at the same node and the derivatives found in the usual way, using one unit area only, the resulting matrix is not unique, for certain forms of the boundary.

Boundary Conditions

Boundary conditions at the free edge are automatically satisfied. The conditions at the rock boundary will, in general, correspond to displacements u_r, v_r, w_r and rotations $(\frac{\partial w}{\partial y})_r$ at any point on the boundary. If node concerned to be situated at the boundary, the value of the displacement gets fixed. If the rock boundary passes in between the nodes, the displacements at the two nodes located on the two sides of the rock line can be interrelated with the rock displacements in the following manner,

$$\frac{u_1 y_2 + u_2 y_1}{y_1 + y_2} = u_r, \quad \frac{v_1 y_2 + v_2 y_1}{y_1 + y_2} = v_r ,$$

$$\frac{w_1 y_2 + w_2 y_1}{y_1 + y_2} = w_r \text{ and } \frac{w_2 - w_1}{y_1 + y_2} = (\frac{\partial w}{\partial y})_r$$

of shells as devised by V.Z.Vlassov[21], represented by forces. A typical feature in this respect is that the influence of the transverse forces Q_1 and Q_2 is taken into consideration both in the equilibrium condition expressing the absence of forces in a direction normal to the middle surface, and in the two directions which are tangential to it.

In view of the fact that arch dams are complex shell like structures with varying thickness in both directions, with double curvatures and complex supporting contour, an admissible simplification has been made of the system of differential conditions. This simplification consists in neglecting the influence of the tangential forces,

$$\frac{\partial S}{\partial x} = \frac{\partial S}{\partial y} = 0$$

This makes it possible to reduce the problem to the solution of a single differential equation in partial derivatives for the sole unknown function of the radial displacement $w = w(x,y)$.

The analysis made of the differential equation demonstrates that it consists of two basic group of terms. Some of them are not connected with the curvature of the shell together with the load term of the right side of the equation. The other group of terms are connected to the curvatures of the shell and express the

effect of the supporting action of an imaginary elastically yielding foundation. The strongest supporting effect so called Winkler's supporting effect which is proportionate to the radial displacement of the imaginary plate w = w(x,y).

6. FINITE DIFFERENCE APPROACH[17]

In the finite difference approach the differential equation defining the unknowns in some system of simple coordinates is established. Once this equation (or equations) are known they are expressed in terms of a finite number of the unknown values at fairly closely spaced points of the co-ordinate network. Similar treatment expresses the boundary conditions in terms of a discrete number of values of the unknown functions. Having thus reduced the continuum problem to the solution of a finite system of simultaneous, linear, equations, solution of this system is obtained by manual (relaxation) methods or by use of the digital computers.

7. FINITE ELEMENT METHOD (Static Analysis)[8,17]

STIFFNESS MATRIX

There are two different approaches to develop a finite element method for general shell structures. In the first approach, the shell is replaced by an assemblage of flat plate elements which are either triangular or quadrilateral in shape. Each plate element

is connected in some fashion to those surrounding it and undergoes both bending and stretching deformations. The second approach is to develop curved shell element that permits exact geometrical representatives of a structure.

FLAT ELEMENT

Robert J. Melosh[14] developed a stiffness matrix for a thin flat-plate triangular element, capable of stretching, bending, shearing, and twisting. The implied deformation state insures that the matrix will yield monotonic convergence of strain energy predictions with gridwork refinement and lower bounds on strain energy. Its successful application to pure bending and pure shearing cases indicates that it is useful in predicting structural behaviour moderately thick plates, i.e. those in which shear deformations may be important but the normal stress unimportant.

O.C. Zienkiewicz and Y.K. Cheung[22] derived a stiffness matrix for a rectangular element. The derivation is more general and can be easily extended to cover any type of elastic behaviour.

The guiding principle is to assume a displacement system throughout the element, which while satisfying equilibrium conditions at all points can be determined uniquely in terms of nodal displacements. Once this displacement system is known it is possible to relate equivalent nodal forces to the nodal displacements

The shell geometry is limited only by the conditions that the surface equations be given in the parametric form. G.Bonnes, G.Dhatt, Y.M. Giroux, and L.P.A.Robichaud[4] derived the curved triangular element for the analysis of doubly curved shell. Gordon E. Strickland, Jr.William A.Laden[19] derived the stiffness matrix for doubly-curved triangular shell element, suitable for the analysis of general non-symmetric shells.

S.Ahmad, B.M. Irons and O.C.Zienkiewicz[1,2] degenerated a general curved isoparametric thick shell element of arbitrary shape. By introducing only some of the usual Navier assumptions, these new shell elements can include shear as well as bending deformations.

The analysis of an arch dam by the finite element method involves the following steps.

(a) The actual dam is considered to be replaced by an equivalent structure made up of a number of elements, of finite size, connected together in such a way that the continuity in the actual structure is preserved to an extent which depends upon the kind of assumptions made in the finite element procedure.

(b) The load-deformation characteristics of each element are found. This is usually in terms of a stiffness matrix for the element referred to coordinates local to that element.

simply by application of the virtual work principle.

CURVED ELEMENTS

The first attempt to develop the curved thin shell element was made by Bogner, Fox and Schmit[5]. Gallagher[10], in his Ph.D. thesis, reports on a (24x24) stiffness matrix constructed by the standard "assumed displacement" method. Mervyn D., Olson and Garry M. Lindberg[15] made an attempt to develop the simplest possible non-conforming representation for a cylindrical shell element. The radial displacement component w is assumed to be a twelve term polynomial in x and y, the longitudinal and circumferential coordinates of the element, respectively. The in-plane displacement components u and v are each assumed in polynomial form upto linear terms in x and cubic terms in y. The expressions for u,v and w are then substituted into the strain energy and kinetic energy integrals from shell theory yielding 28x28 stiffness matrix for cylindrical shell element.

Connor and Brebbia[7] developed the stiffness matrix for a doubly curved thin rectangular finite element. Tahbildar, U.C.[20] had used the same element in his Ph.D. thesis for the static and dynamic analysis of arch dams. B.E. Greene, R.E. Jones, R.W. Mclay and D.R. Strome[11] developed the stiffness and mass matrices for shell elements on a doubly curved surface.

(c) The stiffness matrices referred to local coordinate system are all transformed to relate to a common, global, coordinate system. The individual stiffness matrices may then be added together to form the stiffness matrix for the whole structure.

(d) Load vectors are obtained for each element for water, gravity and temperature loading referred to local coordinates. These are then transformed to the global coordinates and added together to form the load vectors for the whole structure.

(e) From the structure stiffness matrix and the load vectors, the global displacement components at each node are obtained. Stresses, either local or global can then be computed.

2. Referring to the first of the above steps, we have to choose the shape and size of the element, i.e. triangular, rectangular etc. For cylindrical shell structures, the rectangular shape will obviously be preferable.

3. The determination of the stiffness matrix of an element always requires that some assumption shall be made about its behaviour, and from this assumption else follows. The displacement function throughout the

element is assumed to be simple polynomial functions of the coordinate with, in addition, certain assumptions about the way in which each element behaves on its boundary. Bending and in-plane actions are assumed not to be coupled, so that a bending stiffness matrix and an in-plane stiffness matrix are obtained for each element.

4. The nodal forces and nodal displacements, the relationship between which constitutes the stiffness matrix referred to above, are initially described with reference to a set of Cartesian axes, which are peculiar to a single element. Before the forces at a node can be added together, so that together with the external load they can be forced to satisfy equilibrium, it is necessary to resolve them into common directions. This is the process known as transformation to global coordinates.

5. In obtaining load vectors it is advantageous to employ the principle of virtual work to obtain such vectors in a manner consistent with the formation of the stiffness matrix. Crude lumping of load on to nodal coordinates results unavoidable error. Because the load vector and the inertia matrix, which is required for the dynamic analysis, are obtained in a similar way.

6. The addition of stiffness matrices, the imposition of boundary conditions, and the solution of the equations

of the equilibrium is a computational matter.

DYNAMIC ANALYSIS[8]

Restricting attention to the elastic range, the complete evaluation of the effect of an earthquake on a structure can be divided into three parts,

(a) The determination of the stiffness and mass (inertia) properties of the structure,

(b) The calculation of the natural frequencies and mode shapes of the structure.

(c) The evaluation of the response of the structure to a given earthquake ground acceleration. That is, the calculation of the time-dependent displacements and stresses. This requires knowledge of the damping present in the structure.

By employing the finite element method the infinity of degrees of freedom of the arch dam is reduced to n, where n is finite, and each degree of freedom has associated with it a displacement component q_i $(i=1,\ldots,n)$. The vector q then represents the ordered array of nodal displacements, and the simultaneous differential equations of motion can be written in matrix form as

$$M\ddot{q} + C\dot{q} + Kq = -Hq+J$$

where M,C,K and H are referred to as the mass, damping, stiffness and hydrodynamic, or added mass, matrices, respectively, and J is a forcing function. The first three matrices are properties of the dam itself whereas

H is connected with the water in the reservoir. It is assumed that the effect of this water is dependent only upon the accelerations $\ddot{q}$ of the dam.

Stiffness, Load and Mass Matrices

Stiffness and load matrices are obtained as described in the static case. The reason why load matrices are considered here is that the mass matrix is associated with the dynamic load matrix, and, as will be seen, the derivation of this follows from the static load matrix.

In the finite element method, externally applied load can only be associated with the nodal displacement components and these nodal loads must be so assigned that during any virtual displacement the work done by them is equal to the corresponding work done by the actual distributed loading.

Now consider the vibrating rectangular element. The mass is distributed over the accelerating element and the total inertia force is equal to this mass multplied by the acceleration, integrated over the area of the element. This inertia load can only be associated with accelerations of the nodal displacements. The problem is to find the masses to be associated with the nodal accelerations, and this can be solved by noting that the shape function of the acceleration will be the same as the shape function for displacement if vibration in normal modes is assumed. Thus, if the coordinate j is

given. Unit acceleration the inertia load function will be $m(x,y)Y_j(x,y)$, where $m(x,y)$ is the mass per unit area and $Y_j(x,y)$ is the shape function associated with coordinate j. By the principle of virtual work it is now possible to write

$$m_{ji} = \iint m(x,y)Y_j(x,y)Y_i(x,y)\, dA$$

and m_{ji} represents the inertia force acting at coordinate i associated with a unit acceleration of coordinate j. It will be seen that the mass matrix is square, and it is also symmetric.

If the effect of the reservoir water on the dynamic behaviour of an arch dam is thought of as an added mass vibrating with the dam, the equation of motion are given by eqn.(1) and the added mass, or hydrodynamic, matrix can be found in some cases by calculation but more satisfactorily, by an electric potential analogue experiment. The effect of the reservoir water will be to reduce the natural frequencies of the dam as compared with the reservoir empty values.

COMPARISON OF DIFFERENT METHODS AND THEIR SUITABILITY

In the solution of three-dimensional equations of elasticity, the finite difference formulation presented has some disadvantages. Quite large errors apparently develop with low order differences, and higher order differences necessitating rather complex formulation, are required to improve the solution. Also the boundary

equations are complicated whenever the finite difference expressions for higher order differences are lacking in physical significance. The amount of computational work involved in a finite difference solution makes it unsuitable for preliminary design purposes.

This method considers the agreement between radial (horizontal) and tangential displacements and rotations of the vertical axis of the arches and cantilevers but ignores the very important vertical displacements and the rotations of the horizontal axis. The three adjustments radial, tangential and twist are necessary which is a very laborious task and involves enormous calculations. Similarly in complete adjustment method, it requires even larger calculations and consumes a large amount of time. In trial load method, when the dams are thin and have a pronounced downstream overhang the vertical displacements become very important not only because of the influence of the Poisson's ratio but especially because of the effect of the vertical component of the hydrostatic pressure.

The energy formulation has the main merit in reducing the number of independent parameters, required to solve an elasticity problem if, for example, suitable distribution functions are assumed. If the parameters are the displacements at discrete points and if further more a finite difference formulation is used in evaluation

of stresses the requirement of minimum total energy will reduce precisely to standard equilibrium equations of an element. As such, therefore, the approach is identical to that used in other finite difference representations. The finite difference method is unsuitable for preliminary design purposes as it involves large amount computational work. If the thickness and radius of cylindrical arch dam varies from point to point the governing partial differential equations become quite complex. For a doubly curved shell or a dam with variable radius the difficulties for formulation of equations and of the choice of a suitable coordinate system immediately arises.

The application of shell theory to arch dams is difficult due to its irregular shape of the structure and difficult boundary conditions. The complexities involved are due to irregular shape of shell caused not only by variable radii of curvature in the horizontal and vertical directions and the variable thickness of the shell, but also by the foundation abutment profile comprising a spatial curved line and the foundations which are of irregular elastic nature. The solution of the partial differential equations is complicated and tedious because of complex boundary conditions. Therefore simplifying assumptions are made to make the analytical and numerical solution possible, in order to apply the shell theory successfully

to arch dams it is necessary that the thickness of the dam is relatively thin. This is true very often with regard to the upper and middle sections of the dam, but for the lower portions of the dam this is not always the case.

In finite element method a structure is divided in several elements and these elements are assumed to be connected at their junctions called nodal points. Compatibility and equilibrium conditions are established at these points. This is a generalized method of structural analysis and can take into account any form of geometrical shape, thickness variation and boundary conditions.

Keeping in view of above methods and their limitations, finite element method is considered suitable and adopted here for the analysis of the arch dam.

CHAPTER 3

METHOD OF ANALYSIS AND DESCRIPTION OF DATA

In the present work the behaviour of cylindrical arch dam with different geometrical parameters have been studied. In addition to this, an actual profile of an arch dam has been analysed. In the analysis finite element method has been used considering the dam as an assemblage of flat finite elements. Provided the arch is sufficiently thin it is reasonable to assume that initially plane sections across the thickness remain plane after loading and that the stresses correspond to this restriction.

The complete analysis of structure by finite element method involves three separate phases.

1) Structural idealization,

2) Element properties,

3) Analysis of complete structure.

The selection of the finite element system for a particular problem is completely arbitrary. Therefore structures with practically any shape boundaries may be considered. Here for cylindrical arch dams, rectangular element is obviously convenient and therefore considered in the analysis.

The evaluation of various element properties is

the most critical phase of analysis and is described below. The stiffness matrix of a typical element is generated in local coordinate system. The stiffness matrix of the whole structure is obtained by transforming the local coordinate system of an element into global coordinate system and superimposing the stiffnesses of various elements connected at various nodes. Now the algebraic equations can be formed in terms of applied load at various nodes, stiffness matrix and unknown displacements. By applying the boundary conditions and solving the equations, the unknown nodal displacements can be obtained.

STIFFNESS OF A TYPICAL ELEMENT

The surface of the dam is assumed to be divided into small rectangular elements connected to each other and carrying load at their corner points. Continuity between the elements is established by finding at each node six generalised displacement components (three linear displacements and three rotations) such that equilibrium at each node is satisfied.

Each element is subject to 'inplane' or membrane stresses and to transverse bending and it is convenient to establish the characteristic stiffness separately in the phases. Only when combining the elements it will be necessary to convert the directions of forces

and displacements to some common coordinate system.

In-plane Stiffness of an Element

A displacement system is assumed throughout the element which, while satisfying equilibrium conditions at all points, can be determined uniquely in terms of the nodal displacements. Once this displacement system is known it is possible to relate equivalent nodal forces to the nodal displacements simply by application of the virtual work principle.

In the plane of the element only two displacements need to be considered. Let these be u_1 and u_2 in the directions of the coordinate axes x_1 and x_2 as shown in Fig. 20 and be defined by the following polynomials.

$$\left.\begin{aligned} u_1 &= A_1+A_2x_1+A_3x_2+A_4x_1x_2+A_5x_2^2 \\ u_2 &= A_6+A_7x_1+A_8x_2+A_9x_1x_2+A_{10}x_1^2 \end{aligned}\right] \quad \ldots(1)$$

The stresses at any point are defined by elastic relations in terms of strains as

$$\begin{Bmatrix} \sigma_{x_1} \\ \sigma_{x_2} \\ \sigma_{x_1x_2} \end{Bmatrix} = D \begin{Bmatrix} \partial u_1/\partial x_1 \\ \partial u_2/\partial x_2 \\ \partial u_1/\partial x_2+\partial u_2/\partial x_1 \end{Bmatrix} \quad \ldots (2)$$

or in matrix notation simply,

$$\sigma = D\psi$$

where ψ is the strain vector. The matrix $|D|$ takes a

simple form of

$$D = \frac{E}{1-\nu^2}\begin{bmatrix} 1 & \nu & 0 \\ \nu & 1 & 0 \\ 0 & 0 & (1-\nu)/2 \end{bmatrix}$$

in which E is the elastic modulus and ν is the Poisson's ratio. It is applicable for isotropic material.

For anisotropic materials if two dimensional analysis is to be applicable a symmetry of properties must exist, implying at most six independent constants in the $|D|$ matrix. Thus it is always possible to write

$$|D| = \begin{bmatrix} d_{11} & d_{12} & d_{13} \\ & d_{22} & d_{23} \\ (\text{sym}) & & d_{33} \end{bmatrix} \qquad \ldots (4)$$

In a two directional plane behaviour, the well-known equilibrium equations are satisfied given in the absence of body forces, by

$$\left.\begin{aligned} \frac{\partial \sigma_{x1}}{\partial x_1} + \frac{\partial \sigma_{x1x2}}{\partial x_2} &= 0 \\ \frac{\partial \sigma_{x2}}{\partial x_2} + \frac{\partial \sigma_{x1x2}}{\partial x_1} &= 0 \end{aligned}\right\} \qquad \ldots (5)$$

which by substitution of (1) and (2) results in two equations between the constants A.

Substituting now into equation (1) the eight displacements and coordinates of the nodal points it

is possible to evaluate all the constants A in terms of these displacements.

If the nodal displacements are written as a vector

$$u^p = \begin{Bmatrix} u_1^1 \\ u_2^1 \\ u_1^2 \\ u_2^2 \\ u_1^3 \\ u_2^3 \\ u_1^4 \\ u_2^4 \end{Bmatrix}$$

We have for the constants A

$$A = \begin{Bmatrix} A_1 \\ \vdots \\ A_{10} \end{Bmatrix} = C\, u^p \qquad .. (6)$$

From equation (2) it similarly follows that

$$\sigma^p = DBC\, u^p = S^p u^p \qquad .. (7)$$

in which C is a matrix of constant coefficients and B a matrix involving the position coordinates x_1 and x_2.

The matrix s^p is the stress matrix and will enable the stresses to be determined at any point later when the displacements are known. Complete stress matrix is given in Table II.

Let it be assumed now that the only external forces acting on the element are eight statically equivalent forces at the nodes in the directions defined by $\{u\}^p$ and let these forces be labelled $\{F\}^p$. Applying now in turn unit virtual displacements in the appropriate direction we have for the external work done by the forces acting on the element

$$W_e = IF^p \qquad \ldots(8)$$

in which I is the identity matrix.

The internal work corresponding to the same virtual displacement is given by integrating the product of appropriate stresses and strains throughout the element as

$$W_i = \iint \delta\psi^T \sigma^p dx_1 dx_2 \qquad ..(9)$$

in which $\delta\psi$ is the strain system corresponding to nodal displacements I, or by (2) and (6)

$$\delta\psi = BC\{I\} = BC \qquad \ldots(10)$$

Equating these two expressions and substituting (7)

$$IF^p = \iint (BC)^T DBC\{u\}^p \, dx_1 dx_2$$

$$\text{or} \quad F^p = \left[C^T \{B^T DB \, dx_1 dx_2\} C\right] u^p \qquad \ldots (11)$$

The expression in square brackets is the stiffness matrix $|K^p|$ sought and can be evaluated explicitly giving the relation

$$F^p = K^p u^p \qquad \ldots (12)$$

TRANSVERSE BENDING STIFFNESS OF AN ELEMENT

Considering now the behaviour of an element which is subject to the action of transverse forces the usual assumptions of plate theory can be made. As no 'inplane' resultant forces exist the only nodal displacements of interest are a lateral linear movement u_3 in the direction of x_3 and two rotations u_{23} and u_{13} about the directions of x_1 and x_2 axes respectively.

Within the element these three components of displacement are given by a function representing the lateral displacement u_3 as the rotations are simply the derivatives of this with respect to x_1 and x_2.

If u_3 is defined as the following polynomial

$$u_3 = A'_1 + A'_2 x_1 + A'_3 x_2 + \ldots\ldots + A'_{10} x_2^3 + A'_{11} x_1^2 x_2 + A'_{12} x_1 x_2^3 \qquad \ldots (13)$$

The constants A' can be determined uniquely in terms of the twelve nodal displacements.

$$u^B = \begin{Bmatrix} u'_3 \\ u'_{23} \\ \vdots \end{Bmatrix} \qquad \ldots (14)$$

Writing the polynomial in the above form, it has certain advantages. In particular , along any x_1=constant line, the displacement u_3 will vary as a cubic. The

element boundaries or interfaces are composed of such lines. Now a cubic is uniquely defined by four constants. The two end values of slopes and displacement at the ends of the boundaries will therefore define the displacements along this boundary uniquely. As such end values are common to adjacent elements, continuity of u_3 will be imposed all along any interface.

It will be observed that the gradient of u_3 normal to any of the boundaries varies along it in a parabolic way. As on such lines only two values of the normal slopes are defined, the parabola is not specified uniquely and, in general, a discontinuity of normal slope will occur. The function is thus 'non-conforming'.

The constants A_1' to A_{12}' can be evaluated by writing down the twelve simultaneous equations, linking the values of u_3 and its slopes at the nodes when the coordinates take up their appropriate values. For instance,

$$(\theta_{x1})_i = (-\frac{\partial u_3}{\partial x_2})_i \equiv -(A_3'+A_5'x_{1i}+2A_6'x_{2i}+A_8'x_{1i}^2+2A_9'x_{1i}x_{2i} +3A_{10}'x_{2i}^2+A_{11}'x_{1i}^3+3A_{12}'x_{1i}x_{2i}^2)$$

$$(\theta_{x2})_i = (\frac{\partial u_3}{\partial x_1})_i = A_2'+2A_4'x_{1i}+A_5'x_{2i}+3A_7'x_{1i}^2+2A_8'x_{1i}x_{2i} +A_9'x_{2i}^2+3A_{11}'x_{1i}^2x_{2i}+A_{12}'x_{2i}^3$$

$$u_{3i} = A_1'+A_2'x_{1i}+A_3'x_{2i}+A_4'x_{1i}^2+A_5'x_{1i}x_{2i}+A_6'x_{2i}^2+A_7'x_{1i}^3 +A_8'x_{1i}^3x_{2i}+A_9'x_{1i}x_{2i}^2+A_{10}'x_{2i}^3 +A_{11}'x_{1i}^3x_{2i}+A_{12}'x_{1i}x_{2i}^3.$$

Listing all twelve equations we can write, in matrix form

$$\{u\}^B = |C|\{A'\} \qquad \ldots (16)$$

where $|C|$ is a 12x12 matrix depending on nodal coordinates and $\{A'\}$ a vector of the twelve unknown constants. Inverting

$$\{A'\} = |C|^{-1}\{u\}^B \qquad \ldots (17)$$

The curvature and twist at any point of the plate can now be determined in terms of the constants, and therefore

$$\psi = \begin{bmatrix} -\dfrac{\partial^2 u_3}{\partial x_1^2} \\ -\dfrac{\partial^2 u_3}{\partial x_2^2} \\ 2\dfrac{\partial^2 u_3}{\partial x_1 \partial x_2} \end{bmatrix} = BA' = B\,C^{-1}u^B \qquad \ldots (18)$$

The internal moments are related to the curvatures by known expressions from the theory of plates. For orthotropic materials this relationship is determined in terms of four constants

$$\left.\begin{aligned} M_{x1} &= -\left(D_{x1}\frac{\partial^2 u_3}{\partial x_1^2} + D_1\frac{\partial^2 u_3}{\partial x_2^2}\right) \\ M_{x2} &= -\left(D_{x2}\frac{\partial^2 u_3}{\partial x_2^2} + D_1\frac{\partial^2 u_3}{\partial x_1^2}\right) \\ M_{x_1x_2} &= 2D_{x_1x_2}\frac{\partial^2 u_3}{\partial x_1 \partial x_2} \end{aligned}\right| \qquad \ldots (19)$$

or simply $M = D\psi$ ... (20)

where D stands for the appropriate matrix of coefficients.

At this stage it is possible to establish the equivalent values of the nodal forces. By the principle of virtual work, if these forces are statically compatible with the internal forces (M), then, during any virtual displacement, the external work done must be equal to the internal work. In particular, if the displacement is such that it is unity in the direction of a selected external force and zero in the direction of all other forces, the internal work will be the same as the value of this selected force. Taking the virtual displacements δu^B as equal to I (The identity matrix) and writing out the corresponding external work in matrix form, we have

$$W_e = (\delta u^B)^T F^B = I F^B = F^B \qquad \ldots (21)$$

To each of these displacements corresponds an internal work done by the moments equal to

$$W_i = \iint (\delta\psi)^T M \, dx_1 dx_2 \qquad \ldots (22)$$

where

$$\delta\psi = BC^{-1}(\delta u)^B = (BC)^{-1} I = BC^{-1} \qquad \ldots (23)$$

Substituting for $\delta\psi$ and M and equating internal and external work results in

$$\begin{aligned} F^B &= \iint (BC^{-1})^T D BC^{-1} u^B dx_1 dx_2 \\ &= \left[(C^{-1})^T \left\{ \iint B^T D B dx_1 dx_2 \right\} C^{-1} \right] u^B \end{aligned} \qquad \ldots (24)$$

The only matrix dependent on the coordinates x_1 and x_2 in the equation (24) is B and the integration of the central part has to be carried out over the entire area of the element.

The whole expression in the square bracket is simply the required stiffness matrix $|K|$ of the element, while obviously relations (18) and (20) define the internal moments in terms of the nodal displacements giving

$$M = (DBC^{-1})u^B \qquad \ldots (25)$$

or

$$M = \begin{vmatrix} M_{x1} \\ M_{x2} \\ M_{x1x2} \end{vmatrix} = S^B u^B \qquad \ldots (26)$$

where S^B is the stress matrix and given in Table III.

and $F^B = K^B u^B \qquad \ldots (27)$

COMBINED STIFFNESS MATRIX OF AN ELEMENT

If both systems of nodal displacements are acting simultaneously then at each node five components of force are developed and these are given in the five terms of components of displacement. However, as it will be necessary to consider the general equilibrium with respect to the six possible components of force at a node define the vectors of force F and displacement with six components of each node or (24) components in all

$$F = \begin{Bmatrix} F_1^1 \\ F_2^1 \\ F_3^1 \\ F_{13}^1 \\ F_{23}^1 \\ F_{12}^1 \\ \vdots \end{Bmatrix} \quad \text{and} \quad u = \begin{Bmatrix} u_1^1 \\ u_2^1 \\ u_3^1 \\ u_{13}^1 \\ u_{23}^1 \\ u_{12}^1 \\ \vdots \end{Bmatrix} \qquad \ldots (28)$$

With the understanding that $F_{12}^1 = 0$ etc.

$$\text{Now } F = K\,u \qquad \ldots (29)$$

where the element K_{ij} of the matrix is made up from appropriate elements of the K^p and K^B matrices as follows

$$|K_{rs}| \quad \left[\begin{array}{c|ccc|c} |K_{rs}^p| & 0 & 0 & 0 & 0 \\ \hline 0 & & & & 0 \\ 0 & & |K_{rs}^b| & & 0 \\ 0 & & & & 0 \\ \hline 0 & & 0 & & 0 \end{array}\right] \qquad .. (30)$$

The full $|K|$ matrix for an element after transformation to global coordinate system is given in Table I.

TRANSFORMATION TO GLOBAL COORDINATES AND ASSEMBLY OF ELEMENTS

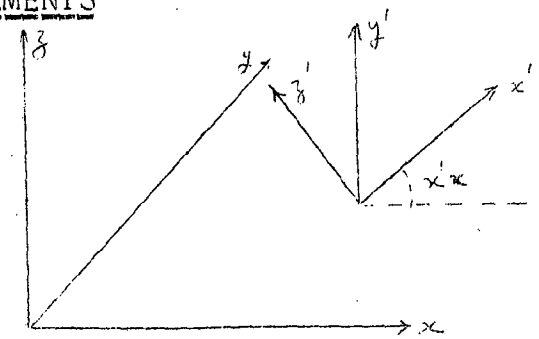

Local and Global Coordinates

Transformation of coordinates to a common global system (which now will be denoted by xyz, and the local system by x'y'z') will be necessary to assemble the elements and to write the appropriate equilibrium equations.

The two systems of coordinates are shown in the above figure. The forces and displacements of a node given in the local system (x'y'z') tranform from the global system by a matrix L giving

$$\{\delta_i'\} = |L|\{\delta_i\} \; ; \; \{F_i'\} = |L|\{F_i\} \qquad .. (31)$$

in which $|L| = \begin{bmatrix} \lambda & 0 \\ 0 & \lambda \end{bmatrix}$ .. (32)

With $|\lambda|$ being a three by three matrix of direction cosines of angles formed between the two sets of axes,

i.e. $$|\lambda| = \begin{bmatrix} \lambda_{x'x} & \lambda_{x'y} & \lambda_{x'z} \\ \lambda_{y'x} & \lambda_{y'y} & \lambda_{y'z} \\ \lambda_{z'x} & \lambda_{z'y} & \lambda_{z'z} \end{bmatrix} \qquad .. (33)$$

in which $\lambda_{xx'}$ = cosine of angle between x and x' axes, etc.

For the whole set of forces acting on the nodes of an element we can therefore write

$$\{\delta'\}^e = |T|\{\delta\}^e \; ; \; \{F'\}^e = |T|\{F\}^e \qquad .. (34)$$

By the rules of orthogonal transformation the stiffness matrix of an element in the global coordinate becomes

$$|K| = |T|^T|K'||T| \qquad .. (35)$$

In both of the above equations $|T|$ is given by

$$|T| = \begin{bmatrix} L & 0 & 0 & \cdots \\ 0 & L & 0 & \cdots \\ 0 & 0 & L & \cdots \\ \cdot & & & \\ \cdot & & & \\ \cdot & & & \end{bmatrix} \qquad .. (36)$$

a diagonal matrix built up of $|L|$ matrices in a number equal to that of the nodes in the element.

It is simple to show that the typical stiffness submatrix now becomes

$$|K_{rs}| = |L|^T|K'_{rs}||L| \qquad .. (37)$$

in which $|K'_{rs}|$ is determined by eqn.(30).

The determination of local coordinates follows a similar pattern. If the origins of both local and global systems are identical then

$$\begin{Bmatrix} x' \\ y' \\ z' \end{Bmatrix} = |\lambda| \begin{Bmatrix} x \\ y \\ z \end{Bmatrix} \quad .. (38)$$

Direction Cosines for Rectangular Elements

Such elements being limited in use to representing a cylindrical or box type of surface it is convenient to take one side of the elements and the corresponding coordinates x' parallel to the global, x, axis. For a typical element ijkm, it is now easy to calculate all the relevant direction cosines.

Direction cosine of x' are, obviously

$$\lambda_{x'x} = 1, \quad \lambda_{x'y}=0, \quad \lambda_{x'z} = 0 \quad .. (39)$$

The direction cosine of the y' axis have to be obtained by consideration of the coordinates of the various nodal points. Thus

$$\lambda_{y'x} = 0$$

$$\lambda_{y'y} = + \frac{y_j - y_i}{\sqrt{|(z_j-z_i)^2+(y_j-y_i)^2|}} \quad .. (40)$$

$$\lambda_{jz} = + \frac{z_j - z_i}{\sqrt{|(z_j-z_i)^2+(y_j-y_i)^2|}}$$

Simple geometrical relations which can be obtained by consideration of the sectional plane passing vertically through ij.

Similarly, from the same section we have for the z' axis

$$\lambda_{z'x} = 0$$

$$\lambda_{z'y} = -\frac{z_j - z_i}{\sqrt{|(z_j-z_i)^2+(y_j-y_i)^2|}}$$

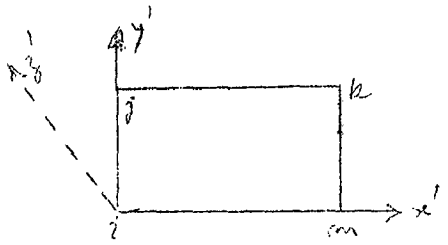

$$\lambda_{z'z} = +\frac{y_j-y_i}{\Sigma\sqrt{|(z_j-z_i)^2+(y_j-y_i)^2|}} \qquad .. (41)$$

The numbering of points in a consistent fashion is important to preserve the correct signs of the expression.

In order to obtain the stiffness matrix of the whole structure, the stiffness of the connecting elements at various modes are superimposed. It is done by first writing the stiffnesses of element in local coordinate system (x', y', z') and then transforming it into the global coordinate system (x,y,z) as explained in equation (35)

The equilibrium of the complete system of elements, which is an expression for nodal point loads in terms of nodal point displacements, can be expressed by the following matrix equations:

$$|P| = |\bar{K}||u| \qquad .. (43)$$

where the stiffness of the complete structure $|\bar{K}|$ can be found by a systematic addition of the stiffness of all elements in the system.

BOUNDARY CONDITIONS

The dam is assumed to be fixed along the foundation and abutment profile. As such the deflections of the

nodal points lying on the profile are zero. In the present analysis boundary conditions have been applied by considering the elements with different edge conditions (either fixed or not fixed). There are eight possible type of such elements as shown below

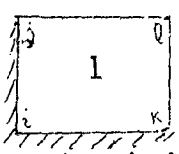

Nodes i,j,k fixed and l not fixed

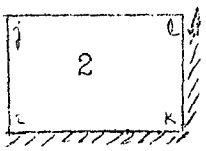

Nodes i,k,l fixed and j not fixed

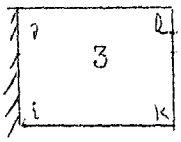

Nodes i,j fixed and k,l not fixed

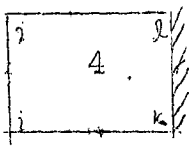

Nodes k,l fixed and i,j not fixed

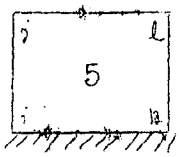

Nodes i,k fixed and j,l, not fixed

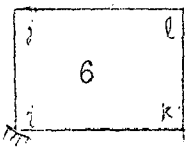

Nodes i fixed and j,k,l not fixed

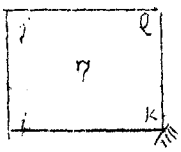

Nodes k fixed and i,j,l not fixed

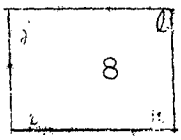

Nodes all not fixed

SOLUTION OF EQUILIBRIUM EQUATIONS

For most practical problems equation (42) represents a system of several hundred equations. In equation (42), $|\bar{K}|$ is a symmetrical band matrix i.e. it has non-zero elements only near the diagonals and zeros at all other places.

For the solution of these algebraic equations two subroutines " LUMAT" and " FOBAC" [6] have been used.

SALIENT FEATURES OF DIGITAL COMPUTER PROGRAM

As only five degrees of freedom (three translation and two rotations) have been considered at each node, it is a 20x20 symmetrical stiffness matrix for a rectangular

element. Only the upper half has been considered and named as shown in the sketch below.

$$\begin{bmatrix} ii & ij & ik & il \\ D_1 & R_1 & R_2 & R_3 \\ & jj & jk & jl \\ & D_2 & R_4 & R_5 \\ & & kk & kl \\ & & D_3 & R_6 \\ & & & ll \\ & & & D_4 \end{bmatrix}$$

20x20

The above sketch constitutes two types of system i.e. (1) the triangular system which is along the diagonal (D_1, D_2, D_3, D_4) and contains 15 values each in different directions at the four nodes of the element and (ii) the rectangular system (R_1, R_2, R_3, R_4, R_5, R_6) and contains 25 values each.

To generate the stiffness matrix of the whole structure, three subroutines i.e. (i) TWEFY, (ii) FIFTN, and (iii) GENER have been written. Subroutine 'GENER' generates the values of submatrices D_1, D_2, D_3, D_4, R_1, R_2, R_3, R_4, R_5, R_6 for all the elements of the structure and 'TWEFY' and 'FIFTN' stores the elements of submatrices in such a way that the diagonal becomes the first column of the element and so on.

The assembled matrix $|\bar{K}|$ of the whole structure is symmetrical and a band matrix. By storing the matrix in the above mentioned form it results in saving of

memory space and computation time.

ANALYSIS OF ARCH DAM

STATIC FORCES

The following cases with different parameters have been considered for the analysis in the present problem.

1. Variation of Base Width to Crest Length Ratio

Three different ratios have been considered keeping the other parameters constant. The details of different parameters are given below.

(i)	Type of dam-	Singly Curved Constant Thickness Cylindrical Arch
(ii)	Height-	99 ft.
(iii)	Thickness-	10 ft.
(iv)	Radius-	150 ft.
(v)	Central Angle-	106°
(vi)	Base width to crest length ratio	(a) 0.432, (b) 0.379 (c) 0.333

2. Variation of Central Angle

Three different central angles with constant crest length have been considered. Details of parameters are given below,

(i)	Type of Dam	- Singly Curved Constant Thickness Cylindrical Arch
(ii)	Height	- 99 ft.
(iii)	Thickness	- 10 ft.
(iv)	Base Width	-114 ft.

(v) Radius - (a) 150 ft.
(b) 175 ft.
(c) 200 ft.

(vi) Corresponding Central Angle (a) 106°
(b) 92°
(c) 80°

(3) Variation of Height

Three different cases have been considered with the following parameters.

(i) Type of Dam- Singly Curved Constant Thickness Cylindrical Arch.

(ii) Thickness - 10 ft.

(iii) Radius- 150 ft.

(iv) Base Width 114 ft.

(v) Central Angle- 106°

(vi) Height- (a) 99 ft.
(b) 120 ft.
(c) 135 ft.

(4) Variation of Thickness in horizontal direction

Three cases with different thicknesses in horizontal direction have been considered. The details of parameters are given below.

(i) Type of dam- Singly curved cylindrical Arch

(ii) Height- 99 ft.

(iii) Radius- 150 ft.

(iv) Central Angle- 106°

(v) Base width- 114 ft.

(vi) Thickness- (a) Constant thickness throughout, 10'.
(b) Thickness increases gradually towards abutments with 1:20 slope.
(c) Thickness increases gradually towards abutments with 1:15 slope

(5) Variation of thickness in Vertical Direction

Three cases have been considered with different thicknesses in vertical direction. The details of parameters are given below,

(i) Type of dam- Singly curved cylindrical arch

(ii) Height - 99 ft.

(iii) Radius- 150 ft.

(iv) Central Angle- 106^{o}

(v) Base Width- 114 ft.

(vi) Thickness- (a) Constant thickness throughout, 10 ft.

(b) Thickness increases gradually towards base with 1:16.5 slope keeping water face vertical.

(c) Thickness increases gradually towards base with 1:11 slope keeping water face vertical

(6) An Actual Profile-

An actual profile of an arch dam in a non-symmetrical valley have been considered with the following parameters.

(i) Type of dam- Singly curved cylindrical Arch.

(ii) Height - 520 ft.

(iii) Radius- 720 ft.

(iv) Central Angle- 92^{o}

(v) Base width- 270 ft.

(vi) Thickness- Varies horizontally as well as vertically.

The radial deflections and stresses of the dams considered for analysis due to external loads at various points have been calculated using finite element method.

The procedure for the same has been described earlier. To calculate stresses, a 'STRESS' subroutine has been written. The stress matrices for 'inplane' as well as 'bending' forces have been given in Tables II and III. The element idealization of the dam along with the developed surface for the typical cases are shown in figs. 1,2 and 3. With 'STRESS' subroutine for bending analysis internal moments are obtained. Stresses are calculated by using flexural formula i.e. $\frac{M}{I} = \frac{f}{y}$.

The various profiles have been divided into a number of finite rectangular elements of various sizes. The number of free nodal points multiplied by five (number of degrees of freedom considered at each node) will give us the number of algebraic equations. Hydrostatic load is assumed to be acting on the nodal points statically equivalent to the pressure acting on half the width of element on either side of the node. The above algebraic equations have been solved to get the deflections and rotations at various nodes by using digital computer and hence the stresses can be calculated by multiplying deflections with the stress matrix. The following datas have been used for the analysis of the arch dam:

Modulus of Elasticity of the material E	$= 2.6 \times 10^6$ psi.
Poisson's ratio μ	= 0.20
Unit weight of water w	= 62.5 lbs/cft.

Density of concrete mass ρ = 144 lbs/cuft.
Water level is assumed upto the top of dam. In the static analysis hydrostatic load as well as dead load have been considered.

EARTHQUAKE TYPE FORCES

Estimation of dynamic forces due to earthquake depends on so many factors such as location, type, form and material of structure. It is always possible to express the dynamic forces as equivalent static loads. As the dynamic forces vary along the height of the structure, it is important to know that variation of forces along the height of structure which may produce the maximum stresses and deflections for the same intensity of shock.

Generally the design practice is to assume a uniform loading along the height. For gravity dams the triangular type of loading and for multistoried buildings a parabolic type of loading is adopted. Keeping in view of the above type of load distribution, three types of load distribution, viz., (i) Rectangular, (ii) Triangular and (iii) Parabolic, have been considered in the present analysis. In order to find the effects of different form of loads for the same shock, base moment as a free cantilever in all the cases has been kept constant and the corresponding seismic coefficients have been calculated as below.

Generally to estimate the dynamic stresses an equivalent static load of 10 percent of gravity acceleration is considered. The same has been considered in the

present analysis.

CALCULATION OF SEISMIC COEFFICIENTS

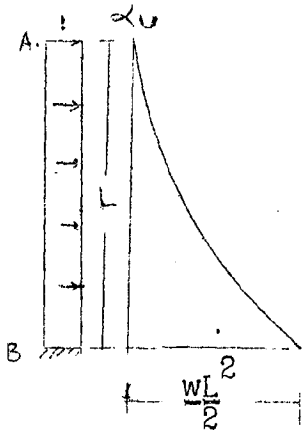

(i) Rectangular Type of Loading

Assuming unit rectangular load acting on the dam as shown. The base moment M_B becomes, i.e.

$$M_B = \alpha_u \frac{wL^2}{2} L^2/2$$

(ii) Triangular type of loading

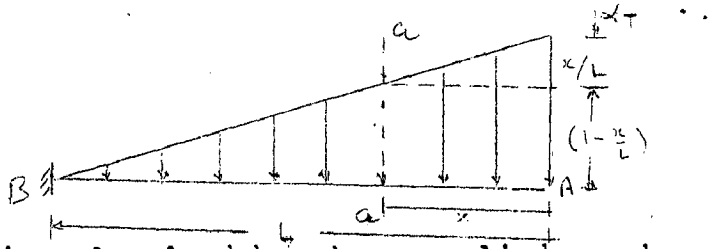

The unit triangular load has been applied as shown in the figure above. To calculate the bending moment at any section consider a section a-a at a distance x from the free end A. The bending moment at this section

$$M_x = (1 - \frac{x}{L}) \frac{x^2}{2} + \frac{x^2}{2L} \cdot \frac{2x}{3}$$

$$M_x = \frac{x^2}{2}(1 - \frac{x}{3L})$$

Therefore base moment $M_B = \frac{L^2}{3}$

Keeping the base moment same as that of the rectangular type of loading, the seismic coefficient comes out to be 0.15 g or, $\alpha_T = 1.5\ \alpha_u$

(iii) Parabolic Type of Loading

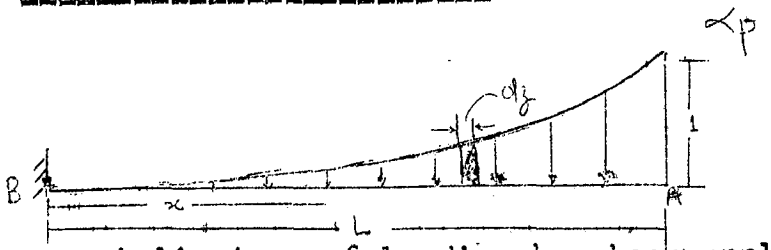

A unit parabolic type of loading has been applied as shown in figure above.

Let the equation of parabola be $y = K x^2$

where K is a constant

at $x = L$, $y = 1$

Therefore $K = 1/L^2$

$$\therefore y = \frac{x^2}{L^2}$$

The moment at any section at a distance x from B is given by

$$M_{x-z} = \frac{z^2}{L^2}\, dz\, (z-x)$$

$$= \frac{1}{L^2}\int_x^L \left[z^3 - z^2 x\right] dz$$

$$= \frac{1}{L^2}\left[\frac{z^4}{4} - \frac{z^3}{3}x\right]_x^L$$

$$= \frac{1}{L^2}\left[\frac{L^4}{4} - \frac{L^3 x}{3} - \frac{x^4}{4} + \frac{x^4}{3}\right]$$

$$= \frac{1}{L^2}\left[\frac{L^4}{4} - \frac{L^3 x}{3} + \frac{x^4}{12}\right]$$

$$M_x = \frac{L^2}{4} - \frac{Lx}{3} + \frac{x^4}{12L^2}$$

Base Moment $M_B = \frac{L^2}{4}$

Keeping the base moment same as that of the

rectangular type of loading, the seismic coefficient comes out to be 0.20 g. or $\alpha_p = 2.0\ \alpha_u$

After knowing the seismic coefficients for all the types of loading , the load vector has been calculated by mutliplying the total load lumped at nodal points with the seismic coefficient at different elevations for each type of loading. Deflections and stresses have been calculated as explained in static case. A comparison of deflections and stresses has been made between all three types of loading. The deflections and stresses have been calculated for the dam im which the thickness increases vertically towards the base which is generally the case in actual practice. In addition to this an actual profile has been studied with such type of loadings. For the different datas of dams analysed for such loadings, Cases 5 and 6 of static analysis may be referred.

DYNAMIC ANALYSIS

For the analysis of the arch dams, finite element method has been employed. By employing this method the infinity of degrees of freedom of the arch dam is reduced to n, where n is finite, and each degree of freedom has associated with it a displacement component.

An arch dam can vibrate in many modes. Practically, only few low frequency modes of the dam are considered for earthquake loading. The fundamental mode of the dam will be excited primarily by the upstream-

down-stream components of the earthquake ground motion.

In the present work, finite element method has been used. In addition to the stiffness matrix, the mass matrix for rectangular finite element has been derived and the fundamental natural frequencies and corresponding mode shapes have been calculated for empty reservoir condition for some typical cases just to have an idea of the range of frequency of the assumed singly curved cylindrical arch dams. The details of the derivation of mass matrix have been given subsequently.

The equation of motion for free vibration system can be written as

$$|M|\{\ddot{x}\} + |K|\{x\} = 0$$

which is of the form $p^2 M\, x = K\, x$

To determine the fundamental frequency and corresponding mode shape the following cases have been considered.

(1) Type of dam - Singly curved constant thickness cylindrical arch in a symmetrical valley.

Height,	- 30 m.
Radius	- 43.25 m
Thickness	- 3.0 m
Central Angle	- 106^0
Base width	- 35 m
Crest length	- 80 m.

(2) Singly curved constant thickness cylindrical Arch in a U-shaped valley with the following parameters,

Height, 99 ft., Radius = 150 ft., Thickness = 10 ft.
Central Angle = 106^0, Base Width = 264 ft.

Fundamental frequencies and mode shapes have been calculated by using matrix iteration[22] procedure for the two cases and a comparison has been made by considering coarse and fine meshes for the first case. The details of calculations for the frequencies are given in Chapter 4.

MASS MATRIX

Plane Stress and Strain

The figure given opposite shows the typical rectangular element considered, with nodes i,j,k,l numbered in the manner shown.

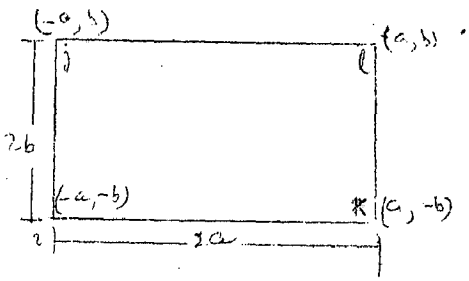

The displacements of a node have two components

$$\{\delta_i\} = \begin{Bmatrix} u_i \\ v_i \end{Bmatrix} \qquad \ldots (43)$$

and the eight components of element displacements are listed as a vector

$$\{\delta\}^e = \begin{Bmatrix} \delta_i \\ \delta_j \\ \delta_k \\ \delta_l \end{Bmatrix} \qquad \ldots (44)$$

The displacements within an element have to be uniquely defined by these eight values. The simplest representation is clearly given by two linear polynomials,

$$\left.\begin{aligned} u &= C_1 + C_2 x + C_3 y + C_4 xy \\ v &= C_5 + C_6 x + C_1 y + C_8 xy \end{aligned}\right| \qquad \ldots (45)$$

The eight constants C can be evaluated easily by solving the two sets of four simultaneous equations which will arise if the nodal coordinates are inserted and the displacements equated to the appropriate nodal displacements. Writing the equations,

$$\left.\begin{aligned} u_i &= C_1 - C_2 a - C_3 b + C_4 ab \\ v_i &= C_5 - C_6 a - C_7 b + C_8 ab \\ u_j &= C_1 - C_2 a + C_3 b - C_4 ab \\ v_j &= C_5 - C_6 a + C_7 b - C_8 ab \\ u_k &= C_1 + C_2 a - C_3 b - C_4 ab \\ v_k &= C_5 + C_6 a - C_7 b - C_8 ab \\ u_l &= C_1 + C_2 a + C_3 b + C_4 ab \\ v_l &= C_5 + C_6 a + C_7 b + C_8 ab \end{aligned}\right| \qquad \ldots (46)$$

We can easily solve the above eight equations and constants C_1 to C_8 can be evaluated in terms of nodal displacements. Finally,

$$u = u_i\left(\frac{1}{4} - \frac{x}{4a} - \frac{y}{4b} + \frac{xy}{4ab}\right) + u_j\left(\frac{1}{4} - \frac{x}{4a} + \frac{y}{4b} - \frac{xy}{4ab}\right)$$
$$+ u_k\left(\frac{1}{4} + \frac{x}{4a} - \frac{y}{4b} - \frac{xy}{4ab}\right) + u_l\left(\frac{1}{4} + \frac{x}{4a} + \frac{y}{4b} + \frac{xy}{4ab}\right) \qquad \ldots (47a)$$

$$v = v_i\left(\frac{1}{4} - \frac{x}{4a} - \frac{y}{4b} + \frac{xy}{4ab}\right) + v_j\left(\frac{1}{4} - \frac{x}{4a} + \frac{y}{4b} - \frac{xy}{4ab}\right)$$
$$+ v_k\left(\frac{1}{4} + \frac{x}{4a} - \frac{y}{4b} - \frac{xy}{4ab}\right) + v_l\left(\frac{1}{4} + \frac{x}{4a} + \frac{y}{4b} + \frac{xy}{4ab}\right) \qquad \ldots (47b)$$

The equations (47a) and (47b) can now be represented in the standard form,

$$\text{i.e. } |N| = \begin{Bmatrix} u \\ v \end{Bmatrix} = |I\ N_i',\ IN_j',\ IN_k',\ IN_l'|\,|\delta|^e \qquad \ldots (48)$$

in which $I = \begin{bmatrix} 1 & 0 \\ 0 & 1 \end{bmatrix}$

$N_i = (\frac{1}{4} - \frac{x}{4a} - \frac{y}{4b} + \frac{xy}{4ab})$ etc.,

If the thickness of the element is t and this is assumed to be constant within the element, we have for the mass matrix

$$|m|^e = \rho\, t \iint |N|^T |N| dx\, dy$$

$$\therefore \quad N_i = \rho\, t \int_{-b}^{b} \int_{-a}^{a} (\frac{1}{4} - \frac{x}{4a} - \frac{y}{4b} + \frac{xy}{4ab}) dx\, dy$$

$$= \rho\, t\, ab$$

$$= \frac{W}{4}$$

Since $W = 4ab\rho t$

Similarly N_j, N_k, N_l can be calculated.

Thus if the mass had been lumped at the nodes in four equal parts the mass matrix contributed by the element would have been,

$$|m|^e = \frac{W}{4} \begin{bmatrix} 1 & 0 & 0 & 0 & 0 & 0 & 0 & 0 \\ 0 & 1 & 0 & 0 & 0 & 0 & 0 & 0 \\ 0 & 0 & 1 & 0 & 0 & 0 & 0 & 0 \\ 0 & 0 & 0 & 1 & 0 & 0 & 0 & 0 \\ 0 & 0 & 0 & 0 & 1 & 0 & 0 & 0 \\ 0 & 0 & 0 & 0 & 0 & 1 & 0 & 0 \\ 0 & 0 & 0 & 0 & 0 & 0 & 1 & 0 \\ 0 & 0 & 0 & 0 & 0 & 0 & 0 & 1 \end{bmatrix}$$

Bending of Plates

Consider a rectangular element ijlk as shown in

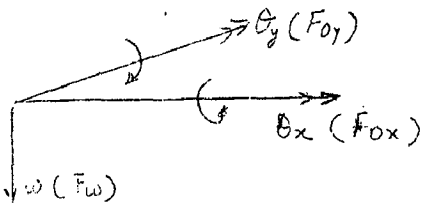

'Forces and Corresponding displacements'

the figure given opposite. At each mode displacements $\{\delta_m\}$ are introduced. These have three components, the first a displacement in z direction, w_n, the second a rotation about the x axis, $(\theta_x)_m$, the third a rotation about y axis $(\theta_y)_n$. Positive directions of the rotation are determined by the righ-hand screw rule and are shown by vectors directed along these axes.

Clearly the slope of w and the rotations are identical (except for sign), i.e.,

$$\left.\begin{aligned} \theta_x &= -\frac{\partial w}{\partial y} \\ \theta_y &= \frac{\partial w}{\partial x} \end{aligned}\right| \qquad .. (49)$$

The nodal displacement vector can therefore be defined as follows at a node i

$$\{\delta_i\} = \begin{Bmatrix} w_i \\ \theta_{xi} \\ \theta_{yi} \end{Bmatrix} = \begin{Bmatrix} w_i \\ -(\frac{\partial w}{\partial y})_i \\ (\frac{\partial w}{\partial x})_i \end{Bmatrix} \qquad .. (50)$$

The slope function is considered simply as the scaler w must be definable in terms of $|\delta|^e$, i.e. in terms of twelve parameters.

A polynomial expression is conveniently used.

$$w = \alpha_1+\alpha_2 x+\alpha_3 y+\alpha_4 x^2+\alpha_5 xy+\alpha_6 y^2+\alpha_7 x^3+\alpha_8 x^2 y+\alpha_9 xy^2+\alpha_{10} y^3+ \alpha_{11} x^3 y+\alpha_{12} xy^3 \qquad .. (51)$$

The constants α_1 to α_{12} can be evaluated by writing down the twelve simultaneous equations linking the values of w and its slopes at the nodes when the coordinates take up their appropriate values.

Listing all the twelve equations we can write, in matrix form,

$$\{\delta\}^e = |C|\{\alpha\} \qquad .. (52)$$

where $|C|$ is a 12x12 matrix depending on nodal coordinates and $\{\alpha\}$ a vector of the twelve unknown constants. Inverting

$$\{\alpha\} = |C|^{-1}\{\delta\}^e \qquad .. (53)$$

It is now possible to write the expression for the displacement within the element in a standard form

$$\text{i.e.} \quad w = |N|\{\delta\}^e = |P||C|^{-1}\{\delta\}^e \qquad .. (54)$$

where,

$$|P| = (1, x, y, x^2, xy, y^2, x^3, x^2y, xy^2, y^3, x^3, x^3y, xy^3) \qquad .. (55)$$

An explicit form of the above expression was derived by Melosh. If the coordinate origin is taken at the centre of the element and equation (54) is written as

$$\{w\} = |N_i,\ N_j,\ N_l,\ N_k|\{\delta\}^e$$

Then,

$$32N_i = X_iY_1\{2(X_1Y_1 - X_2Y_2) - 4X_1X_2 - 4Y_1Y_2, +4bY_1Y_2, -4aX_1X_2\}$$

$$32N_j = X_1Y_2\{2(X_1Y_2 - X_2Y_1) + 4X_1X_2 + 4Y_1Y_2, +4bY_1Y_2, +4aX_1X_2\}$$

$$32N_l = X_2Y_2\{2(X_2Y_2 - X_1Y_1) - 4X_1X_2 - 4Y_1Y_2, +4bY_1Y_2, +4aX_1X_2\}$$

$$32N_k = X_2Y_1\{2(X_2Y_1 - X_1Y_2) + 4X_1X_2 + 4Y_1Y_2, +4bY_1Y_2, -4aX_1X_2\}$$

with $X_1 = (x - a)/a$ $\quad Y_1 = (y-b)/b$

$X_2 = (x + a)/a$ $\quad Y_2 = (y+b)/b$

If a distributed loading q is acting per unit area of an element in direction of w then the contribution of these forces to each of the nodes is

$$|F|_p^e = -\iint |N|^T q \, dx \, dy \qquad .. (56)$$

or $$\{F\}_p^e = \{-|C|^{-1}\}^T \iint |P|^T q \, dx \, dy \qquad .. (57)$$

The integral is again evaluated as shown below. It is noted that in general, all three components of external force at any node will have (non-zero) values.

Determination of translation and rotation contribution at each node

1. Translation

Node i

$$32N_i = X_1Y_1\{2(X_1Y_1 - X_2Y_2) - 4X_1X_2 - 4Y_1Y_2\}$$

$$= \frac{(x-a)(y-b)}{ab}\left[2\left\{\left(\frac{x-a}{a}\right)\left(\frac{y-b}{b}\right) - \left(\frac{x+a}{a}\right)\left(\frac{y+b}{b}\right)\right\} - 4\left(\frac{x+a}{a}\right)\left(\frac{x-a}{a}\right) - 4\left(\frac{y+b}{b}\right)\left(\frac{y-b}{b}\right)\right.$$

$$= \left(\frac{xy-xb-ay+ab}{ab}\right)\left[\frac{2}{ab}\{xy - xb - ay + ab - xy - xb - ay - ab\} - \frac{4}{a^2}(x^2-a^2) - \frac{4}{b^2}(y^2-b^2)\right]$$

$$= -4\left(\frac{xy-xb-ay+ab}{a^2b^2}\right)(xb+ay) - \frac{4}{a^3b}(xy-xb-ay+ab)(x^2-a^2)$$

$$- \frac{4}{ab^3}(xy-xb-ay+ab)(y^2-b^2)$$

$$32F_{wi} = q\int_{-b}^{b}\int_{-a}^{a}\left[-\frac{4}{a^2b^2}(x^2yb - x^2b^2 - 2xyab + xab^2 + xy^2a - a^2y^2 + a^2by)\right.$$

$$- \frac{4}{a^3b}(x^3y - x^3b - x^2ya + x^2ab - xya^2 + xba^2 + a^3y - a^3b)$$

$$\left.-\frac{4}{ab^3}(xy^3 - xy^2b - ay^3 + aby^2 - xyb^2 + xb^3 + ayb^2 - ab^3)\right]dx \, dy$$

$$F_{wi} = qab$$

$$= \frac{W}{4} \quad (\text{since } 4qab=W)$$

Rotations

$$32F_{\theta xi} = q \int_{-b}^{b} \int_{-a}^{a} 4b\, Y_1 Y_2 \, dx\, dy$$

$$= -q \times 8 \times \frac{4}{3} ab^2$$

$$F_{\theta xi} = -\frac{1}{3}qab^2 = -\frac{Wb}{12}$$

Similarly

$$32F_{\theta yi} = 4aX_1X_2\, q$$

$$F_{\theta yi} = q\,\frac{a^2b}{3} = \frac{Wa}{12}$$

Node j

Translation

$$32N_j = X_1Y_2\{2(X_1Y_2-X_2Y_1)+4X_1X_2+4Y_1Y_2\}$$

$$32F_{wj} = q \int_{-b}^{b} \int_{-a}^{a} \Big| \frac{4}{a^2b^2}(x^2yb+x^2b^2-2xyab-xab^2-xy^2a+y^2a^2+ya^2b)$$

$$+ \frac{4}{a^3b}(x^3y+x^3b-x^2ya-x^2ab-xya^2-xa^2b+ya^3+a^3b)$$

$$+ \frac{4}{ab^3}(xy^3+xy^2b-y^3a-y^2ab-xyb^2-xb^3+yab^2+ab^3)\Big]dxdy$$

$$F_{wj} = qab = \frac{W}{4}$$

Rotation

$$32\,F_{\theta xj} = q \int_{-b}^{b} \int_{-a}^{a} 4b\, Y_1 Y_2 \, dxdy$$

$$F_{\theta xj} = q\,\frac{ab^2}{3} = \frac{W\,b}{12}$$

Similarly $32\ F_{\theta yj} = q \int_{-b}^{b} \int_{-a}^{a} 4a\ X_1 X_2\ dx\ dy$

$$F_{\theta yj} = q\ \frac{a^2 b}{3} = \frac{Wa}{12}$$

Similarly for

Node K

$$32\ N_k = X_2 Y_1 \{2(X_2 Y_1 - X_1 Y_2) + 4 X_1 X_2 + 4 Y_1 Y_2\}$$

$$\therefore\ F_{wk} = qab = \frac{W}{4}$$

Rotations

$$32 F_{\theta xk} = q \int_{-b}^{b} \int_{-a}^{a} 4b\ Y_1 Y_2 dx dy$$

$$F_{\theta xk} = \frac{Wb}{12}$$

Similarly

$$32 F_{\theta yk} = q \int_{-b}^{b} \int_{-a}^{a} -4a X_1 X_2 dx dy$$

$$F_{\theta yk} = -\frac{Wa}{12}$$

Node 1

Translation

$$32 N_1 = X_2 Y_2 \{2(X_2 Y_2 - X_1 Y_1) - 4 X_1 X_2 - 4 Y_1 Y_2\}$$

$$\therefore\ F_{w1} = qab = \frac{W}{4}$$

Rotations

$$32\ F_{\theta x1} = q \int_{-b}^{b} \int_{-a}^{a} 4b\ Y_1 Y_2 dx\ dy$$

$$F_{\theta x1} = -q\ \frac{ab^2}{3} = -\frac{Wb}{4}$$

Similarly

$$32\ F_{\theta yl} = q\int_{-b}^{b}\int_{-a}^{a} 4aX_1X_2\,dx\,dy$$

$$F_{\theta yl} = -q\,\frac{a^2b}{3} = -\frac{Wa}{12}$$

Thus the table given below shows the nodal load vector for a uniform loading q.

Load vector for a rectangular element under uniform load 'q'

$$\begin{Bmatrix} F_i \\ \\ \\ F_j \\ \\ \\ F_k \\ \\ \\ F_l \\ \\ \end{Bmatrix} \begin{Bmatrix} F_{wi} \\ F_{\theta xi} \\ F_{\theta yi} \\ F_{wj} \\ F_{\theta xj} \\ F_{\theta yj} \\ F_{wk} \\ F_{\theta xk} \\ F_{\theta yk} \\ F_{wl} \\ F_{\theta xl} \\ F_{\theta yl} \end{Bmatrix} = 4qab \begin{Bmatrix} 1/4 \\ -b/12 \\ a/12 \\ 1/4 \\ b/12 \\ a/12 \\ 1/4 \\ b/12 \\ -a/12 \\ 1/4 \\ -b/12 \\ -a/12 \end{Bmatrix} \qquad \ldots (58)$$

Usually direct strains in the plate are introduced additionally, and the complete problem can be solved only by consideration of the plane stress problem as well as that of bending.

The complete load vector for the element will be as shown on the next page.

$$
\left\{\begin{array}{c} \\ F_i \\ \\ \\ \\ \\ F_j \\ \\ \\ \\ \\ F_k \\ \\ \\ \\ \\ F_l \\ \\ \\ \\ \end{array}\right\}
=
\left\{\begin{array}{l} F_{ui} \\ F_{vi} \\ F_{wi} \\ F_{\theta xi} \\ F_{\theta yi} \\ F_{uj} \\ F_{vj} \\ F_{wj} \\ F_{\theta xj} \\ F_{\theta yj} \\ F_{uk} \\ F_{vk} \\ F_{wk} \\ F_{\theta xk} \\ F_{\theta yk} \\ F_{ul} \\ F_{vl} \\ F_{wl} \\ F_{\theta xl} \\ F_{\theta yl} \end{array}\right\}
= 4qab
\left\{\begin{array}{c} 1/4 \\ 1/4 \\ 1/4 \\ -b/12 \\ a/12 \\ 1/4 \\ 1/4 \\ 1/4 \\ b/12 \\ a/12 \\ 1/4 \\ 1/4 \\ 1/4 \\ b/12 \\ -a/12 \\ 1/4 \\ 1/4 \\ 1/4 \\ -b/12 \\ -a/12 \end{array}\right\}
\qquad \ldots (59)
$$

CHAPTER 4

RESULTS AND CONCLUSIONS

The constant thickness, constant angle dam can be satisfactorily represented by an assembly of plane rectangular elements except in the region of the sloping valley sides. Here a stepped boundary has been used as shown in the developed surface of the air face of the dam with the real valley profile shown by the dashed line in figures 1,2, and 3. In case the thickness varies horizontally, vertically, or in both directions, it has been assumed that the dam is an assemblage of finite elments of various thickness and the thickness for each element is taken as the mean thickness of the element.

STATIC ANALYSIS

DEFLECTIONS - Figures 4a, 4b, 4c, 4d and 4e shows the radial deflections of central cantilever due to hydrostatic load for different cases. The following conclusions can be made.

a) As the base width to crest length ratio decreases, the maximum deflections which occur near about 0.6 height, decreases.

b) As the radius increases or central angle decreases, the deflections increase.

c) As the height increases without any change in the thickness, the deflections increase.

d) As thickness increases horizontally from the centre towards the abutments, the deflections decrease.

e) As the thickness increases vertically towards base, the deflection decreases.

Vertical Stresses due to hydrostatic Load

Figures 5a, 5b, 5c, 5d and 5e shows the vertical stress distribution due to hydrostatic load on the central cantilever on upstream and downstream sides for the different cases. The following conclusions can be made.

a) As the base width to crest length ratio decreases, the compressive and tensile stresses on both the faces go on reducing.

b) As the radius of the dam increases, the compressive and tensile stress on both the faces increases.

c) As the height of the dam increases, the compressive and tensile stress on both the faces increases.

d) As the thickness of the dam increases horizontally towards the abutments, the compressive and tensile stress on both sides increases.

e) As the thickness of the dam increases vertically towards the base, on upstream face the

tensile stress increases and compressive stress reduces while on downstream face the compressive stress increases and tensile stress reduces.

Hoop-Stresses due to Hydrostatic Load

Figures 6a, 6b, 6c, 6d, and 6e shows the distribution of hoop stresses due to hydrostatic load on the central cantilever on upstream face for different cases. From the results it has been concluded that the hoop stresses go on increasing in all the five cases considered.

Vertical Stresses due to Dead Load

Figures 7a, 7b, 7c, 7d and 7e shows the vertical stress distribution due to dead load on the central cantilever on the upstream and downstream sides for the different cases. The following conclusions can be made.

a) As the base width to crest length ratio decreases, the stresses goes on reducing on both the faces,

b) As the radius increases, there is no marked variation of stresses on upstream side while on downstream side the stresses go on reducing slowly.

c) As the height increases, the stresses on both the faces go on increasing.

d) As the thickness increases horizontally or vertically, the stress on both faces reduces.

Hoop-Stresses due to Dead Load

Figures 8a, 8b, 8c, 8d and 8e shows the hoop stress variation for different cases on upstream and downstream sides on central cantilever. The following can be concluded.

a) As the base width to crest length ratio decreases,
   (i) On the upstream face the tensile stresses in the lower third region increases slightly,
   (ii) The compressive stresses in the middle third region increases, and (iii) the compressive stresses in the top third region decreases, while on the downstream face the tensile stresses occur and go on decreasing.
b) As the radius increases the stresses go on reducing slowly on both the faces,
c) As the height increases, the maximum stresses go on increasing on both faces.
d) As thickness increases in horizontal direction, the stresses go on increasing on both faces.
e) As the thickness of the dam increases vertically, the maximum stress reduces on both the sides.

An Actual Profile

Figures 9a shows the deflections of the longest cantilever of the dam in a non-symmetric valley. The problem has been solved for two different meshes,

(i) Coarse mesh, and (ii) Fine mesh. The comparison of the two has been shown. The maximum deflection is of the order of 11 cms. at the crest level.

Figure 9c shows the distribution of vertical and hoop stresses due to hydrostatic load on both the faces. The distribution is more or less symmetrical. Maximum hoop stresses are about 5 times of the maximum vertical stresses.

Figure 9(d) shows the distribution of dead load stresses (vertical as well as hoop) on both the faces. In the middle third portion hoop stresses are maximum and about 1.5 times as that of the maximum vertical stresses.

Figure 10 shows a comparison of radial deflections, and stresses due to hydrostatic load and dead load due to coarse mesh and fine mesh. A good agreement is obtained.

Equivalent Static Earthquake Load

Since the acceleration due to earthquake load varies along the height of the structure, the load will also vary. To determine the shape of loading which may produce the maximum stresses in the structure for the same intensity of shock, three cases of loading, viz., (i) Rectangular, (ii) Triangular, and (iii) Parabolic have been considered in the analysis. The dynamic loads can always be represented by a certain percentage of static loads. A dynamic load of 10 percent gravity acceleration has been considered for different types of loading. Two profiles in which the thickness gradually

increases vertically, have been analysed.

Deflections Figures 11a and 11b show the radial deflections of central cantilever due to the three types of loading for the dam considered. The following conclusions can be made.

(a) The maximum deflection occurs due to parabolic type of loading in the upper third region and minimum by the rectangular load while in the lower 2/3rd region, reverse is the case.

(b) More the rate of increase in thickness, lesser are the deflections.

Vertical Stresses

Figures 12a and 12b shows the vertical stress distribution on the central cantilever due to three types of loading on both the faces. The following can be concluded,

(a) The maximum stresses occur due to parabolic type of loading on both faces.

(b) As the thickness increases vertically, the maximum stress reduces.

Hoop Stresses

Figures 12c and 12d show the variation of hoop stresses on the central cantilever due to three types of loading on both the faces. The following can be concluded.

(a) The maximum hoop stresses occur due to rectangular type of loading in the lower third region on both the faces while in the upper third region it is due to parabolic type of loading.

(b) As the effect of thickness reduces, the parabolic type of loading produces the maximum compressive stresses on the upstream face.

An Actual Profile

An actual profile in an unsymmetrical valley has been analysed for dynamic loads also. Figures 13 and 14 show the distribution of vertical stresses and hoop stresses on both the faces on the longest cantilever. Figure 9(b) shows the radial deflection of the same cantilever due to dynamic loads. The following conclusions can be made.

Deflections

(a) Deflection pattern is same as in other cases.

(b) Maximum deflection at the crest due to parabolic loading is of the order of 18 mm.

Vertical Stresses

(a) The stresses on both the faces are more or less symmetrical.

(b) The maximum stresses are due to parabolic loading throughout the height of the cantilever.

(c) The maximum stress due to parabolic type of loading is about 1.6 times of the maximum stress due to rectangular type of loading.

Hoop-Stress

(a) The stresses on both the faces are more or less symmetrical.

(b) The maximum hoops are produced due to rectangular type of loading in the lower half region. In the top region it is due to parabolic loading.

Combined Stresses

Combined static and dynamic stress variation on both faces are shown in the figures 15,16 and 17 for three cases, viz., (i) Variation of thickness in vertical direction in the ratio 1:16.5, (ii) Variation of thickness in vertical direction in the ratio 1:11, and (iii) An actual profile. In all the cases the vertical and hoop stress variations are shown for, (i) static stresses due to hydrostatic and dead loads, (ii) static loads plus rectangular load, and, (iii) Static loads plus parabolic load. From the curves it is found that-

(a) Maximum vertical stresses are due to static loads plus parabolic load.

(b) Maximum hoop stresses in the lower 2/3rd region is due to static plus rectangular loading with a slight variation with static plus parabolic loading, while in the upper region it is due to static plus parabolic loading.

(c) As the thickness increases , the vertical stresses are reduced while the hoops are

slightly increased.

(d) In case of an actual profile the maximum hoop is about 5 times the maximum vertical stress.

Natural Period of Vibration and Mode Shape of the Dam

Figures18(a) and 18(b) show the fundamental mode shape for (a) symmetrical sloping side valley and (2) (b) U-shaped valley. Figure 18(a) shows the effect of fine mesh also. It is seen that

(a) In sloping side symmetrical valley, the fundamental mode is a symmetric one while in the U-shaped valley it is antisymmetric.

(b) There is only a small variation between fine mesh and coarse mesh results.

(c) Frequency in case of U-shaped valley is slightly less than the frequency due to sloping side valley.

DETAILS OF CALCULATIONS OF FUNDAMENTAL FREQUENCIES

Case I FINE MESH

Data Assumed

Modulus of Elasticity $E = 2.6 \times 10^6$ psi

Wt. density $\rho = 144$ lbs/cu.ft.

$$p^2 = \alpha \frac{Eg}{\rho}$$

$$\sqrt{Eg/\rho} = \sqrt{\frac{2.6 \times 10^6 \times 32.2 \times 144}{144}}$$

$$= 10\sqrt[3]{836}$$

$$= 9140$$

Therefore $p^2 = \frac{0.491976}{900} \times \frac{Eg}{\rho}$

$$= 0.000546 \times \frac{Eg}{\rho}$$

$$\therefore p = 0.0233 \times \frac{9140 \times 30.48}{100} = 0.0233 \times 2790$$

or $p = 65.00$ rad/sec.

Therefore, $f = \frac{p}{2\pi} = \frac{65.00}{6.28} = 10.30$ c/sec.

Coarse Mesh

$$p = 0.0248 \times 2790$$

$$= 69.30 \text{ rad/sec.}$$

or $f = \frac{69.30}{6.28} = 11.00$ c/sec.

Case II - U-Shaped Valley

$$p = 0.0226 \times 2790$$

$$= 63 \text{ rad/sec.}$$

or $f = \frac{63}{6.28} = 10.00$ c/sec.

CONCLUSIONS

Based on the results obtained from the analysis of various profiles with different parameters, the following conclusions may be drawn for safe design of an arch dam-

1. Though V-shaped valley is generally preferred for construction of an arch dam, arch dams are economical to construct in valleys of other shapes also. This study has indicated that the stresses do not increase very rapidly with the shape of valley , other parameters remaining same.

2. Central angle of the cylindrical arch dam may lie between 95° to 110° for economic consideration.On reducing the angle, stresses go on increasing while on increasing it, more volume of concrete mass is required in the dam.

3. Increase in thickness of dam vertically towards the base gives less vertical stresses but more hoops while an increase in thickness horizontally towards the abutments, more vertical as well as hoop stresses are developed in the dam.

4. As the weight of the arch dam is small as compared to the gravity dams, the dynamic stresses in arch dams are very small as compared to the static stresses particularly in moderate earthquake zones.

5. In case of lateral seismic loadings, inverted parabolic type of load distribution produces more vertical

stresses and crest deflections while uniform load distribution produces more hoop stresses and the deflections in the lower 2/3rd region of the dam.

6. Combined static and dynamic (parabolic load distribution) loads give more vertical stresses while static plus rectangular load distribution give slightly more hoop-stresses.

7. In the finite element method, even a coarse mesh gives fairly accurate results in determination of fundamental period and mode shape.

REFERENCES

1. Ahmad, S., Irons, B.M., and Zienkiewicz, O.C., "Curved Thick Shell and Membrane Elements with particular reference to Axisymmetric Problems" Proc. of the Second Conference on Matrix Methods in Structural Mechanics, Wright-Patterson Air Force Base, Ohio, 15-17, Oct.1968.

2. Ahmad, S., Irons, B.M., and Zienkiewicz, O.C., "Analysis of Thick and Thin Shell Structures by Curved Finite Elements" , International Journal for Numerical Methods in Engineering, Vol.2, 419-451 (197C).

3. Allen, D.N. DE G., Chitty, L., Pippard, A.J.S., and Severn, R.T., " The Experimental and Mathematical Analysis of Arch Dams, with special reference to Dokan," Proc. Inst. Civ. Engrs. 5, 198-244(1956).

4. Bonnes, G., Dhatt, G., Giroux, Y.M., and Robichaud, L.P.A., "Curved Triangular Elements for the Analysis of Shells", Proc. of the Second Conference on Matrix Methods in Structural Mechanics, Wright Patterson Air Force Base, Ohio, 15-17 Oct. 1968.

5. Bogner, F.K., Fox, R.L., and Schmit, L.A., "A Cylindrical Shell Discrete Element", AIAA Journal, Vol.5, No.4, April,1967.

6. Chandrasekaran, A.R., "Solution of Banded Stiffness Matrix", A report of Institution of Earthquake Engineering and Seismology, Skopje, Yugoslavia, 1971.

7. Conner, J.J., Jr. and Brebbia, C., "Stiffness Matrix for Shallow Rectangular Shell Element", Journal of the Engineering Mechanics Division, EM5, Proc.of the ASCE., October, 1967.

8. Dennis, T.L., "Proceedings of the Symposium held at the Institute of Civil Engineers, 20-21, March 1968, Institution of Civil Engineers, London.

9. Design Standard No.2, Treatise on Dams, Chap.10, Arch Dams, Bureau of Reclamation, U.S. Department of Interior, Denver, Colorado.

10. Gallagher, R.H., "The Development and Evaluation of Matrix Methods for Thin Shell Structural Analysis", Bell Aerosystems, Buffalo, New York, Report No.8500-902011, June, 1966.

11. Greene, B.E., Jones, R.E., Mclay, R.W., and Strome, D.R., "Dynamic Analysis of Shells using Doubly Curved Finite Element" , Proc. of the Second Conference on Matrix Methods in Structural Mechanics, Write-Patterson Air Force Base, Ohio, 15-17 Oct.1968.

12. Johnson, C.P., "A Finite Element Approximate for the Analysis of Thin Shells" , Ph.D. Thesis, 1967, University of California, Berkeley, Calif.

13. Laginha Serafim, J., Caldeira Rodrigues, J.A., Portela, A., and Milho, M.J., "Complete Adjustment Method for Analysing Arch Dam" , Proc. A.S.C.E., Journal of Structural Division, August 1970.

14. Melosh, R., "A Flat Triangular Shell Element Stiffness Matrix" , Proc. of Conference on Matrix Methods in Structural Mechanics, AFFDL-TR-66-80, Air Force Institute of Technology, October, 1965.

15. Olson, M.D., and Lindberg, G.M., "Vibration Analysis of Cantilevered Curved Plates using a new Cylindrical Shell Finite Element" . Proc. of the Second Conference on Matrix Methods in Structural Mechanics, Wright-Patterson Air Force Base, Ohio, 15-17 October 1968.

16. Rosen, R., and Rubinstein, M.F., "Dynamic Analysis by Matrix Decomposition" , Proc. ASCE, J.Engg. Mechanics Division, April 1968.

17. Rydzewski, J.R., "Theory of Arch Dams" , The International Symposium held at Southampton University, April 1964.

18. Second Interim Report on Research into the Design of Arch Dams, Published by Civil Engineering Research Association, May, 1966.

19. Strickland, G.E., and Luden, W.A., "A Doubly Curved Triangular Shell Element", Proc. of the Second Conference on Matrix Methods in Structural Mechanics, Wright-Patterson Air Force Base, Ohio, 15-17 Oct. 1968.

20. Tahbildar, U.C., "Static and Dynamic Analysis of Arch Dams by the Finite Element Method using Doubly Curved Shell Element", Thesis presented to Southampton University, at Southampton, England, in 1969, in partial fulfilment of the requirement for the Degree of Doctor of Philosophy.

21. Vlassov, V.Z., "General Shell Theory", Moscow, 1949.

22. Zienkiewicz, O.C., and Cheung, Y.K., "Finite Element Method of Analysis for Arch Dam Shells and Comparison with Finite Difference Procedures", Proc. of Symposium on "Theory of Arch Dams" held at Southampton University, London, April 1964.

$$\tau_2 = \frac{2T_2}{t} \qquad .. (3b)$$

Stress-displacement equations

$$N_x = D\left[u' + \mu\left(v^o + \frac{w}{z}\right) - (1+\mu)\alpha T_1\right] \qquad .. (4a)$$

$$N_y = D\left[v^o + \frac{w}{z} + \mu u' - (1+\mu)\alpha T_1\right] \qquad .. (4b)$$

$$N_{xy} = N_{yx} = D\,\frac{1-\mu}{2}\left[u^o + v'\right] \qquad .. (4c)$$

$$M_x = B\left[w'' + \mu\, w^{oo} - (1+\mu)\alpha\, \tau_2\right], \qquad .. (4d)$$

$$M_y = B\left[w^{oo} + \mu w'' - (1+\mu)\alpha\, \tau_2\right], \qquad .. (4e)$$

$$M_{xy} = M_{yx} = B(1-\mu)w'^{o} \qquad .. (4f)$$

With the help of the above equations we obtain finally the three basic equations,

$$\left[Du'\right]' + \frac{1-\mu}{2}\left[Du^o\right]^o + \mu\left[Dv^o\right]' + \frac{1-\mu}{2}\left[Dv'\right]^o + \mu\left[D\frac{w}{z}\right]' - (1+\mu)\alpha\left|DT_1\right|' + X = 0, \qquad .. (5a)$$

$$\frac{1-\mu}{2}\left[Du^o\right]' + \mu\left[Du'\right]^o + \frac{1-\mu}{2}\left[Dv'\right]' + \left[Dv^o\right]^o + \left[D\,\frac{w}{z}\right]^o - (1+\mu)\alpha\left[DT_1\right]^o + Y = 0 \qquad .. (5b)$$

$$\begin{aligned}
&\left[Du'z'\right]' + \frac{1-\mu}{2}\left[Du^o z^o\right]' + \mu\left[Du'z^o\right]^o + \frac{1-\mu}{2}\left[Du^o z'\right]^o - \mu\,\frac{D}{z}u' + \frac{1-\mu}{2}\left[Dv'z^o\right]' \\
&+\mu\left[Dv^o z'\right]' + \frac{1-\mu}{2}\left[Dv'z'\right]^o + \left[Dv^o z^o\right]^o - \frac{D}{z}v^o + \left[Bw''\right]' + \mu\left[Bw^{oo}\right]'' \\
&+2(1-\mu)\left[Bw'^o\right]'^o + \mu\left[Bw''\right]^{oo} + \left[Bw^{oo}\right]^{oo} + \mu\left[D\,\frac{w}{z}\,z'\right]' \\
&+\left[D\,\frac{w}{z}z^o\right]^o - \frac{D}{z^2}w - (1+\mu)x\alpha\Big\{\left[DT_1 z'\right]' + \left[DT_1 z^o\right]^o - D\,\frac{T_1}{z} + \\
&+\left[B\tau_2\right]'' + \left[B\tau_2\right]^{oo}\Big\} + Z = 0
\end{aligned} \qquad .. (5c)$$

Boundary Conditions

For the abutments and the base of the dam the boundary conditions, for cases without perimetral joints are,

APPENDIX 'B'

Assumptions

Besides the usual assumptions of the classical theory of thin elastic shells we can assume that for ease of construction double curvature arch dams of constant angle type are usually designed in such a way that vertical curvature and twist of their middle-surface are not very accentuated i.e.

$z \cong R_0$, $z'^2 \ll 1$, $z^{02} \ll 1$

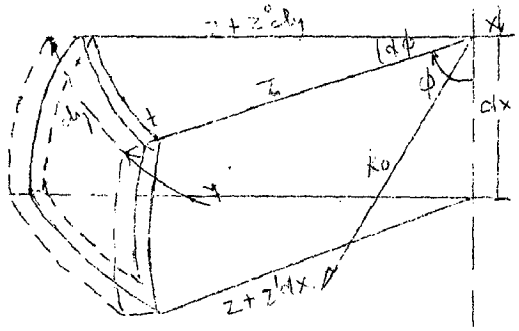

Fig.1 Shell-Element in Cylindrical Coordinate

(a) Stress resultants

$$N_x = \int \sigma_x \, dh, \qquad N_y = \int \sigma_y \, dh, \qquad .. (1a,b)$$

$$N_{xy} = \int \tau_{xy} dh = N_{yx} = \int \tau_{yx} dh, \qquad .. (1c)$$

$$Q_x = \int \tau_{xz} dh, \quad Q_y = \int \tau_{yz} dh, \qquad ...(1d,e)$$

$$M_x = \int \sigma_x h \, dh, M_y = \int \sigma_y h dh \qquad ...(1f,g)$$

$$M_{xy} = \int \tau_{xy} h dh = M_{yx} = \int \tau_{yx} h dh \qquad .. (1h)$$

(b) Equations of equilibrium

$$N'_x + N^o_{xy} + X = 0, \qquad .. (2a)$$

$$N^o_y + N'_{yx} + y = 0, \qquad .. (2b)$$

$$Q'_x + Q^o_y - N_y/z + Z = 0, \qquad .. (2c)$$

$$M'_x + M^o_{xy} + N_x z' + N_{xy} z^o - Q_x = 0, \qquad .. (2d)$$

$$M^o_y + M'_{yx} + N_y z^o + N_{yx} z' - Q_y = 0. \qquad .. (2e)$$

(c) Variation of Temperature

$$T(x,y,h) = T_1(x,y) + h T_2(x,y) \qquad .. (3a)$$

$$u = 0, \quad v = 0, \quad w = 0 \qquad .. \quad (7a\text{-}c)$$

$$w' = w^{o} = 0. \qquad .. \quad (7d)$$

and for cases with perimetral joints,

$$u = 0, \quad v = 0, \quad w = 0, \qquad .. \quad (8a\text{-}c)$$

$$M_x = M_y = 0 \qquad .. \quad (8d)$$

For the crest of the dam the boundary conditions are,

$$M_x = 0, \quad N_{xy} - \frac{M_{xy}}{z} = 0 \qquad .. \quad (9a,b)$$

$$M_x = 0, \quad Q_x + M^{o}_{yx} = 0 \qquad .. \quad (9c,d)$$

APPENDIX 'A'

The analysis was made in terms of the three component displacements at any point in the structure. The six components of stress are given,

$$\frac{1+\sigma}{E}\overline{rr} = \frac{\partial u}{\partial r} + \frac{\sigma}{1-2\sigma}\left(\frac{\partial u}{\partial r} + \frac{u}{r} + \frac{1}{r}\cdot\frac{\partial w}{\partial \theta} + \frac{\partial v}{\partial z}\right),$$

$$\frac{1+\sigma}{E}\overline{\theta\theta} = \frac{1}{r}\cdot\frac{\partial w}{\partial \theta} + \frac{u}{r} + \frac{\sigma}{1-2\sigma}\left(\frac{\partial u}{\partial r} + \frac{u}{r} + \frac{1}{r}\cdot\frac{\partial w}{\partial \theta} + \frac{\partial v}{\partial z}\right),$$

$$\frac{1+\sigma}{E}\overline{zz} = \frac{\partial v}{\partial z} + \frac{\sigma}{1-2\sigma}\left(\frac{\partial u}{\partial r} + \frac{u}{r} + \frac{1}{r}\cdot\frac{\partial w}{\partial \theta} + \frac{\partial v}{\partial z}\right), \qquad \ldots (1)$$

$$\frac{1+\sigma}{E}\overline{\theta z} = \frac{1}{2}\left(\frac{1}{r}\cdot\frac{\partial v}{\partial \theta} + \frac{\partial w}{\partial z}\right),$$

$$\frac{1+\sigma}{E}\overline{zr} = \frac{1}{2}\left(\frac{\partial u}{\partial z} + \frac{\partial v}{\partial r}\right),$$

$$\frac{1+\sigma}{E}\overline{r\theta} = \frac{1}{2}\left(\frac{\partial w}{\partial r} - \frac{w}{r} + \frac{1}{r}\cdot\frac{\partial u}{\partial \theta}\right)$$

where partial differential Young's modulus and σ Poisson's ratio.

The partial differential equations which govern the displacements are,

$$(1-\sigma)\left(\frac{\partial^2 u}{\partial r^2} + \frac{1}{r}\frac{\partial u}{\partial r} - \frac{u}{r^2}\right) + \frac{1-2\sigma}{2}\left(\frac{1}{r^2}\cdot\frac{\partial^2 u}{\partial \theta^2} + \frac{\partial^2 u}{\partial z^2}\right) - \frac{3-4\sigma}{2}\cdot\frac{1}{r^2}\cdot\frac{\partial w}{\partial \theta} + \frac{1}{2}\frac{\partial^2 v}{\partial r\,\partial z} + \frac{1}{2}\cdot\frac{1}{r}\cdot\frac{\partial^2 w}{\partial r\,\partial \theta} = 0$$

$$(1-\sigma)\frac{\partial^2 v}{\partial z^2} + \frac{1-2\sigma}{2}\left(\frac{\partial^2 v}{\partial r^2} + \frac{1}{r}\cdot\frac{\partial v}{\partial r} + \frac{1}{r^2}\cdot\frac{\partial^2 v}{\partial \theta^2}\right) + \frac{1}{2}\cdot\frac{1}{r}\cdot\frac{\partial u}{\partial \theta} + \frac{1}{2}\cdot\frac{1}{r}\cdot\frac{\partial^2 w}{\partial \theta\,\partial z} + \frac{1}{2}\cdot\frac{\partial^2 u}{\partial r\,\partial z} = 0$$

$$(1-\sigma)\frac{1}{r^2}\cdot\frac{\partial^2 w}{\partial \theta^2} + \frac{1-2\sigma}{2}\left(\frac{\partial^2 w}{\partial r^2} + \frac{1}{r}\cdot\frac{\partial w}{\partial r} - \frac{w}{r^2} + \frac{\partial^2 w}{\partial z^2}\right) + \frac{3-4\sigma}{2}\cdot\frac{1}{r^2}\frac{\partial u}{\partial \theta} + \frac{1}{2}\cdot\frac{1}{r}\cdot\frac{\partial^2 u}{\partial r\,\partial \theta} + \frac{1}{2}\cdot\frac{1}{r}\cdot\frac{\partial^2 v}{\partial \theta\,\partial z} = 0 \qquad \ldots (2)$$

These equations must be solved subject to certain boundary conditions.

Table -1

Stiffness Matrix, $|K|$ of an Element in global coordinate system

$$|K| = \begin{bmatrix} D_1 & R_1 & R_2 & R_3 \\ & D_2 & R_4 & R_5 \\ & & D_3 & R_6 \\ & & & D_4 \end{bmatrix}$$

$$|D_1| = \begin{bmatrix} (Ap^{-1}+Bp)\cos^2\theta + FF\sin^2\theta & DF\cos\theta & -(Ap^{-1}+Bp)\sin\theta\cos\theta + FF\sin\theta\cos\theta & -GF\sin\theta\cos\theta & HF\sin\theta \\ & (Ap+Bp^{-1}) & -DF\sin\theta & 0 & 0 \\ & & (Ap^{-1}+Bp)\sin^2\theta + FF\cos^2\theta & -GF\cos^2\theta & HF\cos\theta \\ & & & RF\cos^2\theta & -15\nu t^2\cos\theta \\ & & & & VF \end{bmatrix}$$

$$|D_2| = \begin{bmatrix} (Ap^{-1}+Bp)\cos^2\theta + FF\sin^2\theta & -DF\cos\theta & -(Ap^{-1}+Bp)\sin\theta\cos\theta + FF\sin\theta\cos\theta & GF\sin\theta\cos\theta & HF\sin\theta \\ & Ap+Bp^{-1} & +DF\sin\theta & 0 & 0 \\ & & (Ap^{-1}+Bp)\sin^2\theta + FF\cos^2\theta & GF\cos^2\theta & HF\cos\theta \\ & & & RF\cos^2\theta & 15\nu t^2\cos\theta \\ & & & & VF \end{bmatrix}$$

$$|D_3| = \begin{bmatrix} (Ap^{-1}+Bp)\cos^2\theta + FF\sin^2\theta & -DF\cos\theta & -(Ap^{-1}+Bp)\sin\theta\cos\theta + FF\sin\theta\cos\theta & -GF\sin\theta\cos\theta & -HF\sin\theta \\ & Ap+Bp^{-1} & DF\sin\theta & 0 & 0 \\ & & (Ap^{-1}+Bp)\sin^2\theta + FF\cos^2\theta & -GF\cos^2\theta & -HF\cos\theta \\ & & & RF\cos^2\theta & 15vt^2\cos\theta \\ & & & & VF \end{bmatrix}$$

$$|D_4| = \begin{bmatrix} (Ap^{-1}+Bp)\cos^2\theta + FF\sin^2\theta & DF\cos\theta & -(Ap^{-1}+Bp)\sin\theta\cos\theta + FF\sin\theta\cos\theta & GF\sin\theta\cos\theta & -HF\sin\theta \\ & Ap+Bp^{-1} & -DF\sin\theta & 0 & 0 \\ & & (Ap^{-1}+Bp)\sin^2\theta + FF\cos^2\theta & GF\cos^2\theta & -HF\cos\theta \\ & & & RF\cos^2\theta & -15vt^2\cos\theta \\ & & & & VF \end{bmatrix}$$

$$|R_1| = \begin{bmatrix} (Cp^{-1}-Bp)\cos^2\theta + IF\sin^2\theta & EF\cos\theta & -(Cp^{-1}-Bp)\sin\theta\cos\theta + IF\sin\theta\cos\theta & -JF\sin\theta\cos\theta & KF\sin\theta \\ -EF\cos\theta & -Ap+Bp^{-1} & EF\sin\theta & 0 & 0 \\ -(Cp^{-1}-Bp)\sin\theta\cos\theta + IF\sin\theta\cos\theta & -EF\sin\theta & (Cp^{-1}-Bp)\sin^2\theta + IF\cos^2\theta & -JF\cos^2\theta & KF\cos\theta \\ +JF\sin\theta\cos\theta & 0 & JF\cos^2\theta & SF\cos^2\theta & 0 \\ KF\sin\theta & 0 & KF\cos\theta & 0 & WF \end{bmatrix}$$

$$|R_2| = \begin{bmatrix} (-Ap^{-1}+Bp)\cos^2\theta + LF\sin^2\theta & -EF\cos\theta & -(-Ap^{-1}+Bp)\sin\theta\cos\theta + LF\sin\theta\cos\theta & MF\sin\theta\cos\theta & +NF\sin\theta \\ EF\cos\theta & Cp-Bp^{-1} & -EF\sin\theta & 0 & 0 \\ -(-Ap^{-1}+Bp)\sin\theta\cos\theta + LF\sin\theta\cos\theta & EF\sin\theta & (-Ap^{-1}+Bp)\sin^2\theta + LF\cos^2\theta & MF\cos^2\theta & NF\cos\theta \\ MF\sin\theta\cos\theta & 0 & MF\cos^2\theta & TF\cos^2\theta & 0 \\ -NF\sin\theta & 0 & -NF\cos\theta & 0 & XF \end{bmatrix}$$

$$|R_3| = \begin{bmatrix} (-Cp^{-1}-Bp)\cos^2\theta + OF\sin^2\theta & -DF\cos\theta & -(-Cp^{-1}-Bp)\sin\theta\cos\theta + OF\sin\theta\cos\theta & PF\sin\theta\cos\theta & QF\sin\theta \\ -DF\cos\theta & -Cp-Bp^{-1} & DF\sin\theta & 0 & 0 \\ -(-Cp^{-1}-Bp)\sin\theta\cos\theta + OF\sin\theta\cos\theta & DF\sin\theta & (-Cp^{-1}-Bp)\sin^2\theta + OF\cos^2\theta & PF\cos^2\theta & QF\cos\theta \\ -PF\sin\theta\cos\theta & 0 & -PF\cos^2\theta & UF\cos^2\theta & 0 \\ -QF\sin O & 0 & -QF\cos\theta & 0 & YF \end{bmatrix}$$

$$|R_4| = \begin{bmatrix} (-Cp^{-1}-Bp)\cos^2\theta + OF\sin^2\theta & DF\cos\theta & -(-Cp^{-1}-Bp)\sin\theta\cos\theta + OF\sin\theta\cos\theta & -PF\sin\theta\cos\theta & QF\sin\theta \\ DF\cos\theta & -Cp-Bp^{-1} & -DF\sin\theta & 0 & 0 \\ -(-Cp^{-1}-Bp)\sin\theta\cos\theta + OF\sin\theta\cos\theta & -DF\sin\theta & (-Cp^{-1}-Bp)\sin^2\theta + OF\cos^2\theta & -PF\cos^2\theta & QF\cos\theta \\ PF\sin\theta\cos\theta & 0 & PF\cos^2\theta & UF\cos^2\theta & 0 \\ -GF\sin\theta & 0 & -QF\cos\theta & 0 & YF \end{bmatrix}$$

$$|R_5| = \begin{bmatrix} (-Ap^{-1}+Bp)\cos^2\theta + LF\sin^2\theta & EF\cos\theta & -(-Ap^{-1}+Bp)\sin\theta\cos\theta + LF\sin\theta\cos\theta & -MF\sin\theta\cos\theta & NF\sin\theta \\ -EF\cos\theta & Cp-Bp^{-1} & EF\sin\theta & 0 & 0 \\ -(-Ap^{-1}+Bp)\sin\theta\cos\theta + LF\sin\theta\cos\theta & -EF\sin\theta & (-Ap^{-1}+Bp)\sin^2\theta + LF\cos^2\theta & -MF\cos^2\theta & NF\cos\theta \\ -MF\sin\theta\cos\theta & 0 & -MF\cos^2\theta & TF\cos^2\theta & 0 \\ -NF\sin\theta & 0 & -NF\cos\theta & 0 & XF \end{bmatrix}$$

$$|R_6| = \begin{bmatrix} (Cp^{-1}-Bp)\cos^2\theta + IF\sin^2\theta & -EF\cos\theta & -(Cp^{-1}-Bp)\sin\theta\cos\theta + IF\sin\theta\cos\theta & -JF\sin\theta\cos\theta & -KF\sin\theta \\ EF\cos\theta & -Ap+Bp^{-1} & -EF\sin\theta & 0 & 0 \\ -(Cp^{-1}-Bp)\sin\theta\cos\theta + IF\sin\theta\cos\theta & +EF\sin\theta & (Cp^{-1}-Bp)\sin^2\theta + IF\cos^2\theta & -JF\cos^2\theta & -KF\cos\theta \\ JF\sin\theta\cos\theta & 0 & JF\cos^2\theta & SF\cos^2\theta & 0 \\ -KF\sin\theta & 0 & -KF\cos\theta & 0 & WF \end{bmatrix}$$

where,

$p=a/b$, $p^{-1}=b/a$, $A=60+\frac{30\nu^2}{1-\nu}$, $B=22.5(1-\nu)$, $C=30-\frac{30\nu^2}{1-\nu}$

$DF=22.5(1+\nu)$, $EF=22.5(1-3\nu)$, $FF=(42-12\nu+60p^2+60p^{-2})t^2/ab$

$GF=(30p+3p^{-1}+12\nu p^{-1})t^2/b$, $HF=(30p^{-1}+3p+12\nu p)t^2/a$,

$IF=(-42+12\nu-60p^2+30p^{-2})t^2/ab$, $JF=[30p+3(1-\nu)p^{-1}]t^2/b$

$KF=(15p^{-1}-3p-12\nu p)t^2/a$, $LF=(-42+12\nu-60p^{-2}+30p^2)t^2/ab$,

$MF=(-15p+3p^{-1}+12\nu p^{-1})t^2/b$, $NF=[30p^{-1}+3(1-\nu)p]t^2/a$,

$OF=(42-12\nu-30p^2-30p^{-2})t^2/ab$, $PF=[-15p+3(1-\nu)p^{-1}]t^2/b$

$QF=[15p^{-1}-3(1-\nu)p]t^2/a$, $RF=20p+4(1-\nu)p^{-1}]t^2$

$SF=[10p-(1-\nu)p^{-1}]t^2$, $TF=[10p-4(1-\nu)p^{-1}]t^2$

$UF=[5p+(1-\nu)p^{-1}]t^2$, $VF=[20p^{-1}+4(1-\nu)p]t^2$

$WF=[10p^{-1}-4(1-\nu)p]t^2$, $XF=[10p^{-1}-(1-\nu)p]t^2$, $YF=[5p^{-1}+(1-\nu)p]t^2$

Table 2. Stress Matrix for 'In Plane' Forces.

$$\frac{E}{(1-\nu^2)ab}$$

-b	$-\nu a$	0	νa	b	0	0	0
$-\nu b$	-a	0	a	νb	0	0	0
-ma-nb	-mb-na	ma+nb	-mb+na	-ma+nb	mb+na	ma-nb	mb-na
0	$-\nu a$	-b	νa	0	0	b	0
0	-a	$-\nu b$	a	0	0	νb	0
-ma+nb	-mb-na	ma-nb	-mb+na	-ma-nb	mb+na	ma+nb	mb-na
-b	0	0	0	b	-va	0	νa
$-\nu b$	0	0	0	νb	-a	0	a
ma-nb	-mb+na	ma+nb	-mb-na	-ma+nb	mb-na	ma-nb	mb+na
0	0	-b	0	0	$-\nu a$	b	νa
0	0	$-\nu b$	0	0	-a	νb	a
-ma+nb	-mb+na	ma-nb	-mb-na	-ma-nb	mb-na	ma+nb	mb+nb

$$m = \frac{1-v}{4}, \quad n = v/2$$

$$\sigma^P = S^P u^P$$

Table 3. Stress (Moment) Matrix for Bending Forces

$$\frac{Et^3}{12(1-\nu^2)ab} \times$$

$6p^{-1}+6\nu p$	$-4\nu a$	$4b$	$-6\nu p$	$-2\nu a$	0	$-6p^{-1}$	0	$2b$	0	0	0
$6\nu p^{-1}+6p$	$-4a$	$4\nu b$	$-6p$	$-2a$	0	$-6\nu p^{-1}$	0	$2\nu b$	0	0	0
$-(1-\nu)$	$(1-\nu)b$	$-(1-\nu)a$	$1-\nu$	0	$(1-\nu)a$	$1-\nu$	$-(1-\nu)b$	0	$-(1-\nu)$	0	0
$-6\nu p$	$2\nu a$	0	$6p^{-1}+6\nu p$	$4\nu a$	$4b$	0	0	0	$-6p^{-1}$	0	$2b$
$-6p$	$2a$	0	$6\nu p^{-1}+6p$	$4a$	$4\nu b$	0	0	0	$-6\nu p^{-1}$	0	$2\nu b$
$-(1-\nu)$	0	$-(1-\nu)a$	$1-\nu$	$(1-\nu)b$	$(1-\nu)a$	$1-\nu$	0	0	$-(1-\nu)$	$-(1-\nu)b$	0
$-6p^{-1}$	0	$-2b$	0	0	0	$6p^{-1}+6\nu p$	$-4\nu a$	$-4b$	$-6\nu p$	$-2\nu a$	0
$-6\nu p^{-1}$	0	$-2\nu b$	0	0	0	$6\nu p^{-1}+6p$	$-4a$	$-4\nu b$	$-6p$	$-2a$	0
$-(1-\nu)$	$(1-\nu)b$	0	$1-\nu$	0	0	$1-\nu$	$-(1-\nu)b$	$-(1-\nu)a$	$-(1-\nu)$	0	$(1-\nu)a$
0	0	0	$-6p^{-1}$	0	$-2b$	$-6\nu p$	$2\nu a$	0	$6p^{-1}+6\nu p$	$4\nu a$	$-4b$
0	0	0	$-6\nu p^{-1}$	0	$-2\nu b$	$-6p$	$2a$	0	$6\nu p^{-1}+6p$	$4a$	$-4\nu b$
$-(1-\nu)$	0	0	$1-\nu$	$(1-\nu)b$	0	$1-\nu$	0	$-(1-\nu)a$	$-(1-\nu)$	$-(1-\nu)b$	$(1-\nu)a$

$$p = a/b, \quad p^{-1} = b/a$$

$$M^P = S^B U^B$$

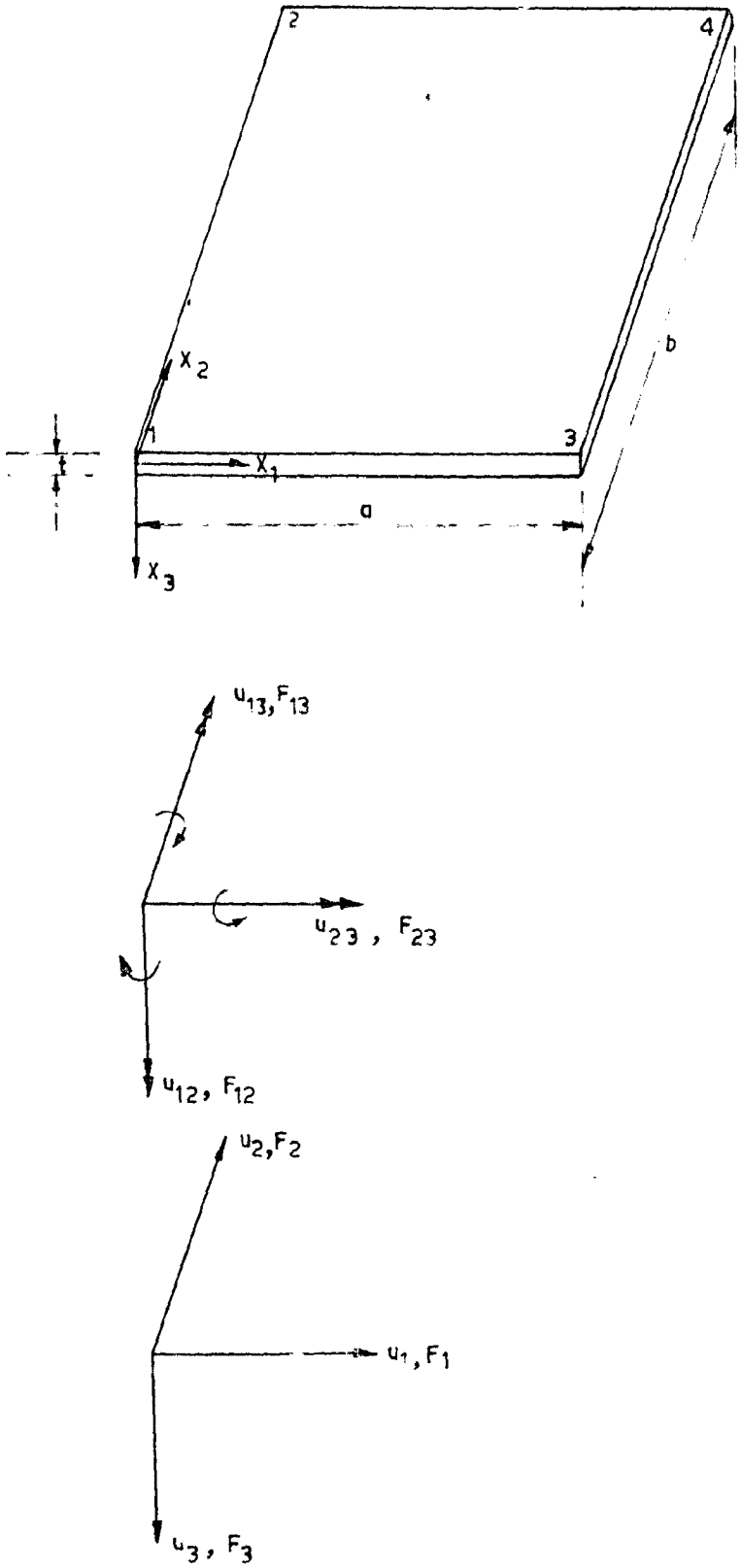

A TYPICAL ELEMENT

FIG. 20

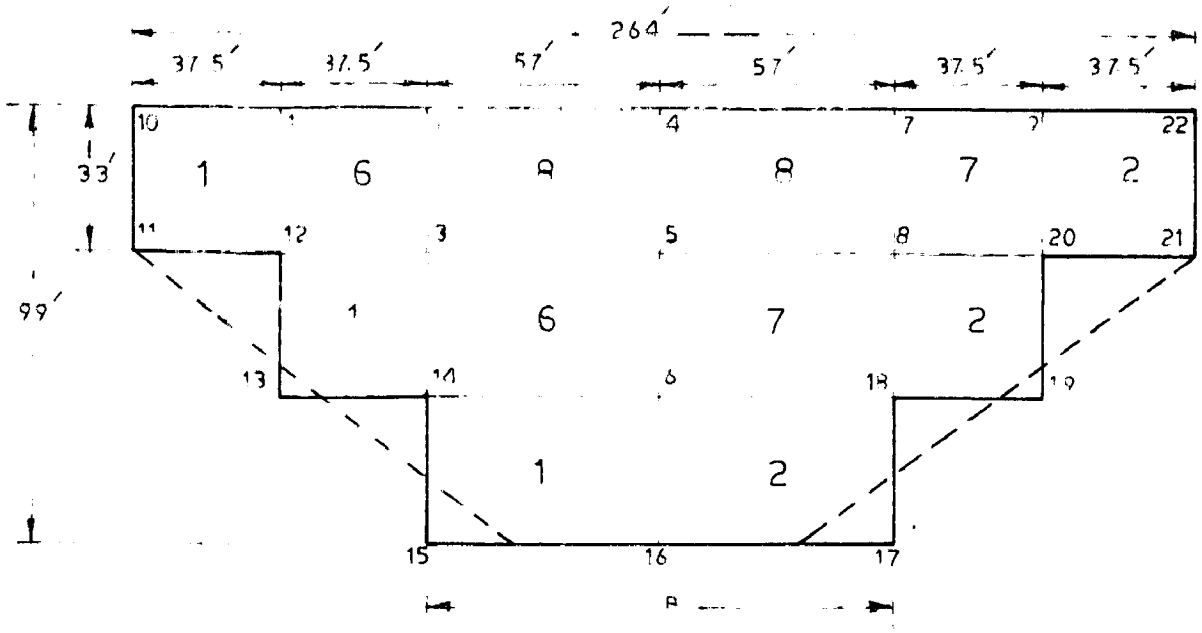

FIG. 1

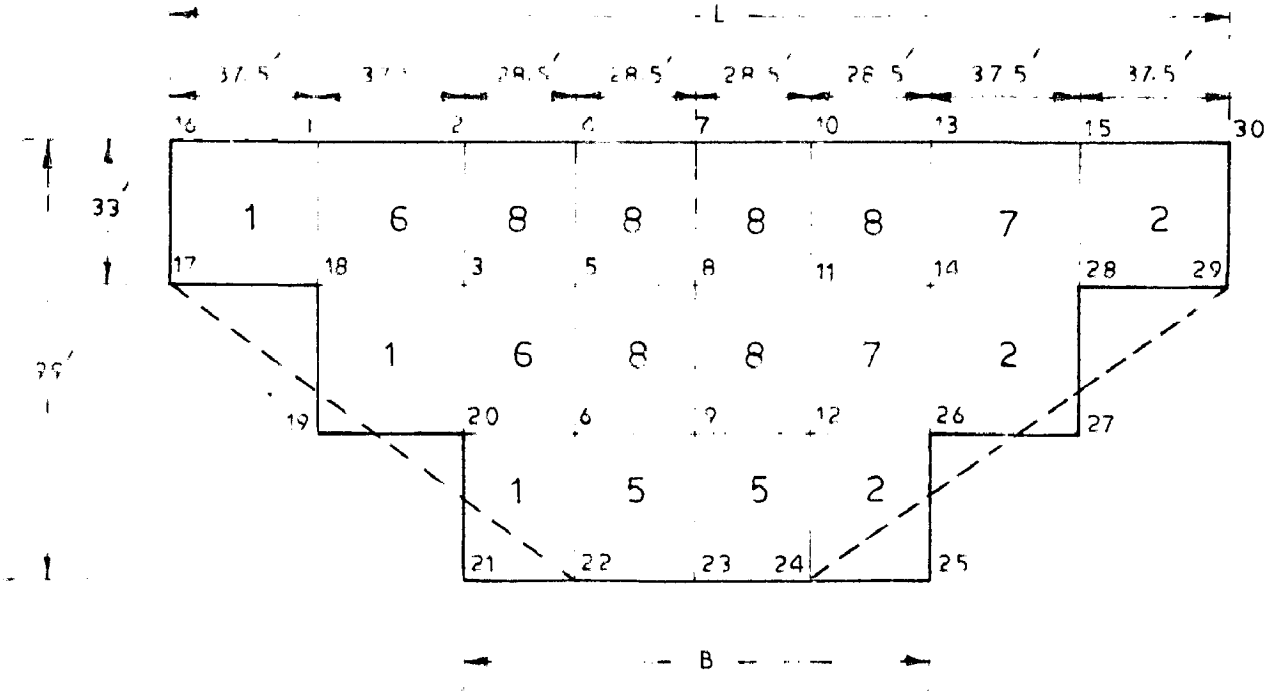

FIG. 2

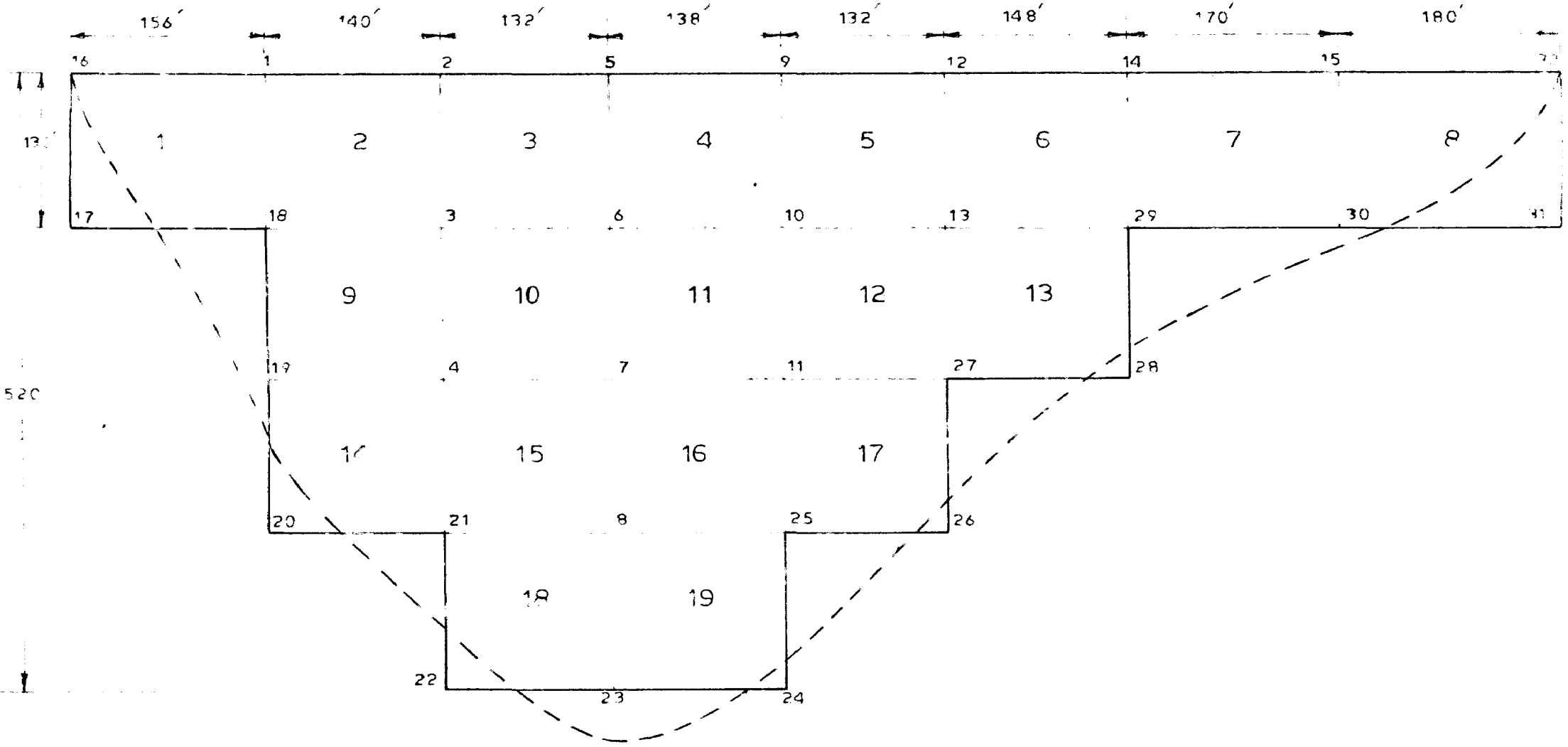

FIG. 3 _ DEVELOPED - SURFACE - OF AN ACTUAL PROFILE

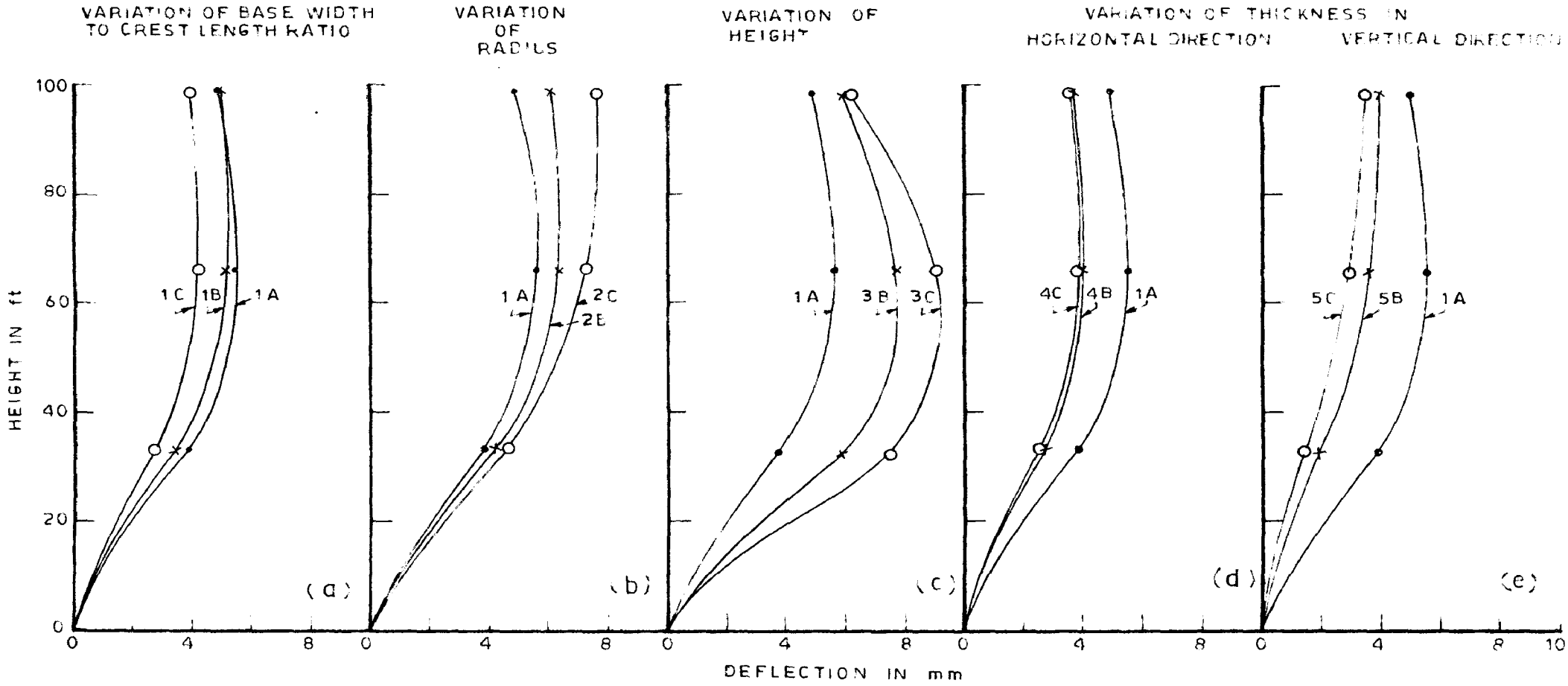

FIG. 4 _ RADIAL DEFLECTION OF CENTRAL CANTILEVER DUE TO HYDROSTATIC LOAD

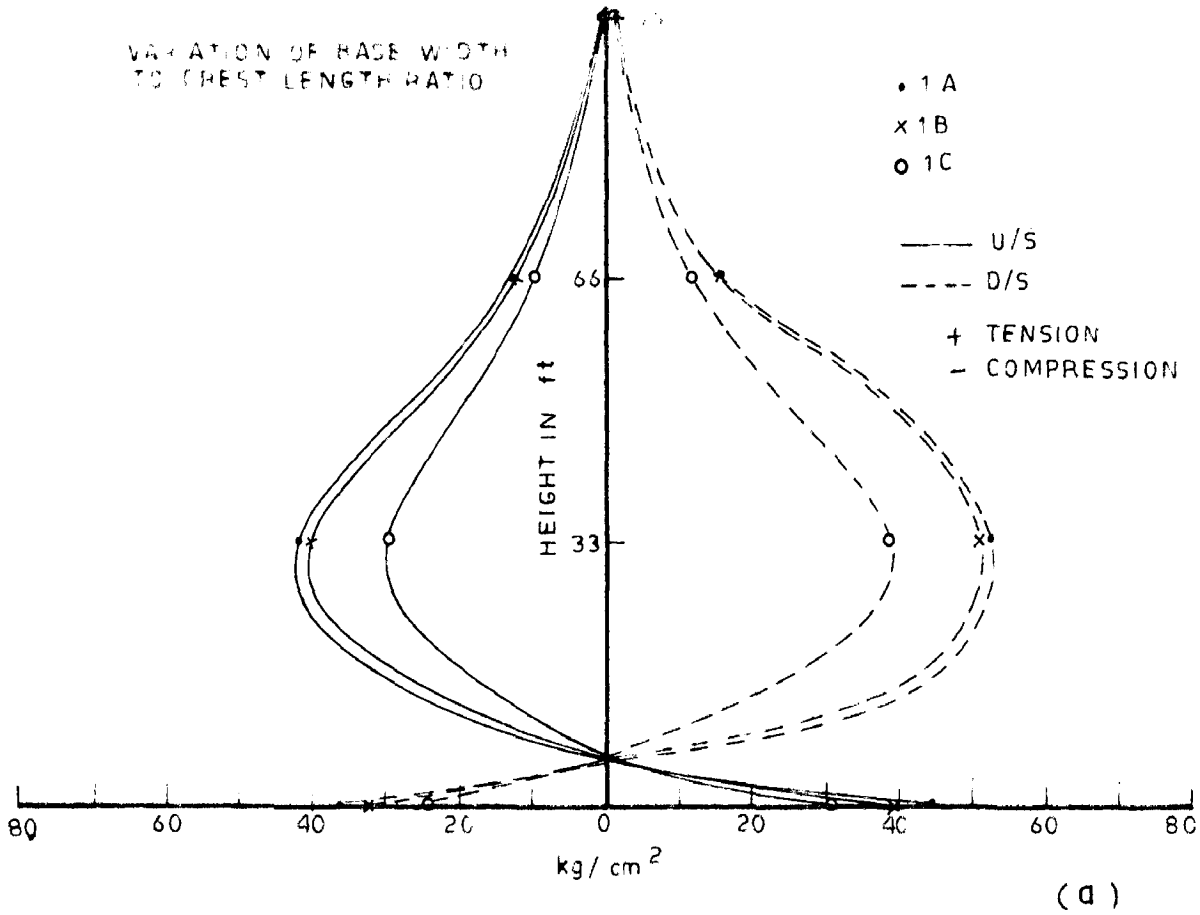

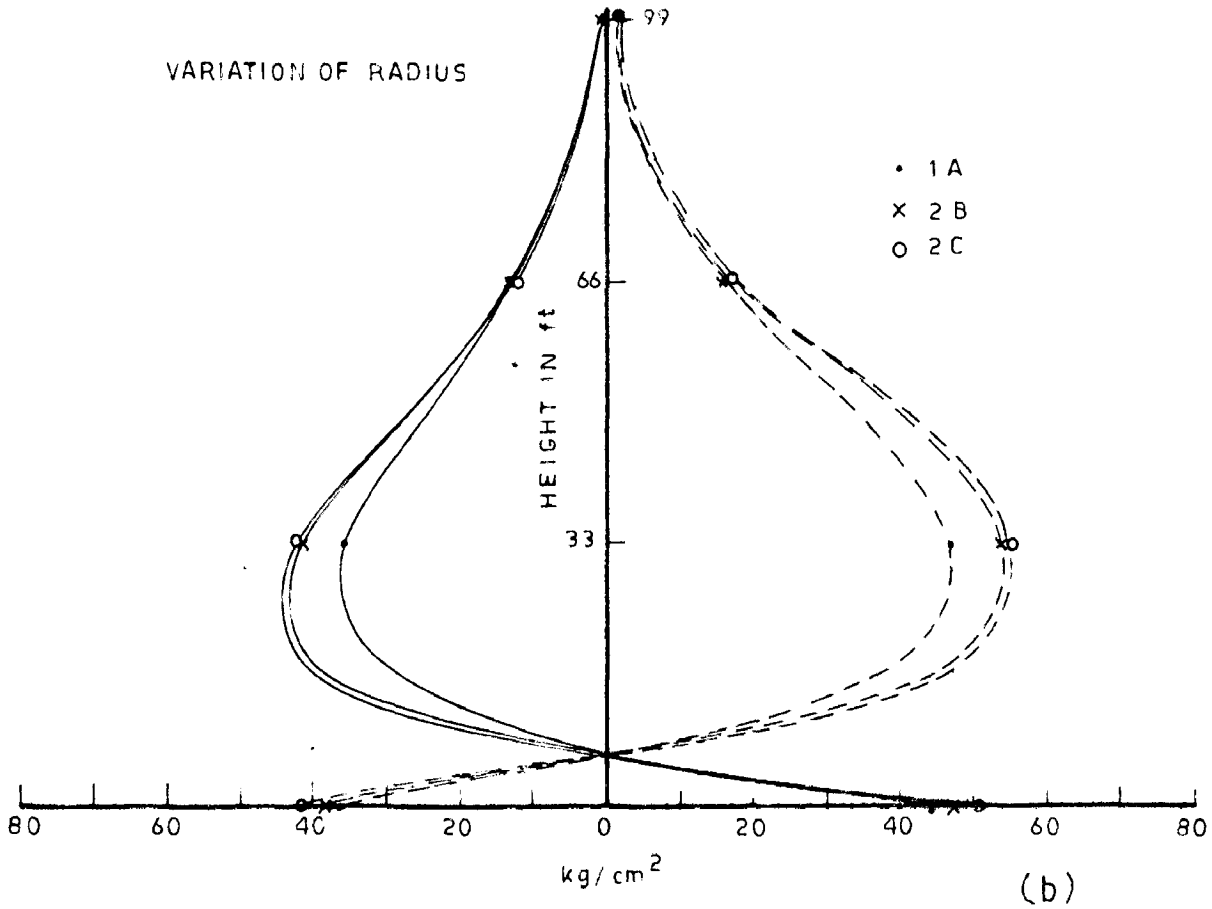

FIG 5 _ VERTICAL STRESSES DUE TO WATER LOAD

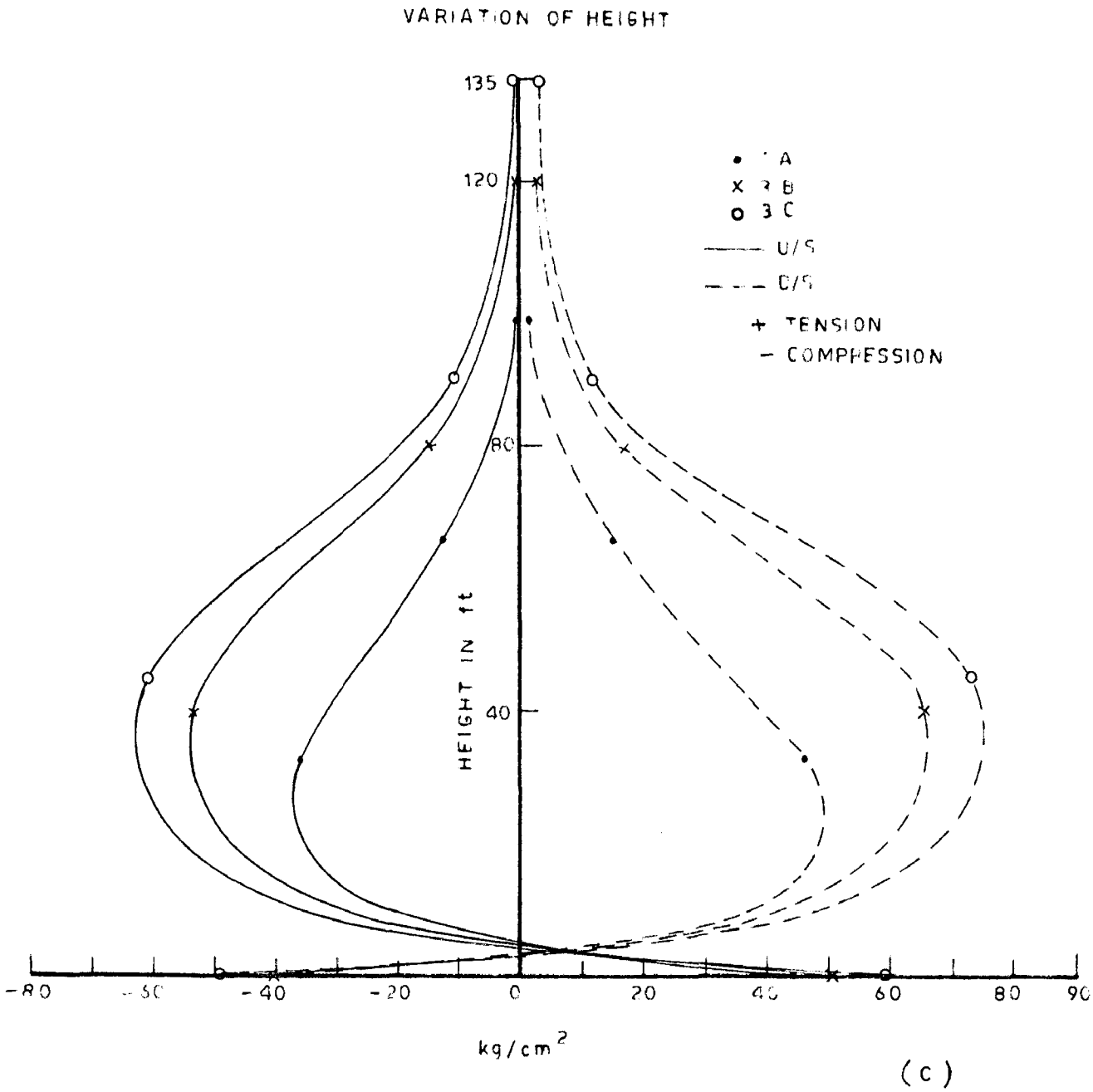

FIG. 5 _VERTICAL STRESSES DUE TO WATER LOAD

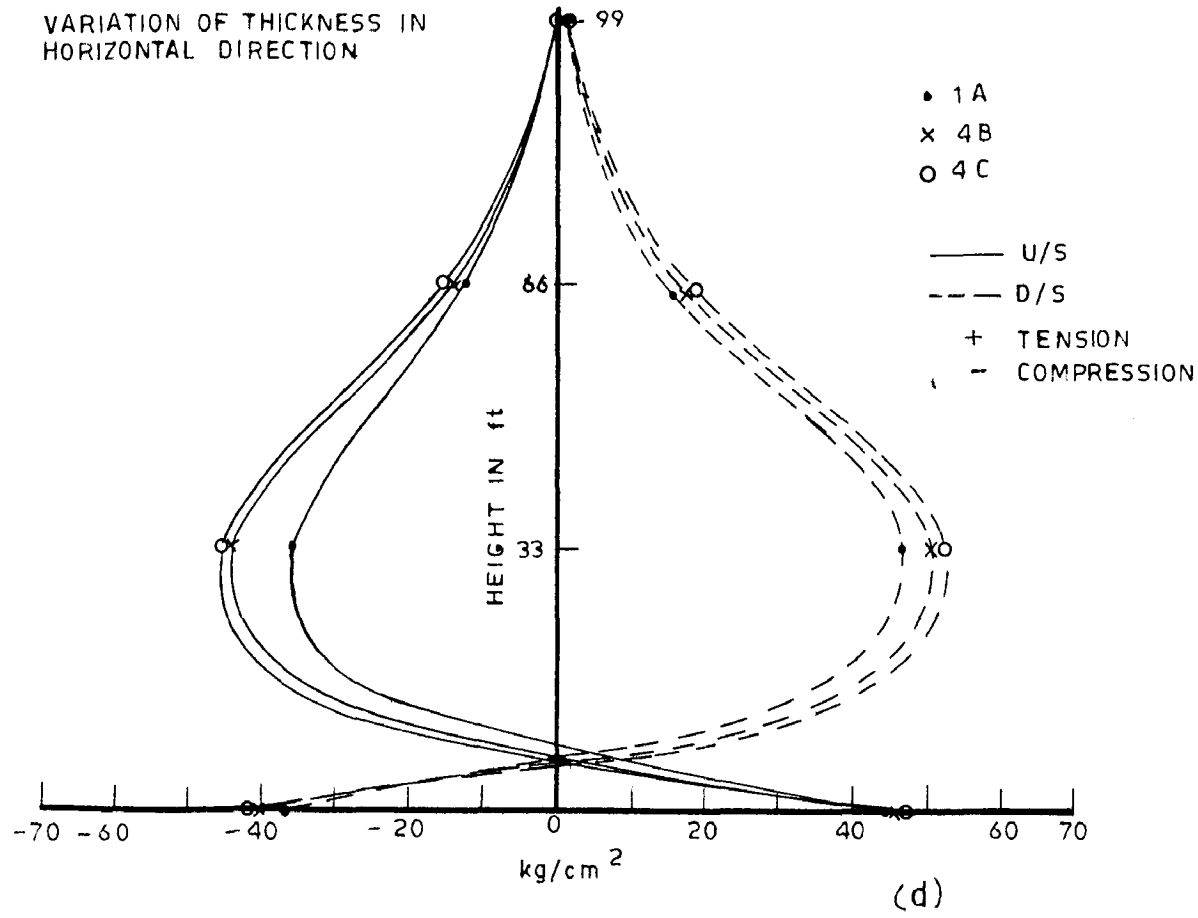

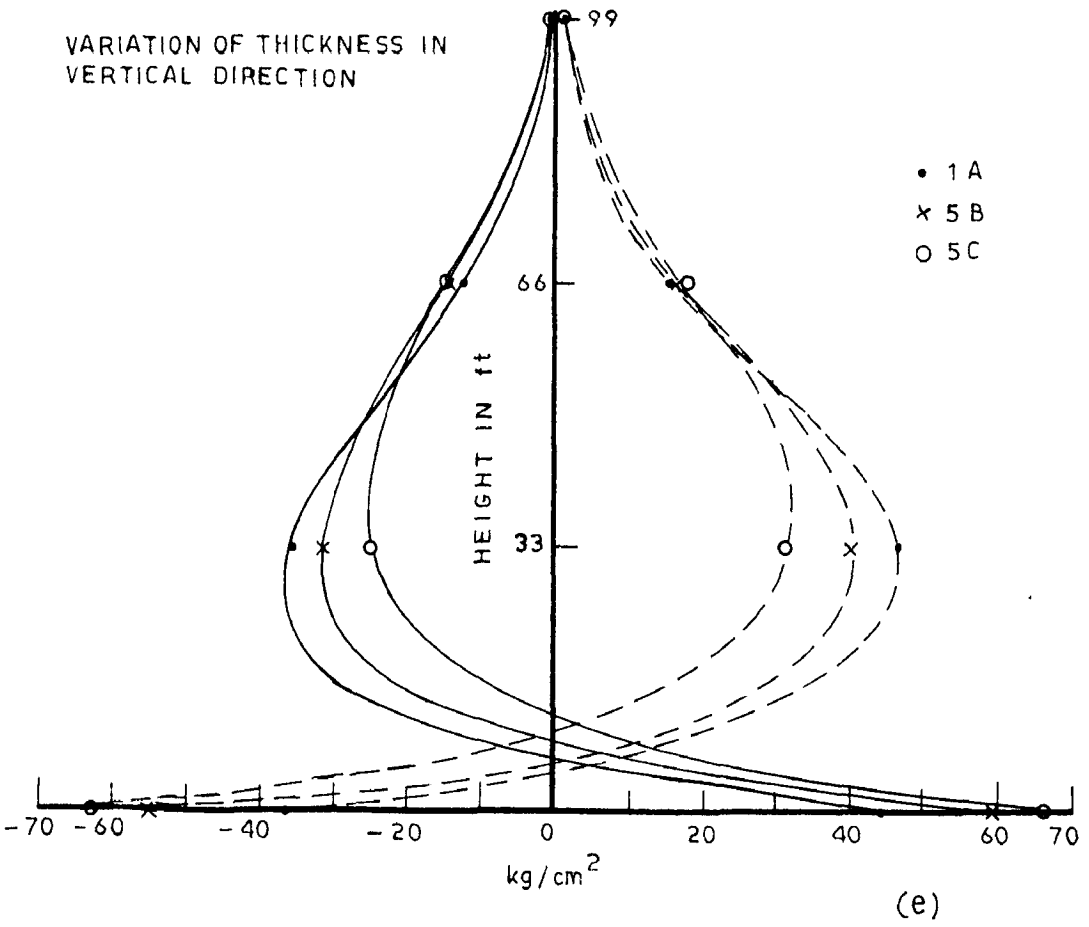

FIG. 5 _VERTICAL STRESSES DUE TO WATER LOAD

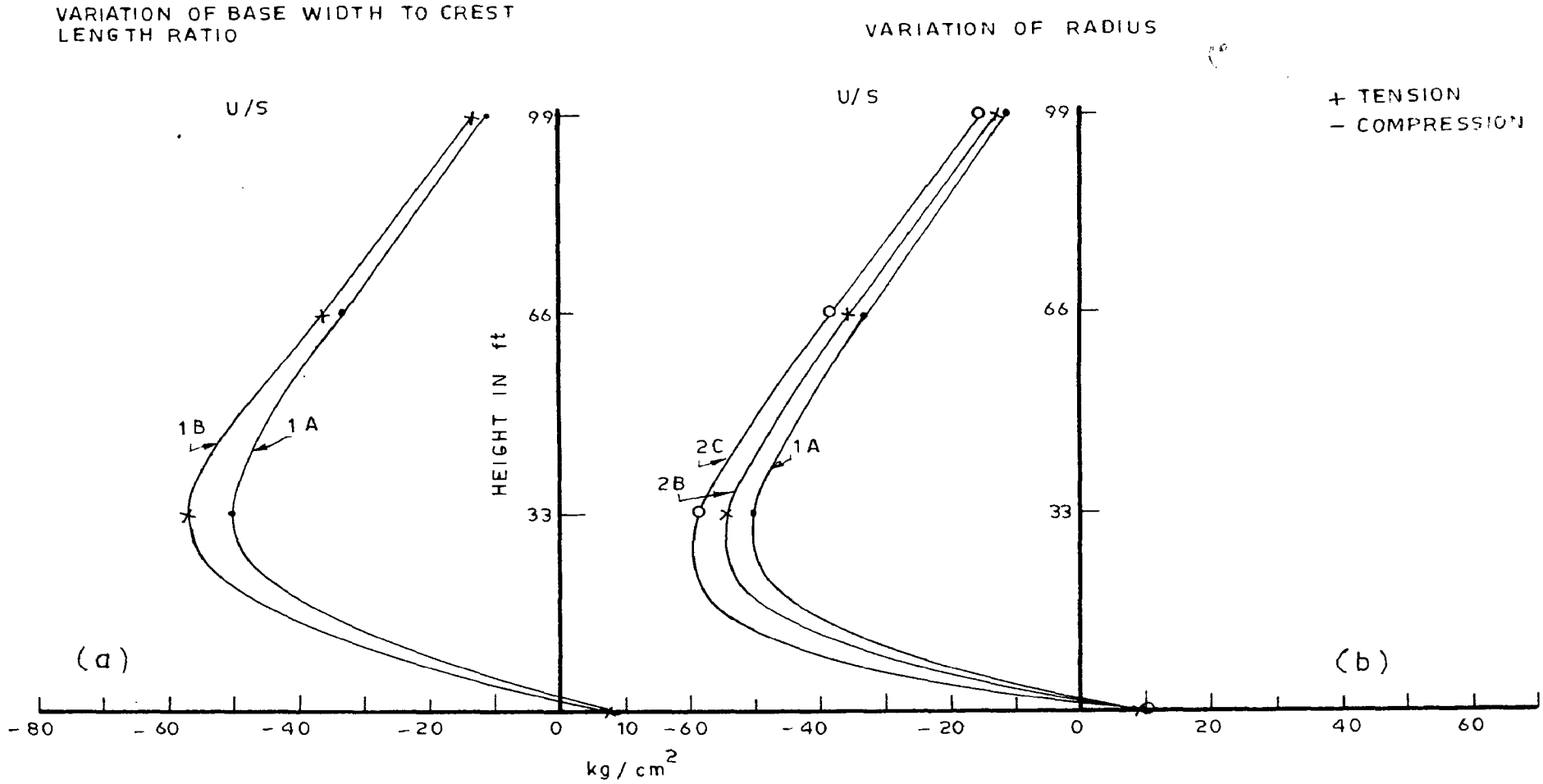

FIG. 6 _HOOP STRESSES ON CENTRAL CANTILEVER WATER LOAD

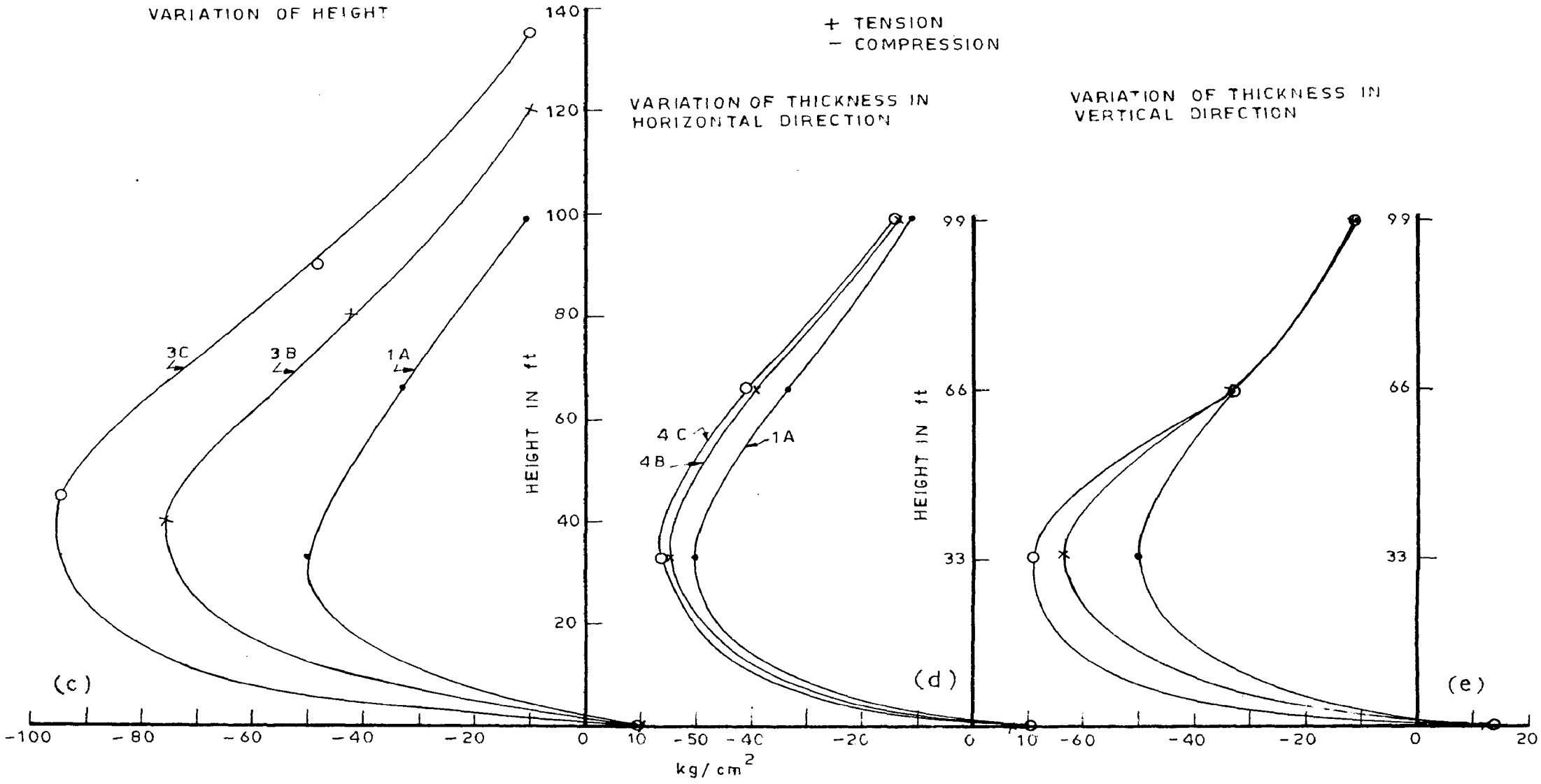

FIG. 6 _HOOP STRESSES DUE TO WATER LOAD

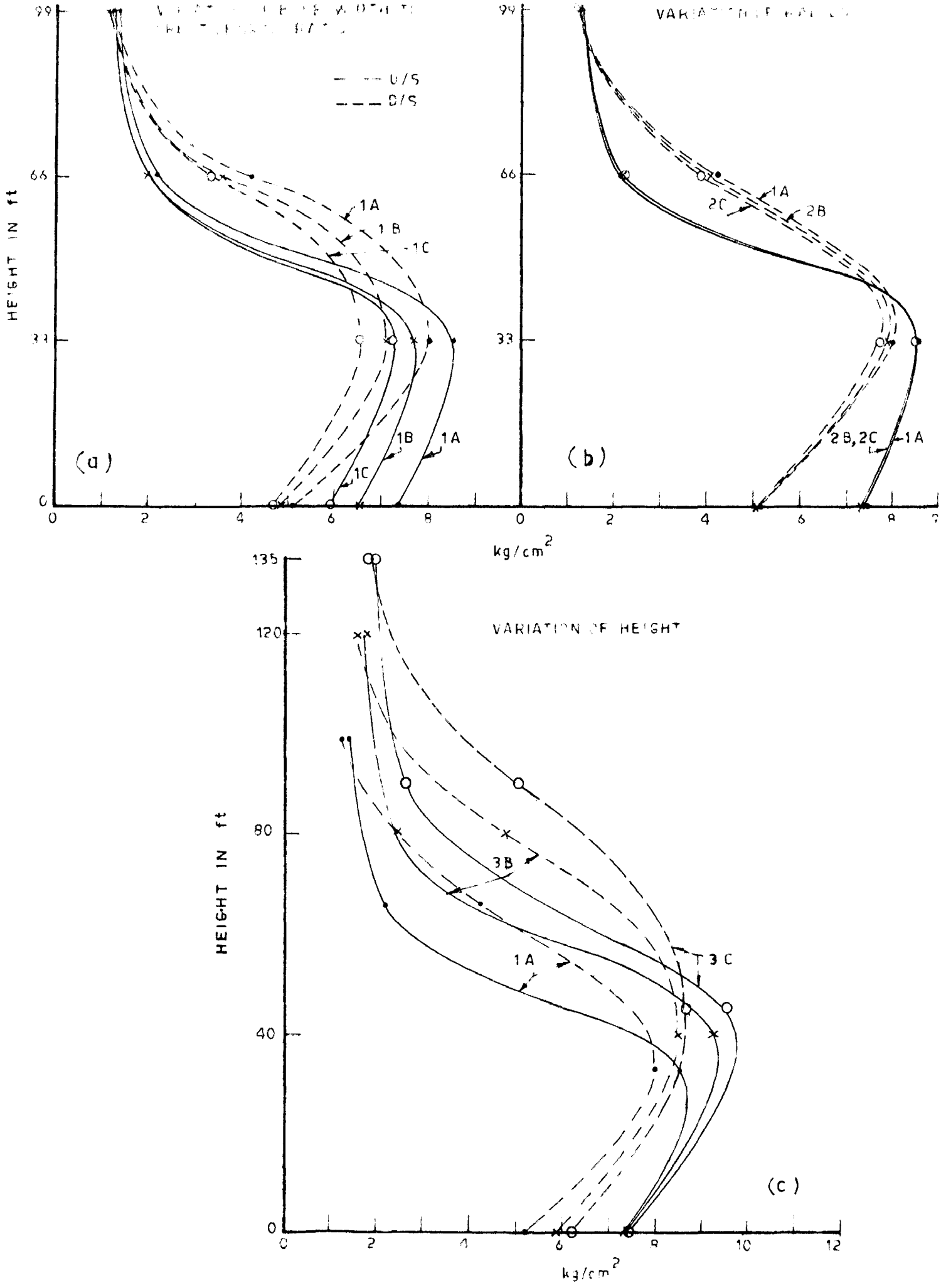

FIG. 7 _VERTICAL STRESSES ON CENTRAL CANTILEVER DEAD LOAD

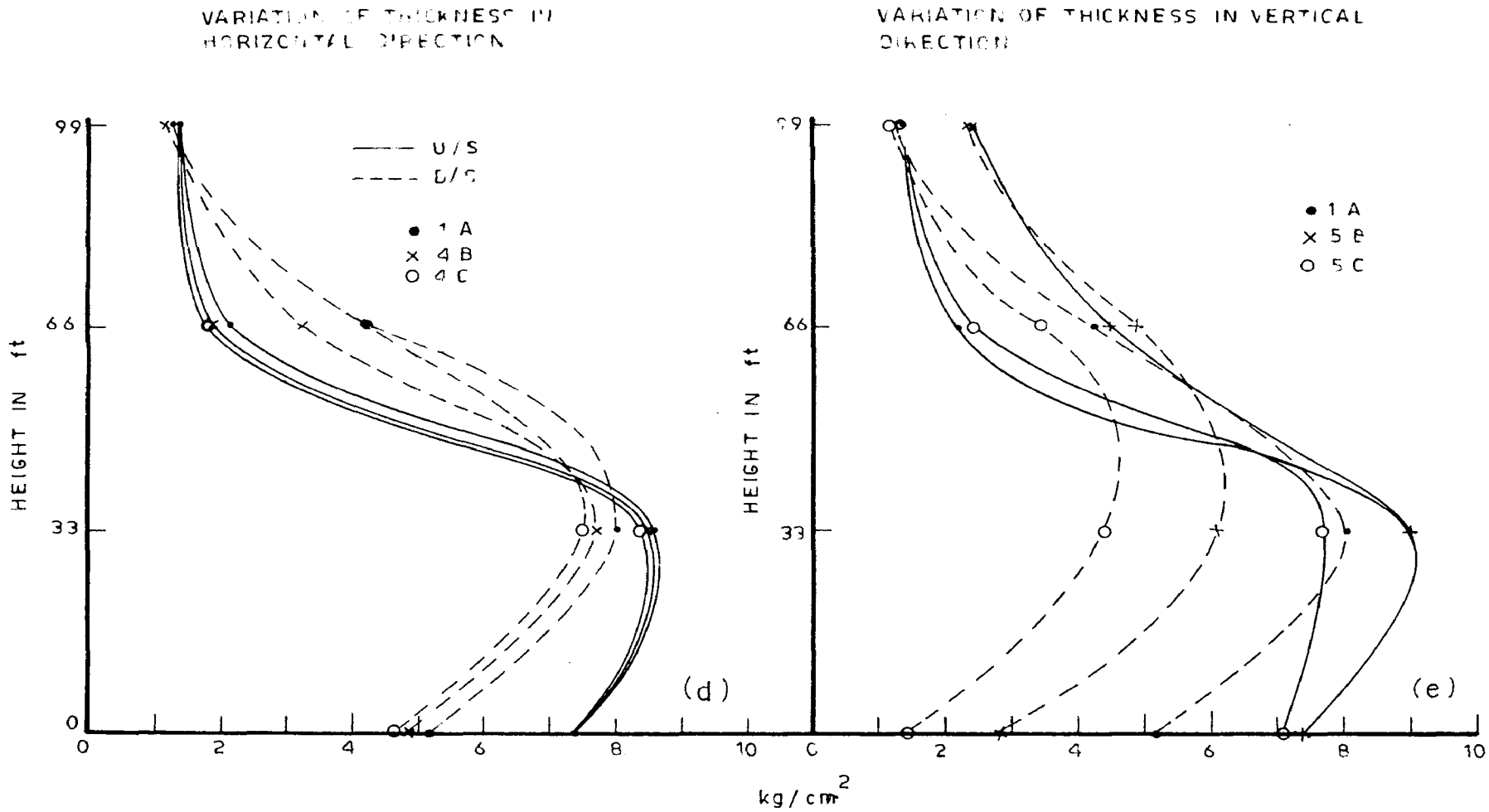

FIG. 7 _ VERTICAL STRESSES ON CENTRAL CANTILEVER DUE TO DEAD LOAD

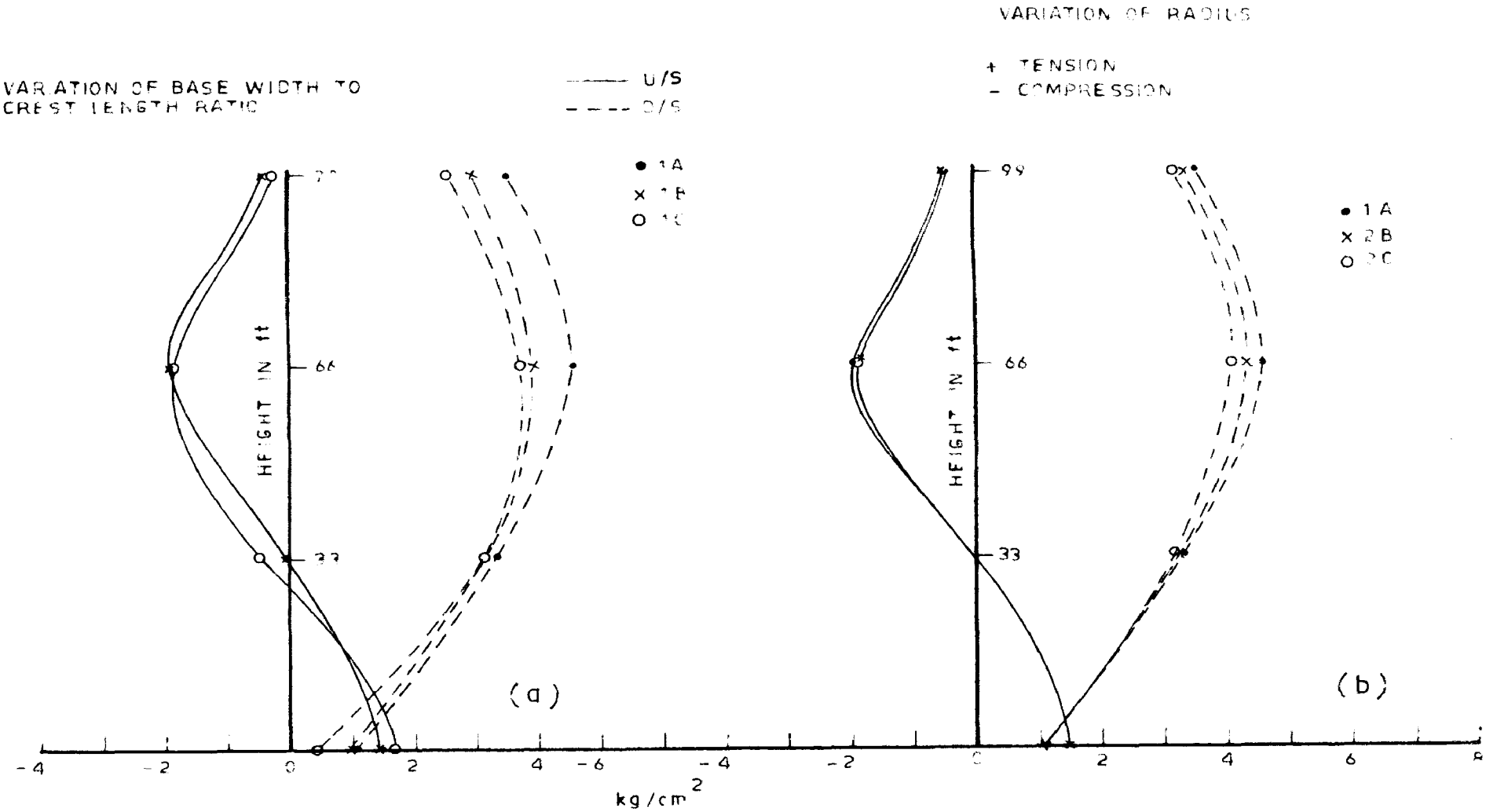

FIG 8 _ HOOP STRESSES ON CENTRAL CANTILEVER DEAD LOAD

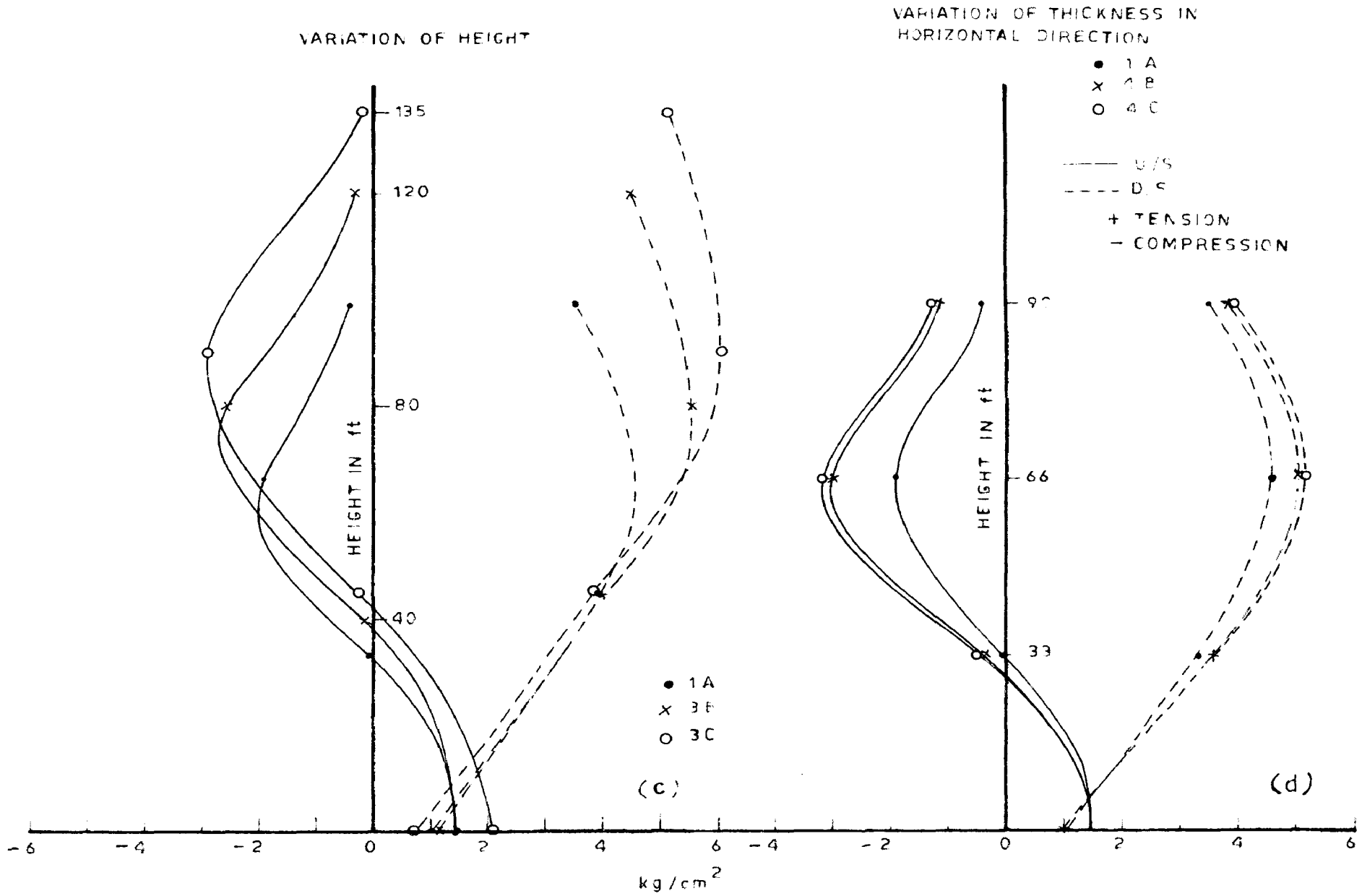

FIG. 8 _HOOP STRESSES DUE TO DEAD LOAD

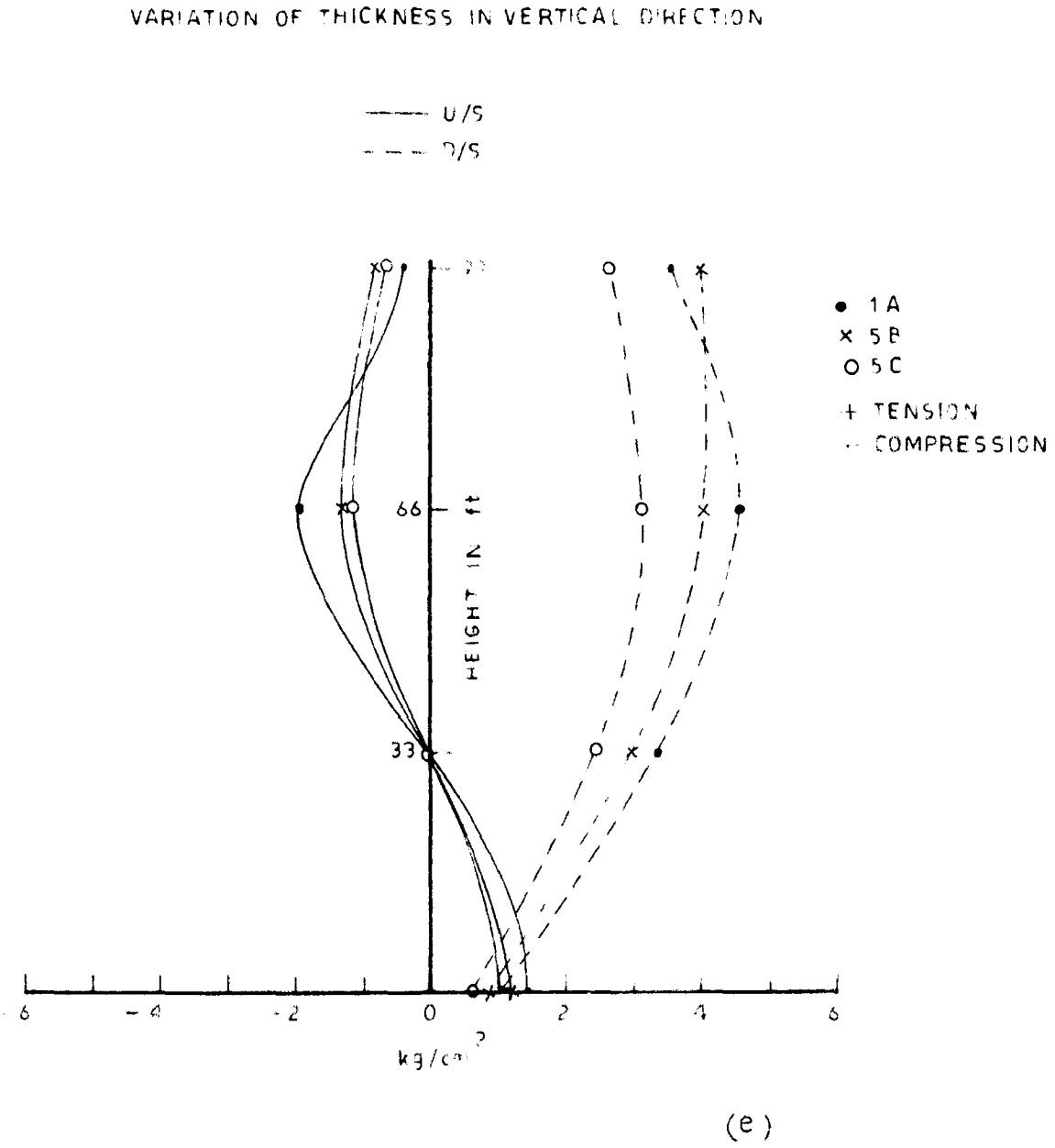

FIG 8 _HOOP STRESSES DUE TO DEAD LOAD

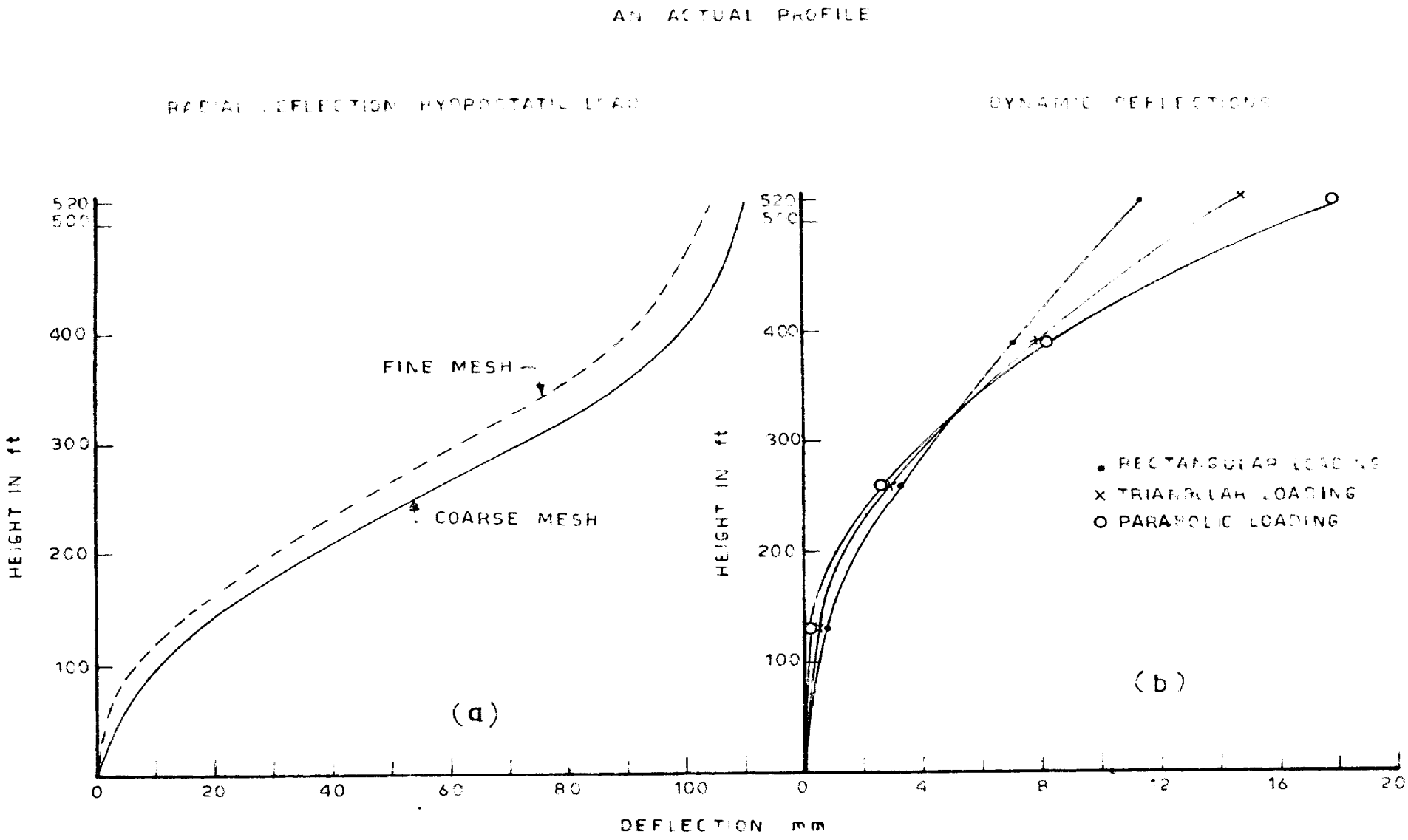

FIG. 9 _ RADIAL DEFLECTION OF LONGEST CANTILEVER

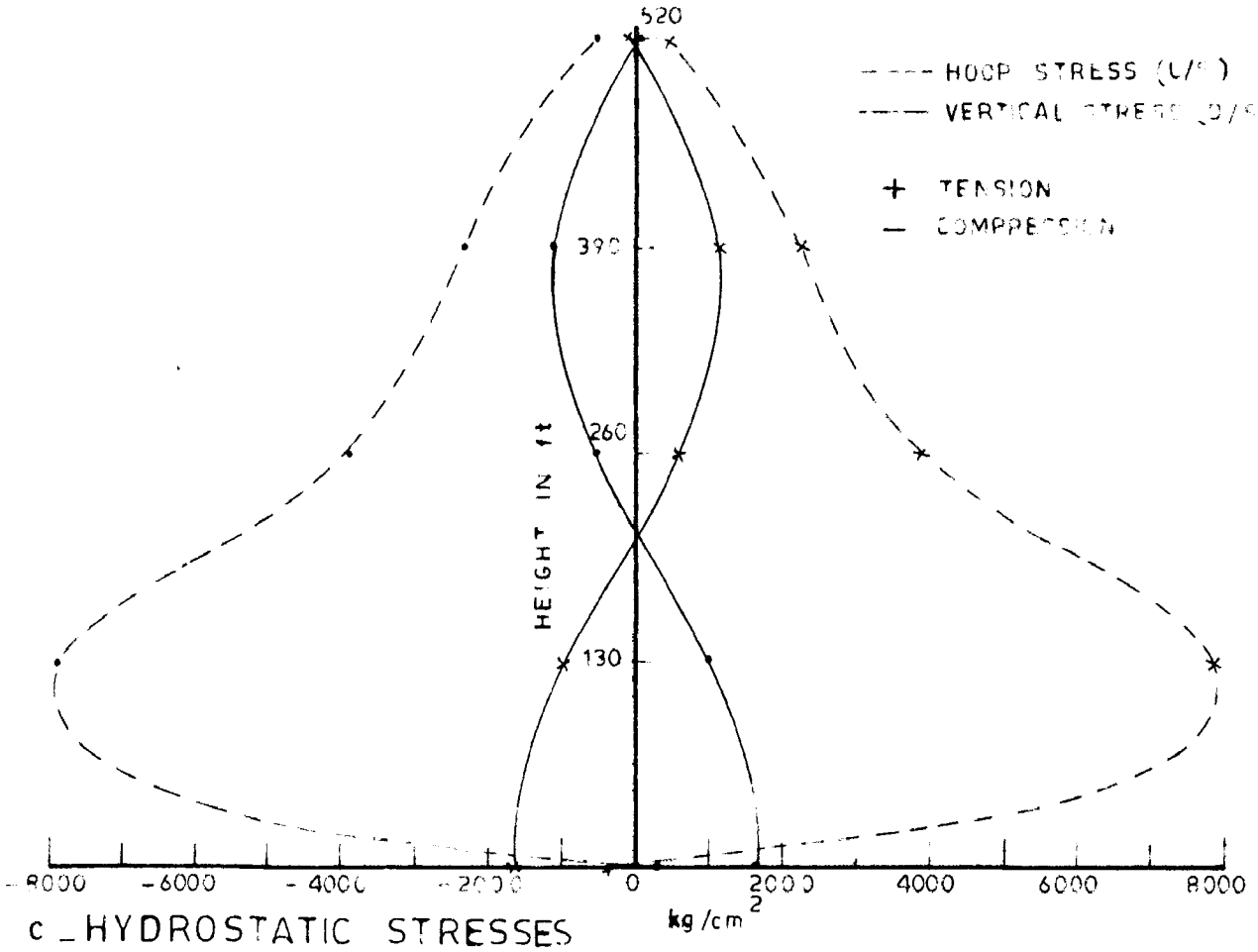

c _ HYDROSTATIC STRESSES

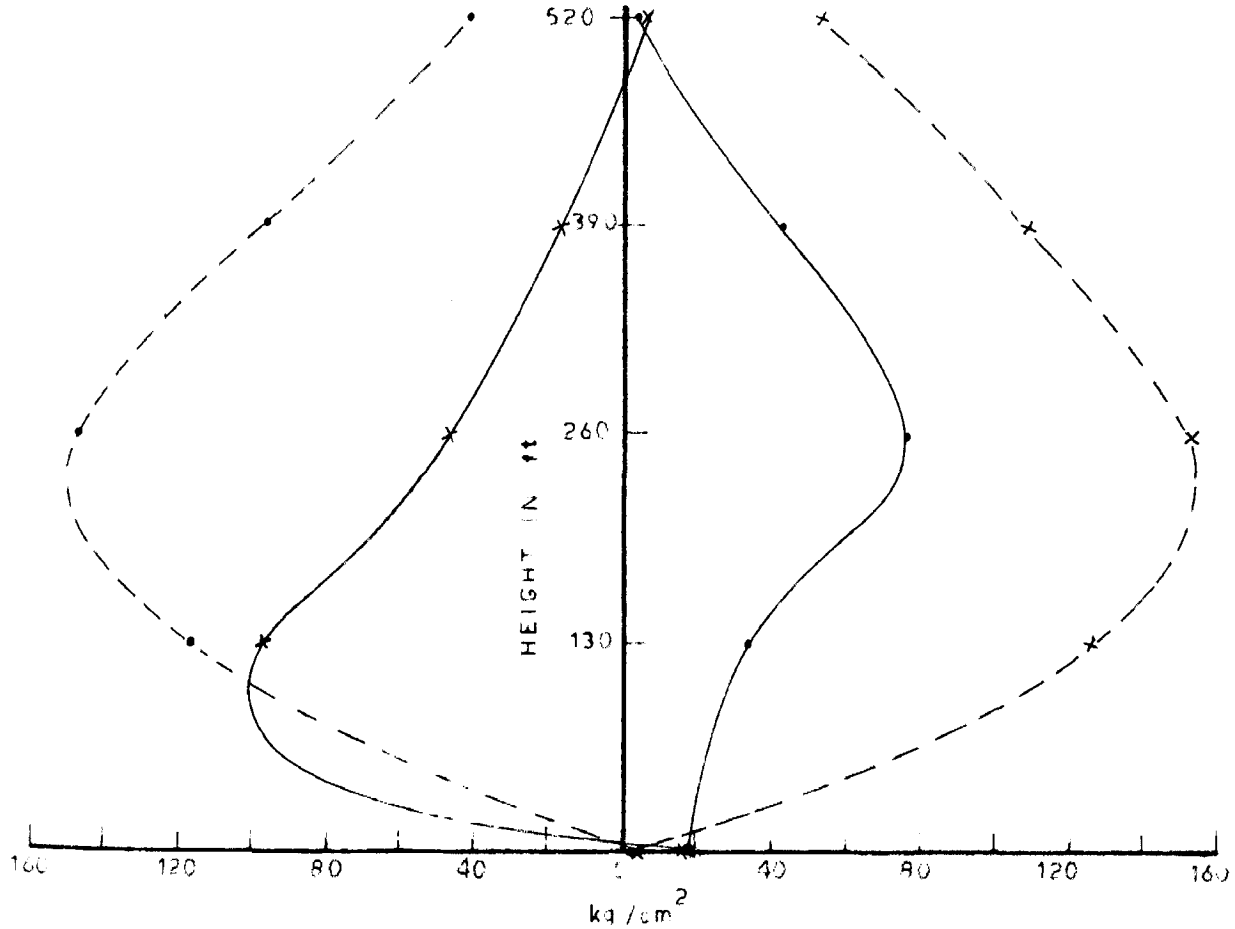

d _ DEAD LOAD - STRESSES

FIG. 9

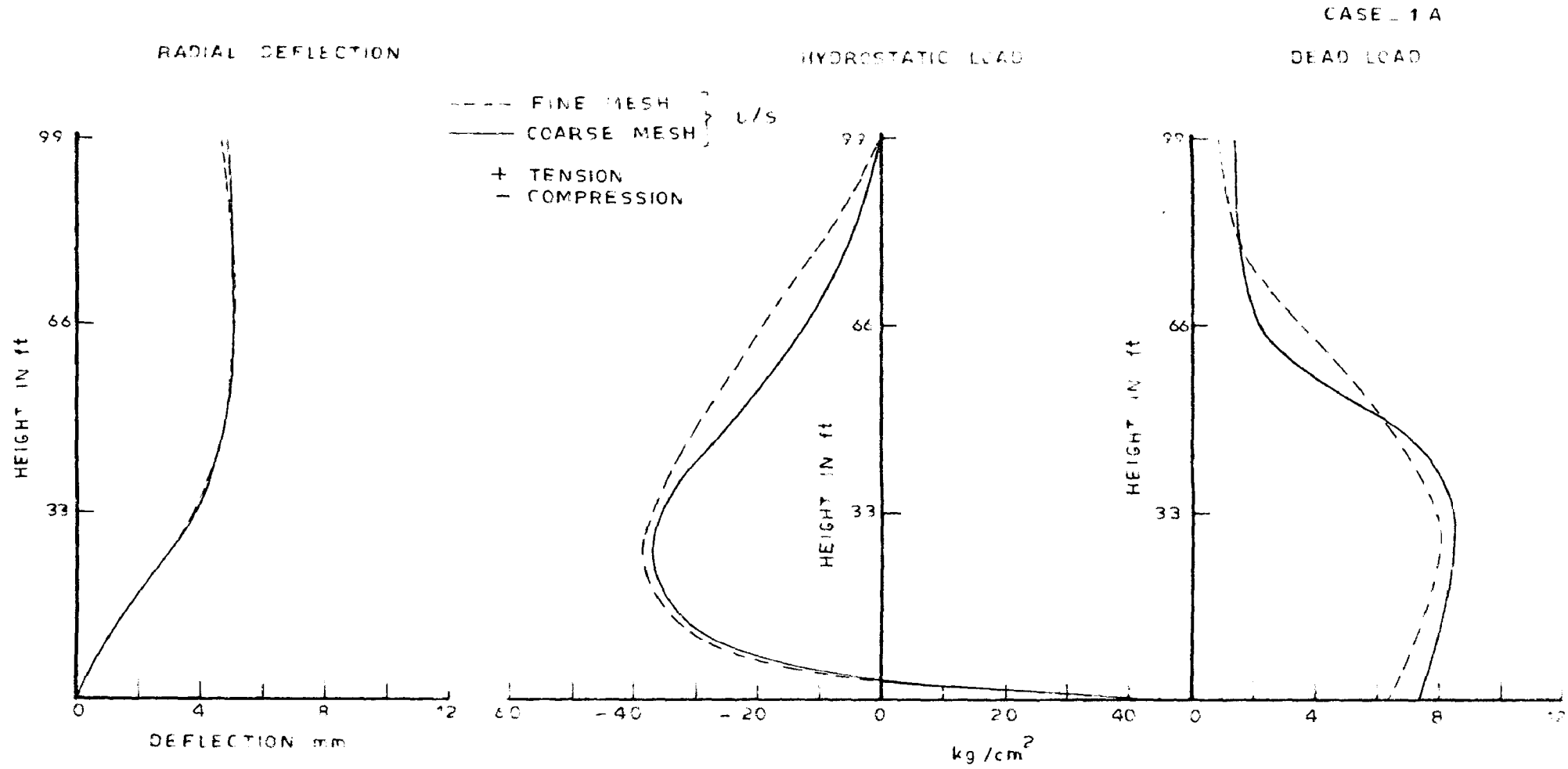

FIG.10 _ COMPARISION OF DEFLECTION AND VERTICAL STRESSES

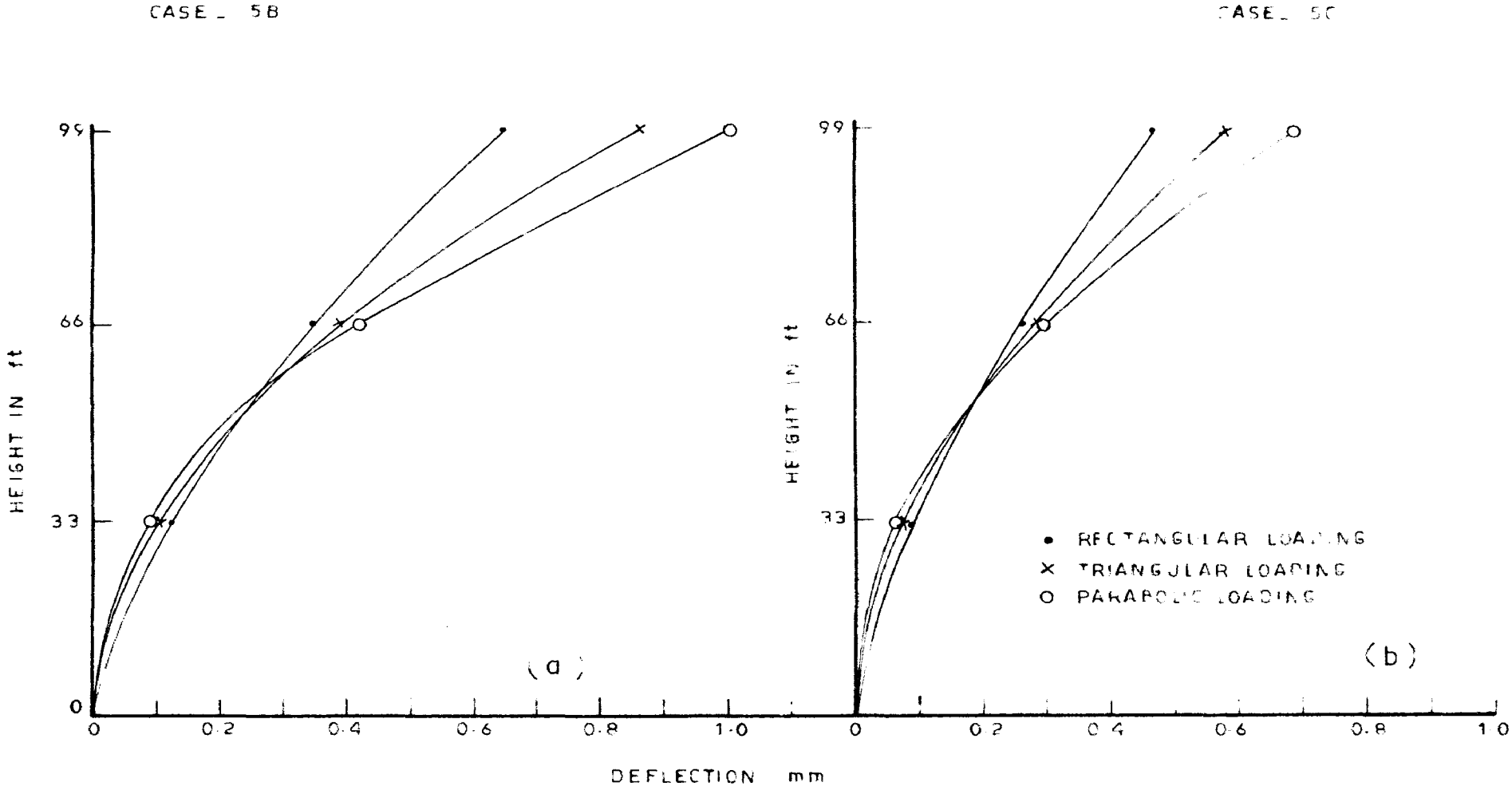

FIG 11 _ DEFLECTION DUE TO DYNAMIC LOADING

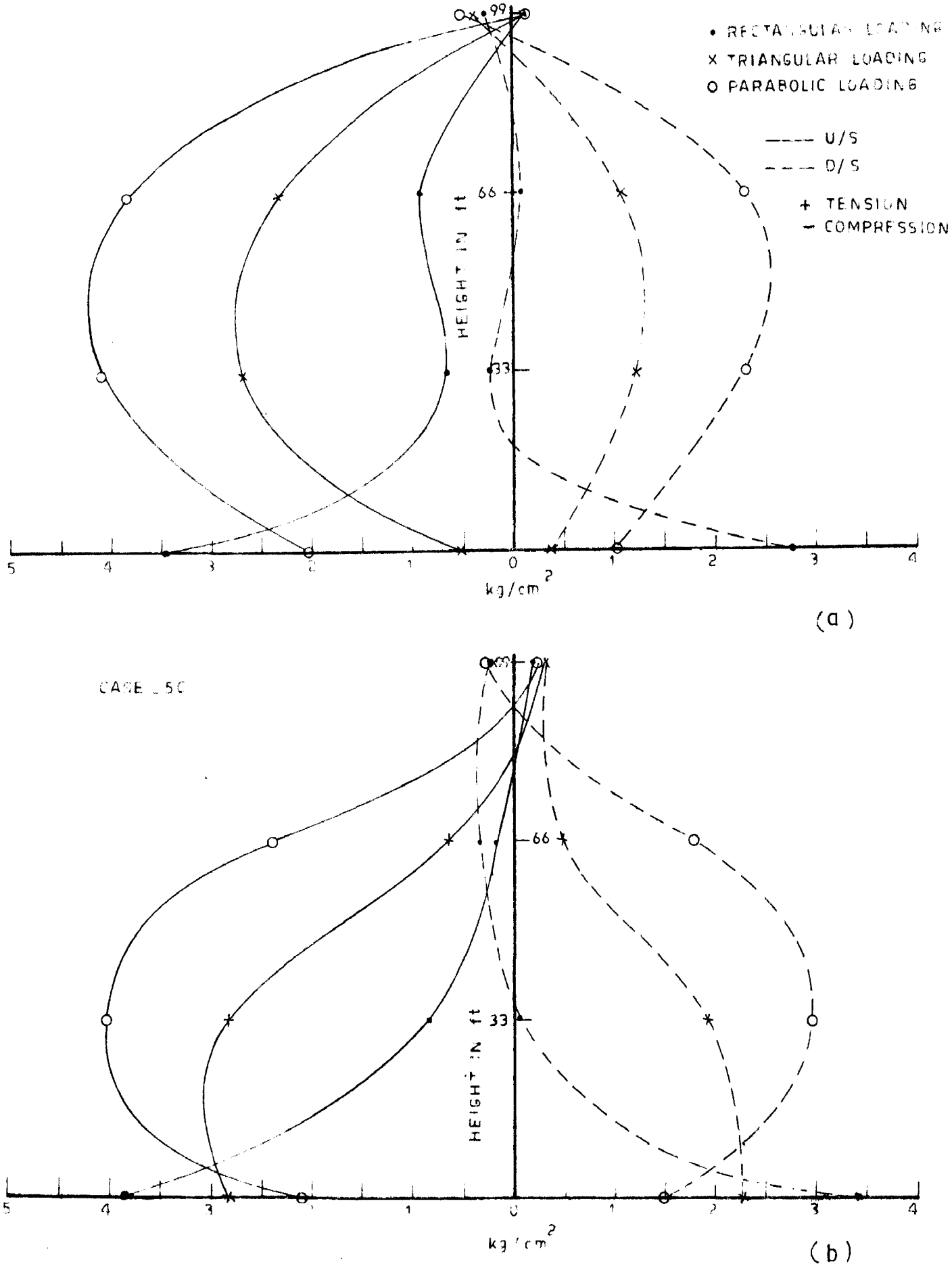

FIG 12 - VERTICAL STRESS (DYNAMIC CASE)

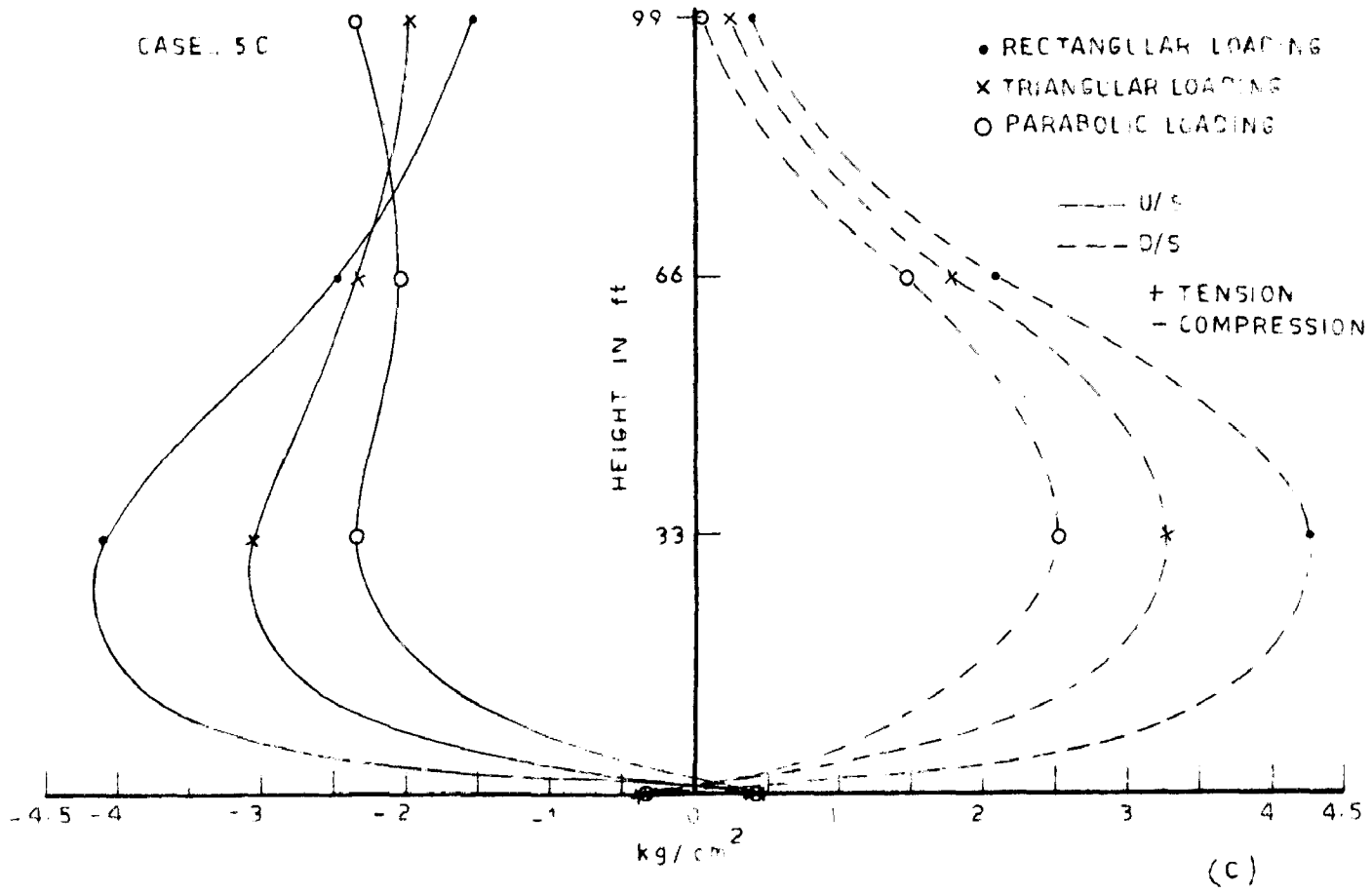

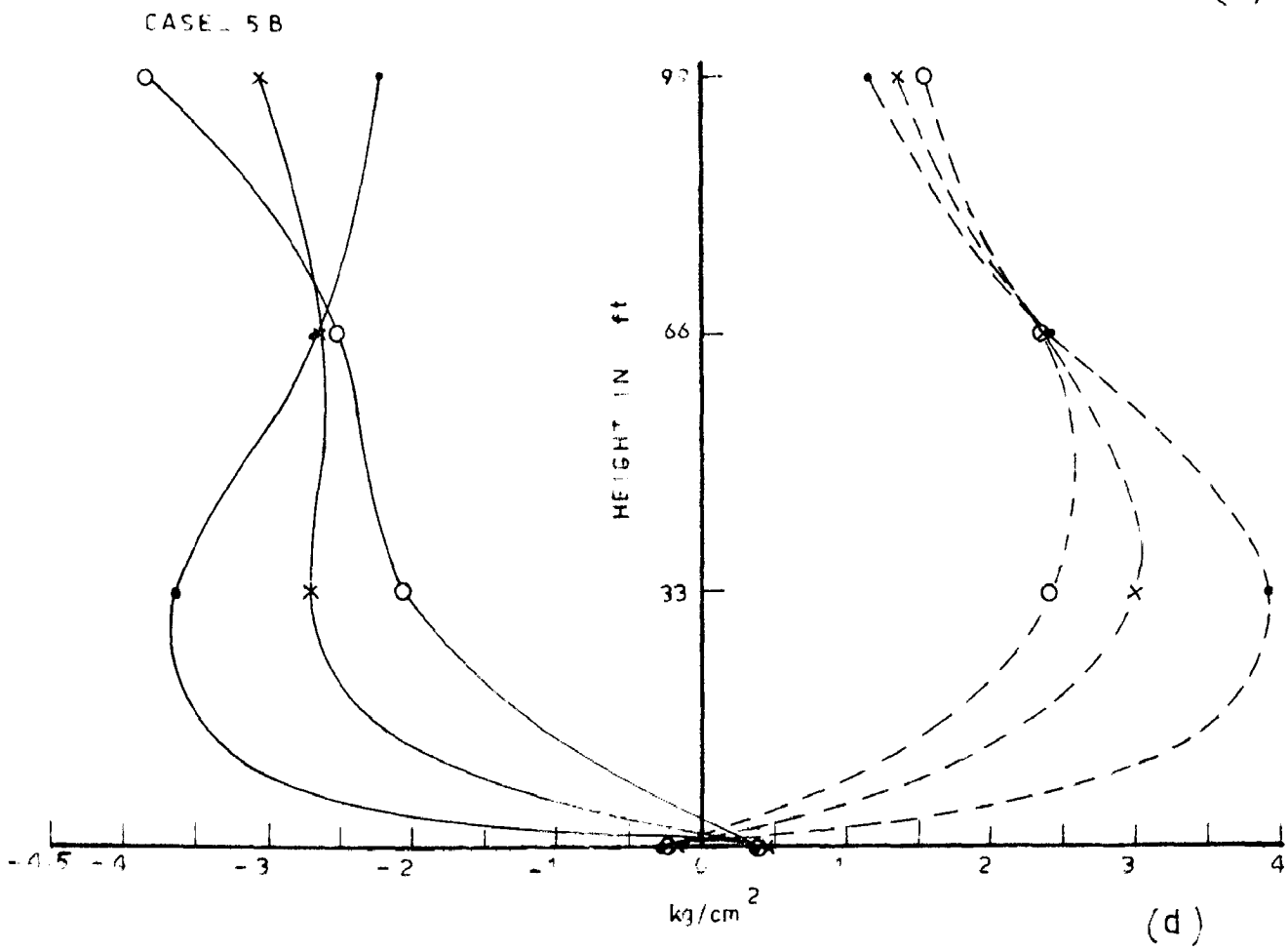

FIG. 12 _ HOOP-STRESSES (DYNAMIC CASE)

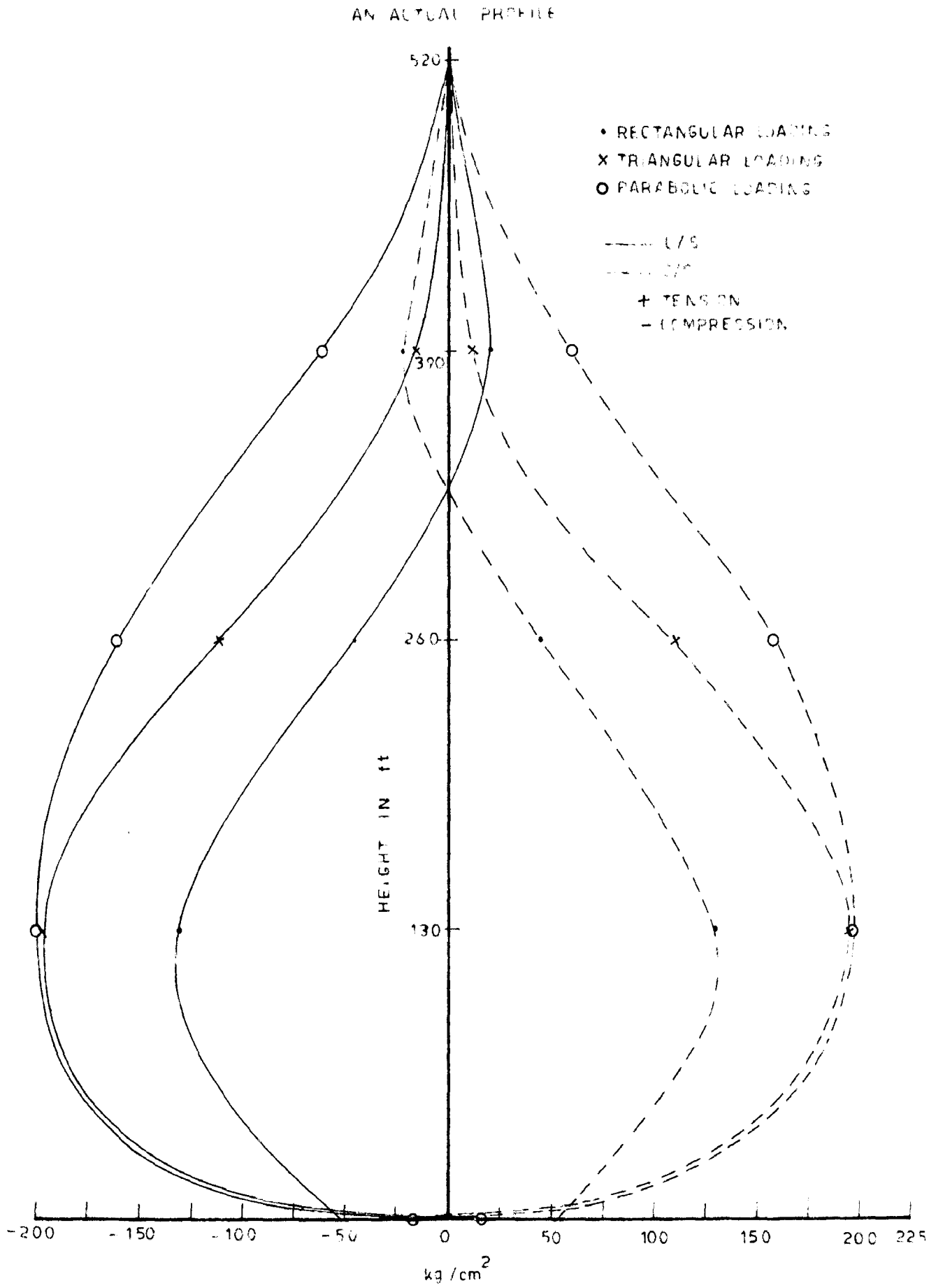

FIG.13 _ VERTICAL STRESSES (DYNAMIC CASE)

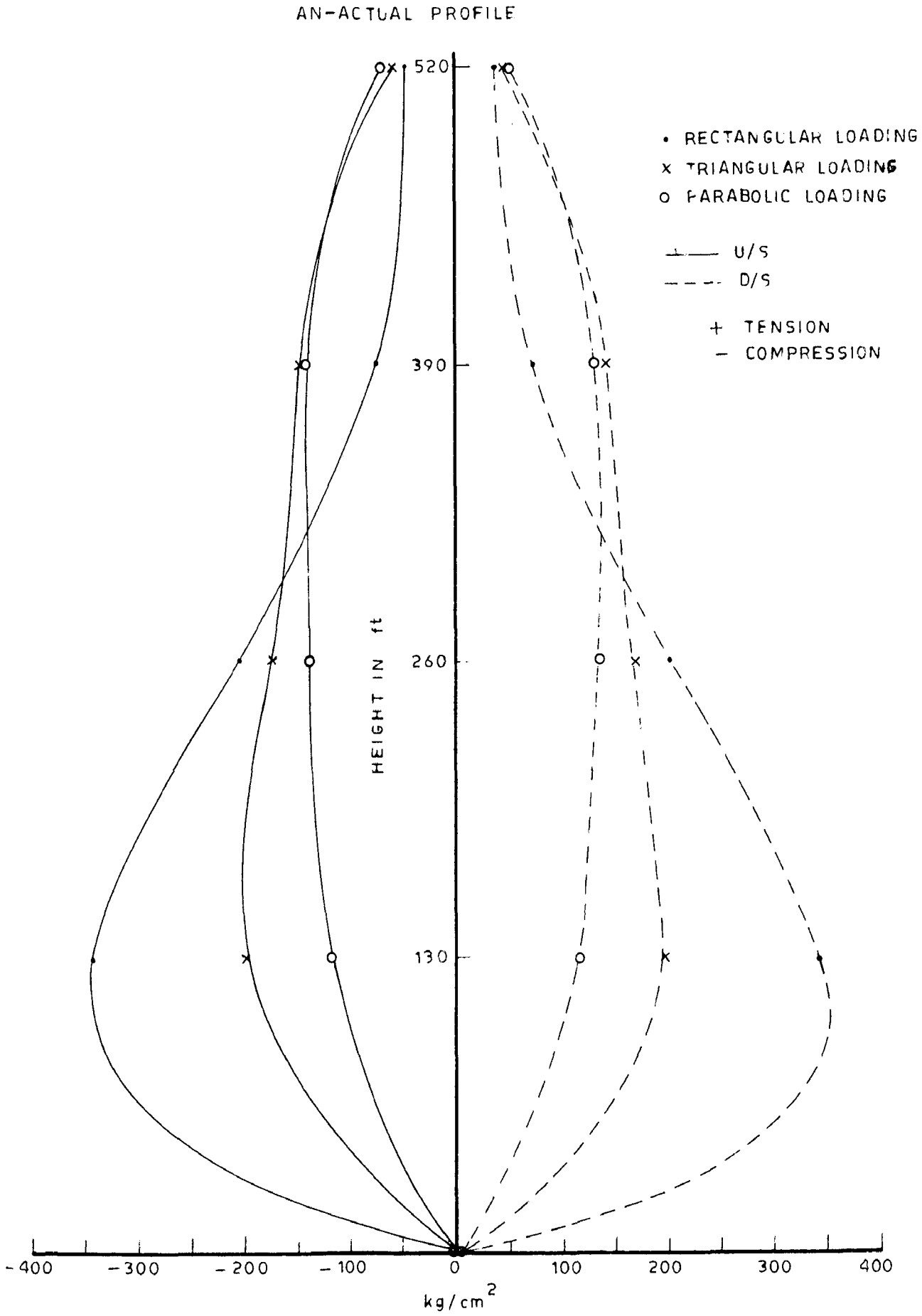

FIG. 14 _HOOP- STRESSES (DYNAMIC CASE)

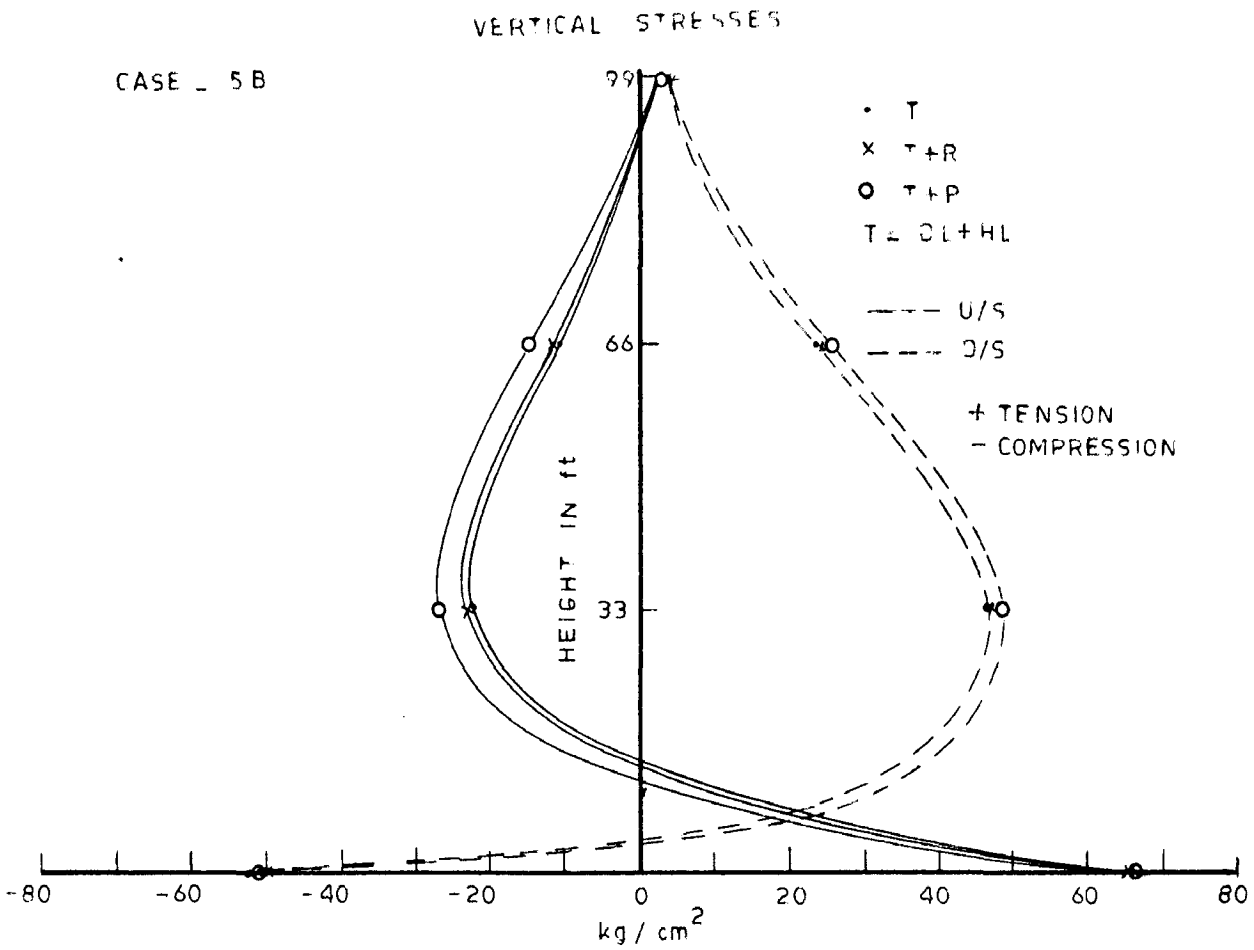

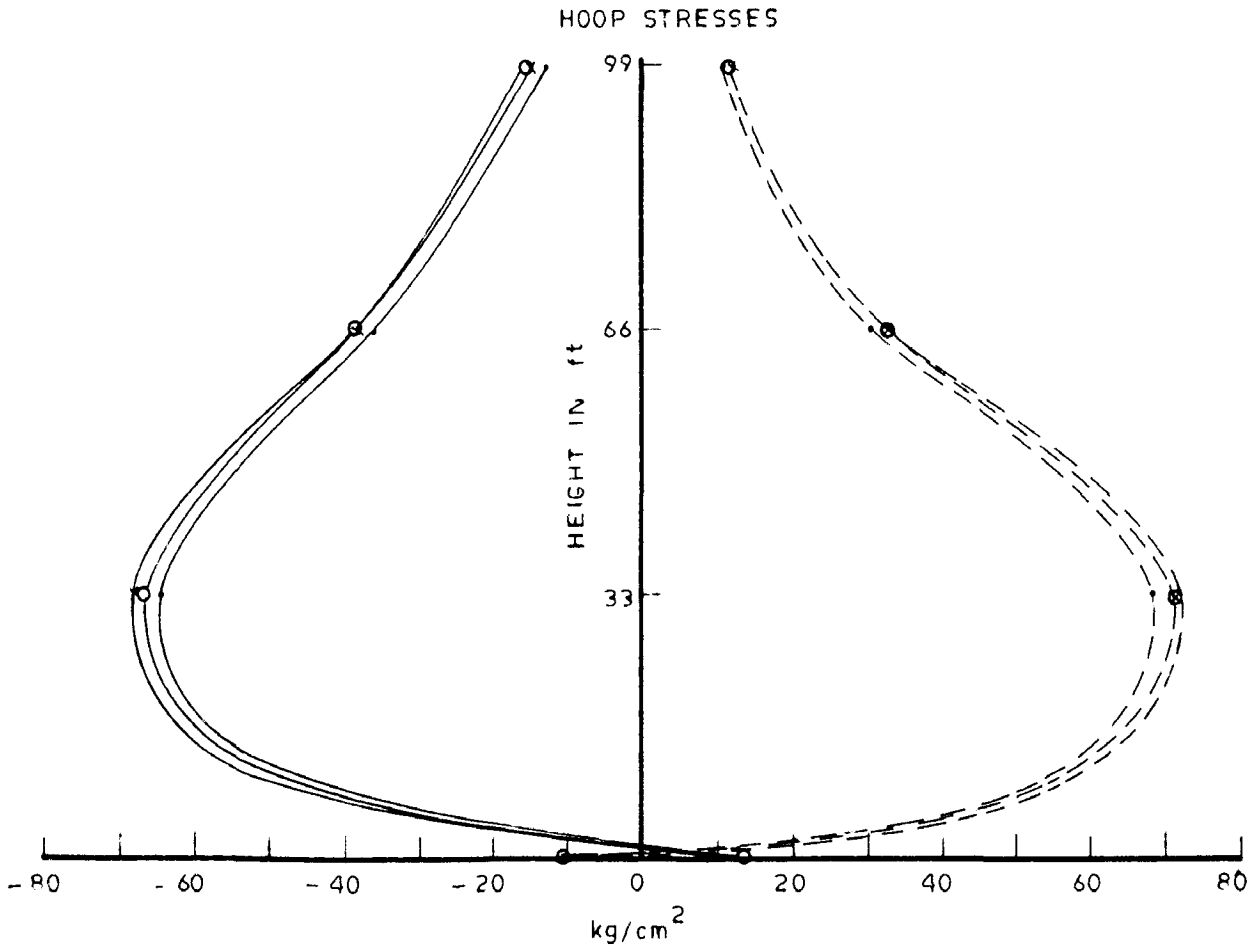

FIG. 15 _ COMBINED STRESSES

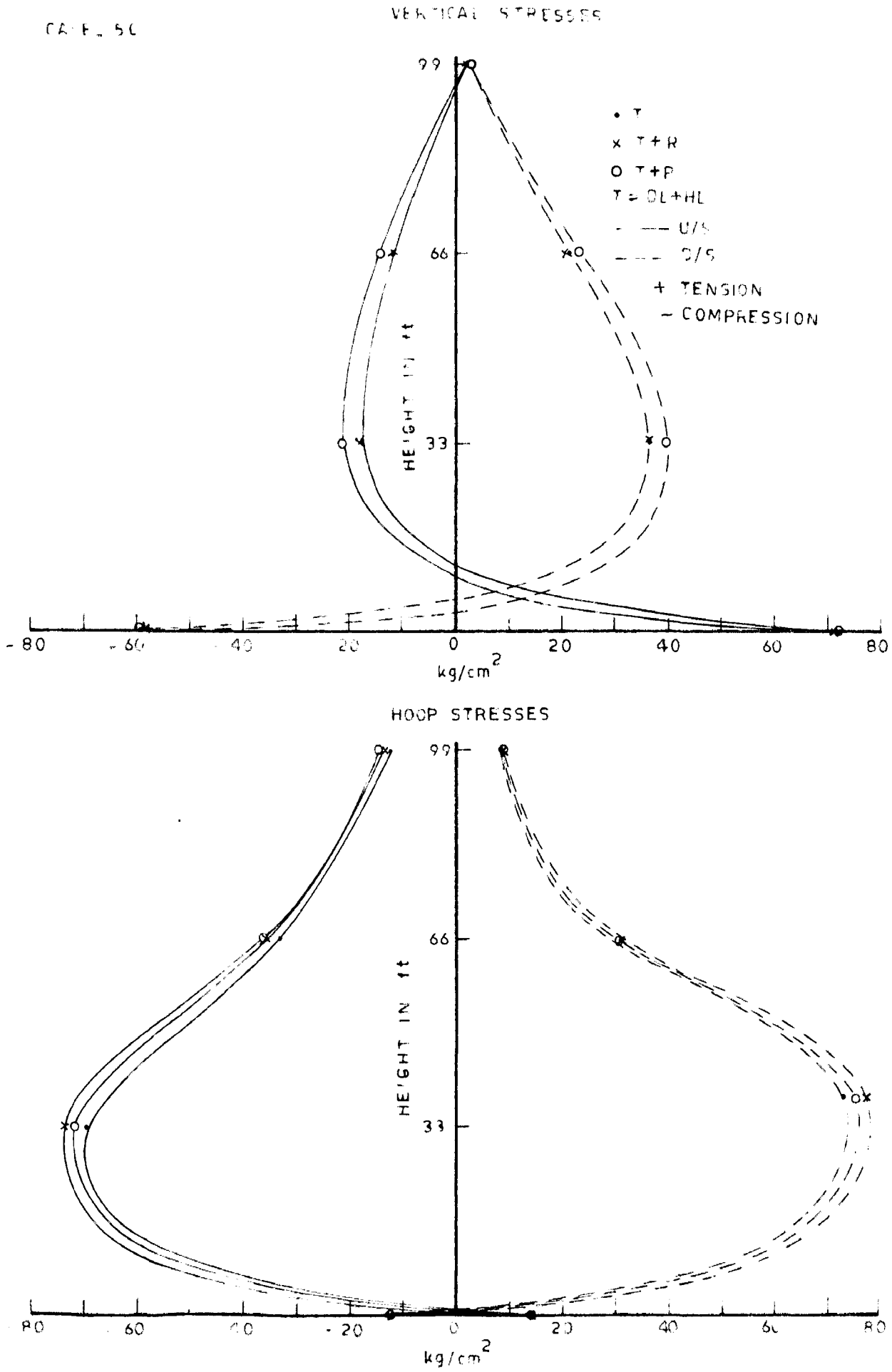

FIG.16 _ COMBINED STRESSES

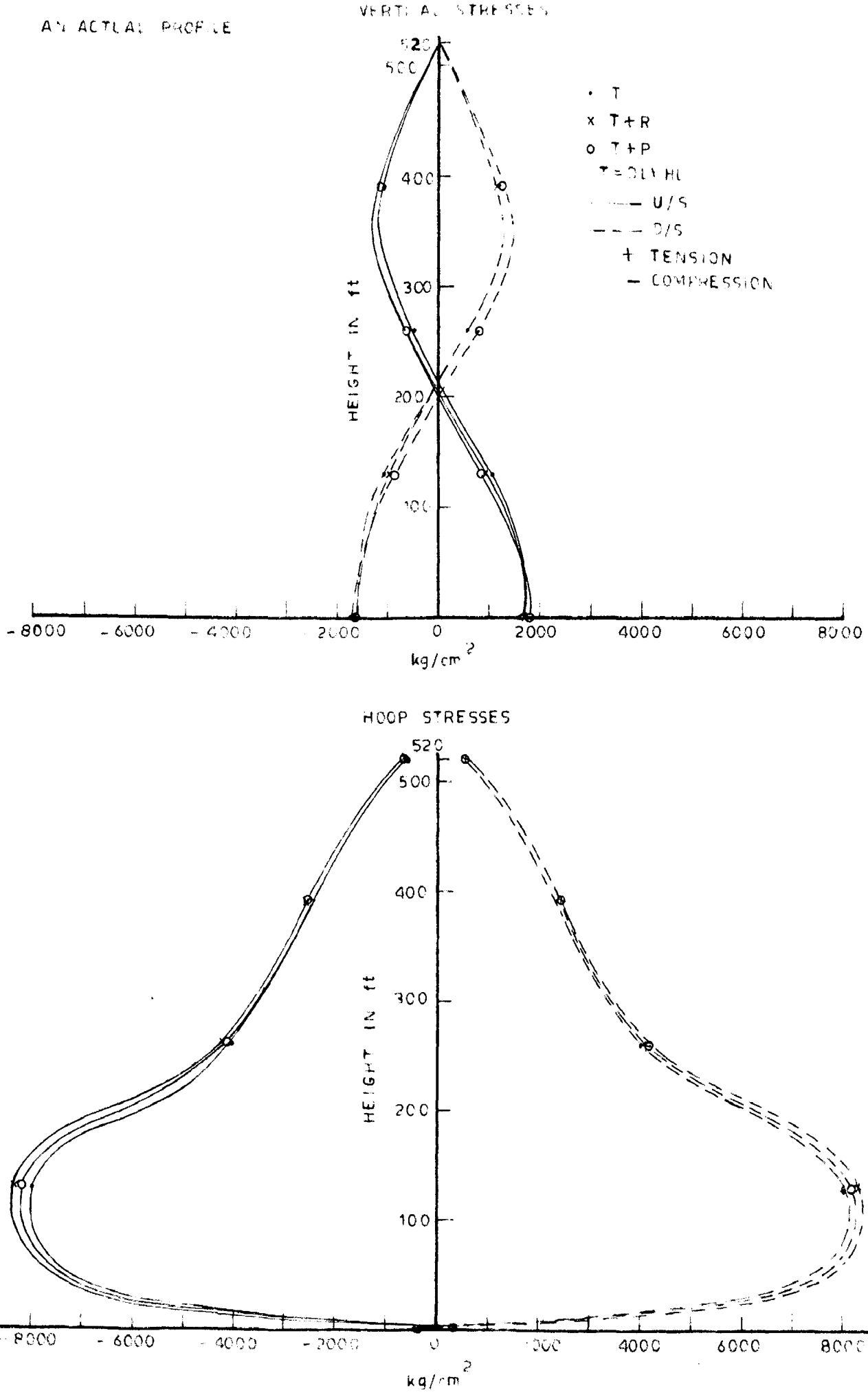

FIG. 17 _ COMBINED STRESSES

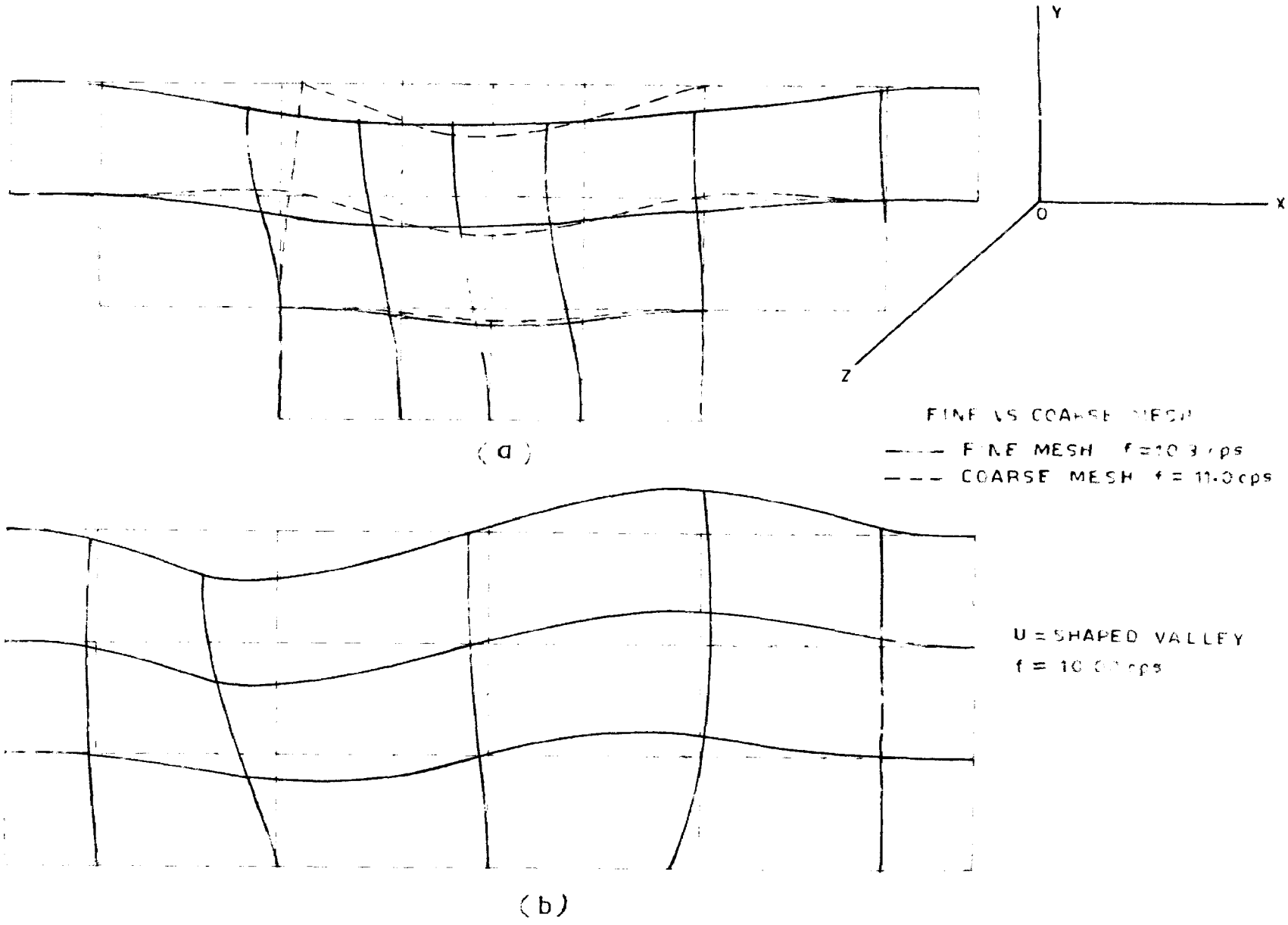
Y
X
O
Z
FINE VS COARSE MESH
FINE MESH f = 10.3 cps
COARSE MESH f = 11.0 cps
(a)
U-SHAPED VALLEY
f = 10.0 cps
(b)

FIG. 18

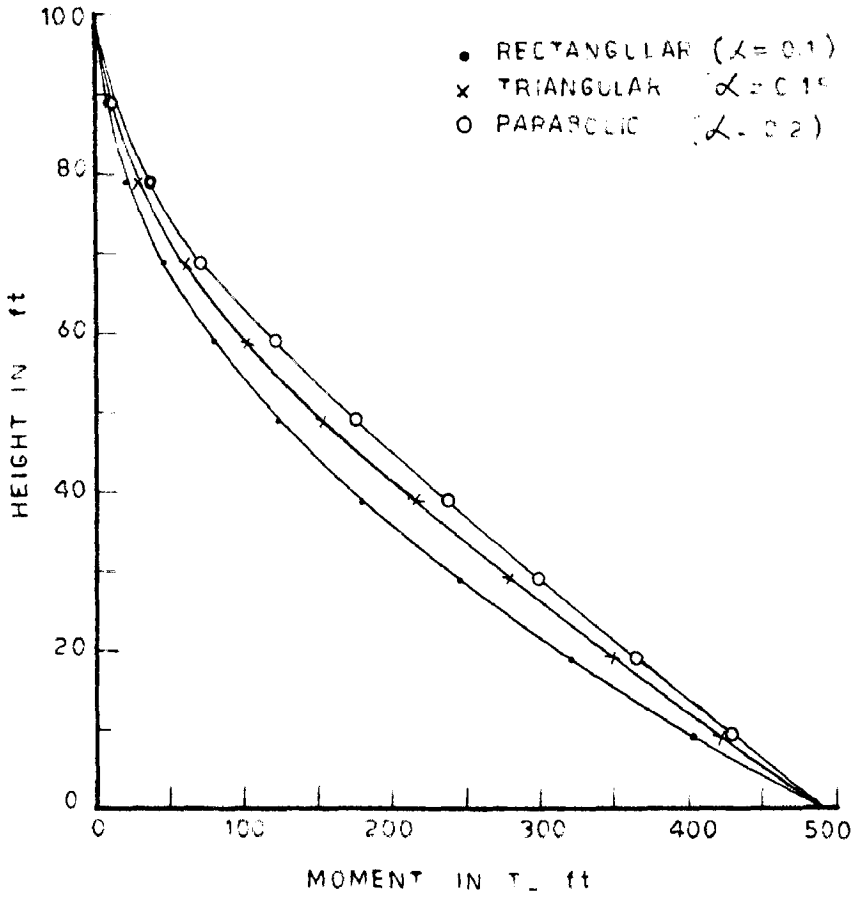
100
80
60
40
20
0
HEIGHT IN ft
0
100
200
300
400
500
MOMENT IN T_ ft
• RECTANGULAR (α = 0.1)
× TRIANGULAR α = 0.15
O PARABOLIC (α = 0.2)

FIG. 19